University of Nevada, Reno

Beyond a Company of Soldiers: Exploring Phenotypic Integration across the Multivariate Human Growth and Development Phenotype

A dissertation submitted in partial fulfillment of the requirements for the degree of Doctor of Philosophy in Anthropology

by

Christopher Aaron Wolfe

Dr. Kyra E. Stull / Dissertation Advisor

May, 2023

THE GRADUATE SCHOOL

We recommend that the dissertation
prepared under our supervision by

Christopher Aaron Wolfe

entitled

Beyond a Company of Soldiers: Exploring Phenotypic Integration across the Multivariate Human Growth and Development Phenotype

be accepted in partial fulfillment of the
requirements for the degree of

Doctor of Philosophy

Kyra E. Stull, Ph.D.
Advisor

G. Richard Scott, Ph.D.
Committee Member

Marin A. Pilloud, Ph.D.
Committee Member

Michael H. Price, Ph.D.
Committee Member

Perry J. Williams, Ph.D.
Graduate School Representative

Markus Kemmelmeier, Ph.D., Dean
Graduate School

May, 2023

Abstract

Traditional studies exploring the interrelationships between growth and development traits have lacked the data necessary to fully describe the multivariate growth and development phenotype and the statistical methodology to quantify the complex interrelationships between varied trait types. Subsequently, human growth and development are often defined by a series of contrasts via the juxtaposition of seemingly disjoint processes in skeletal diaphyseal growth, skeletal ossification and fusion, and development of the dentition. In conjunction with robust data sources from the Subadult Virtual Anthropology Databases (SVAD), this work introduces a Mixed Discrete-Continuous Gaussian copula to explore the multivariate human growth and development phenotype. A copula is a probabilistic function that explicitly models the interrelationships between traits and describes the joint structure of the multivariate relationships.

Fifty-four growth traits are collected from the United States sample in SVAD (n = 1,316). These traits include 18 measurements associated with diaphyseal dimensions collected from six long bones, 20 scores of both epiphyseal fusion and primary ossification centers, and 16 scores of dental development across the left-sided mandibular and maxillary dentition. All data are collected from computed tomography (CT) images and includes demographic information such as an individual's chronological age and biological sex. The joint probability distribution of the 54 growth traits and the underlying dependency structure are fit to a Mixed Discrete-Continuous Gaussian copula using the gradient-based Markov Chain Monte Carlo algorithm known as Hamiltonian

Monte Carlo within the Stan probabilistic programming environment. Six total copula models are fit: the first model utilizes the full dataset, the next three models use subsets of the full dataset representing the individual developmental stages of infancy, childhood, and juvenile/adolescence, and the last two models use subset of the full dataset representing biological males and females.

Results from the full model show that relationships are strongest within each growth module. Further, traits that develop across similar developmental windows show stronger positive correlations as compared to traits that grow and develop during separate periods. These relationships are similar between males and females suggesting that, independent of age, multivariate growth and development processes are the same across the sexes. When considering developmental stages, the results show that the multivariate phenotype presents with different relationships between variables across ontogeny with the strongest relationships between growth and development modules tied to active growth and development periods. Importantly, the skeletal growth, skeletal development, and dental development modules can be further divided into additional units that themselves have various levels of dependence.

The copula demonstrates that the relationships between broad growth modules cannot be summarized via a few pairwise correlations taken at one point during ontogeny. Instead, analyses should be conducted with as much trait information as possible and at various points throughout ontogeny. In the future, copulas could also be extended to additional applications in biological anthropology including research in bioarchaeology and paleoanthropology, method formation in forensic anthropology, and the estimation

and imputation of missing data. In sum, the Mixed Discrete-Continuous Gaussian copula provides the most comprehensive analysis to date of the multivariate human growth and development phenotype and lays the groundwork for future research into the growing, developing, multivariate human.

Dedication

To Mom, Dad, Gary, and Scott – for your unwavering support on this amazing journey.

To Rachel – my forever partner-in-crime, I Love You.

Acknowledgements

Perhaps it is no small irony that my unwittingly long dissertation on the importance of the multivariate human growth and development phenotype would not be if not for a multivariate system of support.

To my dissertation committee:

Dr. Kyra Stull – What started as a random skype conversation in December 2017 about the smallest possibility you may take students the next year, turned into a wonderful five-year journey from Reno to Milan and back. From learning to "write more specific" or learning to ask the tough questions even if the answers were uncomfortable, you have taught me to be a better researcher, statistician, teacher, mentor, and overall better human. There are not enough words to express my gratitude and I am excited to continue to work together and collaborate long into the future.

Drs. Marin Pilloud and G. Richard Scott – From the countless hours in the anatomy lab to the constant musings about tooth metrics and morphology, I am forever grateful for everything you have taught me in the classroom and beyond. Our interactions have pushed me to think outside of the box, provided new avenues to explore the immensity of human phenotypic variation, and taught me to continually evolve and re-imagine what it means to be a biological anthropologist into the future.

Drs. Perry Williams and Michael Price – You both have put up with *countless* emails from me seeking stats help and clarification. And Mike, we have sat on zoom for hours

discussing the finer points of identifiability and joint probability distributions. I am forever grateful for everything you have taught me. This is the most “statsy” paper I have ever written, and I could not accomplish it without teaching and guidance from you both.

To the Stan community:

The Mixed Discrete-Gaussian copula is possible because of Stan and the Stan community. I have spent innumerable hours writing posts, combing through the discourse, answering Stan admins, and seeking ways to model the log probability distribution of a Gaussian copula. I have spoken to more individuals than I can count and been given advice by even more than I can name. However, there are several individuals who must be acknowledged even though they may never see this dissertation. To Benjamin Goodrich, Bob Carpenter, Andrew Johnson, Sean Pinkney, Niko Huurre, John Hall, Brian Ward, and Martin Modrak, this dissertation is a product of your answers to my incessant questions and constant requests to check code, I am forever grateful for your help and teaching. I am a better statistician and Bayesian because of each of you.

To my amazing friends:

From southern Delaware to St. Louis, San Marcos, Reno, and everywhere in between, you have stood by me throughout this long incredible journey. We laughed, cried, drank too much, hung out too little, and no matter what, we never lost contact. You are my

unwavering pillars in life and this dissertation is a product of all your support throughout all these years.

To my family:

Mom and Dad – your bird is flying high. I finally made it. Simply saying ‘thank you’ is not enough. You have loved and supported me every step of the way. I am here because of your love, support, and devotion to all of my dreams, no matter how far from home they have taken me. Scott – for always being there even when life got crazy with twins of your own, I love you. And to my twin, Gary. You have always been my biggest supporter. I could not imagine this life and this journey without your constant calls checking in, your random Rosie snapchats, and your unconditional support no matter how far away I have ended up.

And, to Rachel Provazza:

The love of my life and forever partner in crime. This dissertation is as much mine as it is yours. You took a leap in 2016 to move to the ‘middle of nowhere’ Texas and have been on this journey with me ever since. You have loved me no matter what, sacrificed so much to pick up and move more than once, and kept the lights on even when I was close to tears because of my [low] bank account. You are my best friend. You are my forever and always. Here’s to the next chapter and every adventure in between. I Love You.

Table of Contents

List of Tables

List of Figures

"... progress toward maturity is more like the progress of an informal group of friends on a walk than like the progress of a company of soldiers in strict formation moving at a constant rate of speed… some run ahead, others lag behind and even stop to rest; yet, all reach the same goal in the normal course of events."

(Lamons and Gray, 1958)

Chapter 1 – Introduction

Human growth and development are often defined by a series of contrasts via the juxtaposition of seemingly disjoint processes in skeletal diaphyseal growth, skeletal ossification and fusion, and development of the dentition. Yet, differences in kind surrender to a dynamic interplay of interrelationships that construct growing individuals not as a series of disconnected prefabricated units put together haphazardly at the final build phase, but instead as a continuously integrated whole adult body. How do such relationships vary across ontogeny? Do bones and teeth move uniformly together like regimented soldiers? Do some meander seemingly disconnected from others? Or do some move ahead, while others lag in their own distinct trajectories? The purpose of this dissertation is to investigate the interrelationships between skeletal diaphyseal growth, skeletal ossification and fusion, and development of the dentition. With the advent of robust data sources and the introduction of an innovative multivariate statistical technique to biological anthropology, the results show that growth and development are neither one trait nor one process, but a series of interconnected pathways moving in conjunction towards biological adulthood.

The study of human growth and development has a long history across the natural and social sciences. This includes an early fascination with the pace of individual changes in stature (Scammon, 1927), explication of broad theories in relative growth (Huxley, 1932; Thompson, 1917), the historic and contemporary longitudinal analyses of individual growth and development processes (e.g., Bogin, 1999; Cameron & Bogin, 2012; Eveleth & Tanner, 1990; Tanner, 1981), and modern approaches studying the evolution of the uniquely human growth and development trajectory (e.g., Bogin &

Smith, 1996; Cameron, Bogin, Bolter, & Berger, 2017; Leigh, 2001; Leigh & Park, 1998; Smith, 1992; Stulp & Barrett, 2016). Each of the studies delves into the complex (epi)genetic and environmental factors underpinning the *independent* processes of skeletal growth, skeletal development, and dental development. While important in delineating patterns of "normal" growth processes or highlighting broad trends paramount to applications as wide-ranging as public health or forensic anthropology, there exists an implicit quandary to such analyses: why study each process independently when we know it is an *integrated* human body? The human phenotype, or the observable characteristics of an individual's biology, is inherently multivariate. We are born with upwards of 300 bones that later ossify into 206 adult elements. We first develop 20 deciduous teeth that are lost during development, giving way to 32 permanent adult teeth. Skeletal growth traits, skeletal development traits, and dental development traits make up a portion of the infinitely large multivariate human phenotype. The realization that growth and development processes are a component of a larger multivariate structure leads to the main premise of this study: human growth and development traits do not vary independently, but instead, reflect a network of relationships tied to developmental, functional, and physiological interactions acting through ontogeny (Armbruster, Pelabon, Bolstad, & Hansen, 2014).

The recognition that growth and development processes are reflective of a web of trait-by-trait relationships connected within a larger multivariate system is not novel to bioanthropological research. Historic studies, although contradictory, show varying levels of (in)dependence between skeletal growth, skeletal development, and dental development (e.g., Demirjian, Buschang, Tanguay, & Patterson, 1985; Demisch &

Wartmann, 1956; Lamons & Gray, 1958; Lewis & Garn, 1960). What is more, multivariate analyses with growth traits are commonplace across forensic anthropology and studies into chronological age estimation. Such work has long lamented the superior performance of multivariate techniques over that of univariate or single indicator techniques (e.g., De Tobel et al., 2020; Fieuws et al., 2016; Konigsberg, 2015; Stull & Armelli, 2021; Stull, Corron, & Price, 2021). Yet, even with historical precedence and robust multivariate methods, a complete accounting of the relationship between skeletal growth, skeletal development, and dental development is *missing* from contemporary research. Why? What are these previous studies missing? First, the historic research into interrelationships between traits relied upon longitudinal analyses of often non-diverse samples from select locations in the United States. As a result, the analyses did not collect the *multivariate* series of traits necessary to fully explore the growth and development phenotype nor are they representative of the diverse array of growth and development expression present in a more diverse, contemporary United States. Second, the chronological age estimation techniques are still just that – predictive tools of importance to narrowing down the list of unidentified children in a medico-legal setting or providing an accurate estimate of age for studies of individuals in the past. Their methods, while multivariate, are designed for an efficient, yet valid estimation of an individual's age and not an explication of the interrelationships between traits. And while the structure of integration [correlations or covariances] is critical to such validity, either the full suite of growth and development traits are not included or, if they are, adjustments are made to their structure to increase statistical efficiency (Stull, Chu, Corron, & Price, 2022). As a result, both robust data sources and appropriate statistical techniques are necessary to fill

in the gap in understanding of the multivariate human growth and development phenotype.

With the advent of robust virtual anthropological resources and the formulation of a multivariate statistical model known as Gaussian copula, this study expands upon historic analyses of interrelationships between traits and introduces a novel statistical approach to the study of the multivariate human growth and development phenotype. Virtual anthropology utilizes diverse data domains across varied sources from hospital and/or medical examiner settings to the digitization of raw skeletal and/or anatomical material from museums and skeletal collections (Colman et al., 2019; Weber, 2015). The importance of such sources lies in their ability to encapsulate a *more complete* picture of the multivariate phenotype across diverse settings. Put a different way, virtual anthropology allows the collection and analysis of the multivariate set of traits necessary to study the interrelationships between skeletal growth, skeletal development, and dental development. Specifically, the Subadult Virtual Anthropology Database (SVAD) – a repository that includes skeletal growth traits, skeletal development traits, and dental development traits – provides the data for the current study (Stull & Corron, 2022). In conjunction with data from SVAD, this study introduces a Mixed Discrete-Continuous Gaussian copula to the study of the multivariate human growth and development phenotype and the interrelationships therein. A copula is a probabilistic function that explicitly models the interrelationships between random variables(Skylar, 1959). In this dissertation, these random variables are growth and development traits, where the copula describes the joint structure of the multivariate phenotype between such traits. Therefore, with improved data sources to capture the whole suite of traits underlying skeletal

growth, skeletal development, and dental development, and with the introduction of a copula to explicitly model the relationships between such traits, this dissertation expands upon and provides further evidence that human growth processes are not independent, but instead, interconnected and related in the growing, developing, multivariate human ontogeny.

The objective of this dissertation is ***to develop a novel statistical method to quantify trait interrelationships and provide biologically interpretable results***. The research goals are met through the incorporation of a large sample of growth and development markers and a statistical technique, known as a copula, to biological anthropology. A large sample of individual growth traits ($M = 54$) are collected from the United States sample in SVAD ($n = 1{,}316$). These traits include 18 measurements associated with diaphyseal dimensions across all six long bones, 20 scores of both epiphyseal fusion and primary ossification centers, and 16 scores of dental development across the left-sided mandibular and maxillary dentition. All data are collected from computed tomography (CT) images and includes demographic information such as an individual's chronological age and biological sex. The joint probability distribution of the 54 growth traits and the underlying dependency structure are fit to a Mixed Discrete-Continuous Gaussian copula (Smith & Khaled, 2012) using the gradient-based Markov Chain Monte Carlo algorithm known as Hamiltonian Monte Carlo within the Stan probabilistic programming environment (Stan Development Team, 2022). The results of the modeling process give way to a series of posterior samples for all parameters that describe both the behavior of individual growth traits and the correlation structure that underlies the multivariate system of traits. In the results, this correlation structure is

analyzed across all individuals in the study as well as between subsets of the data related to developmental stage (infancy, childhood, and juvenile + adolescence) and biological sex (male and female). The results are then contextualized in a discussion describing how these analyses expand upon historic work, enhance our understanding of human variation and human growth, and provide for a myriad of applications across biological anthropology and human biology. At the end, not only will this work add a new statistical technique to the study of multivariate human phenotypic variation, but it will provide the most comprehensive look at the multivariate human growth and development phenotype and the dynamic interrelationships that construct growing individuals from birth to adulthood.

Chapter 2 – The Integrated Human Growth and Development Phenotype

Fundamentally, this is a study about relationships. A study about the connections between three developmental components that broadly characterize not only the processes of growth and development, but also the role of such processes in patterning biological variation in the broadest sense. I focus on the components of skeletal growth, skeletal development, and dental development, and specifically their role in patterning phenotypic variation in a human population from the United States. The connections or relationships between each of these components are broadly subsumed under the term phenotypic integration or the patterns of interaction or interrelationships between phenotypic traits (Armbruster, Pelabon, Bolstad, & Hansen, 2014; Pigliucci, 2003). While integration may refer to any number of interactions such as functional, evolutionary, developmental, or morphological, the current study focuses on developmental integration, which is synonymous with ontogenetic integration. That is, this dissertation explores the relationship between phenotypic traits that arise during ontogeny or the period from when an individual is born until they reach biological adulthood. The remainder of this chapter reviews human growth and development and specifically skeletal growth, skeletal development, and dental development in the context of developmental integration. First, I provide a broad introduction to growth and development, followed by a specific review of integration, then I describe what, if anything, historical studies may say about integration in human growth and development traits, and lastly, how developmental integration may be related to other concepts describing human variation including plasticity and canalization.

2.1 Defining Growth and Development

Human growth and development are complex processes representing a dynamic and synergistic balance between underlying (epi)genetic mechanisms and external environmental stimuli. Bogin (1999) defines each of these terms separately. Growth is defined as any quantitative increase in size or mass. Development is a much broader concept related to a) progression of biological changes from an undifferentiated state to a highly organized, specialized state, and b) progression and refinement of behaviors expected by society. A related, yet distinct concept is that of maturation, which refers to the timing and tempo of the above developmental progressions towards a mature state. Importantly, maturation represents the process or movement towards an end state – in biological growth, this represents the beginning of adulthood. Similar to Bogin's definition of maturation, Agarwal (2016) defines development as the "pathway" [trajectory] of biological milestones along the life cycle. As a synthesis of these broad definitions, this work will use growth to refer to progressive and incremental changes in size and morphology (*e.g.* an increase in bone/diaphyseal length and breadth) and will use development to refer to the progression of changes from an immature to a mature state (e.g. dental development and skeletal fusion and ossification) (Šešelj, 2013).

The growth and development phenotype represents a complex network of individual traits and processes mediated through a multitude of cultural, genetic, and environmental forces (Baker, 1997). Beginning with Lasker (1969), biological anthropologists sought to document and explain such phenotypic variability across these complex networks of interrelationships. Lasker (1969) and Frisancho (2009) expounded

on the importance of human growth and development to studies of phenotypic variability. However, their use of the term adaptation to describe non-heritable physiological adjustments during an individual's life cycle often leads to confusion and conflation with tautological neo-Darwinian notions related to fitness and natural selection (Ellison & Jasienska, 2007; Gould & Lewontin, 1979; Hicks & Leonard, 2014). For this reason, there is a distinction between Darwinian concepts of adaptation related to the primacy of genetic heritability and that of phenotypic plasticity related to the malleability of form through a complex, integrated system of epigenetic, genetic, behavioral, and environmental factors (Kuzawa & Bragg, 2012) .

Underlying each individual component of growth and development, such as skeletal growth, are observed differences or variation between individuals. For example, the length of the femoral diaphysis at any given age is not uniform across every individual. Studies of variation within each component of growth and development (e.g., Demirjian, Goldstein, & Tanner, 1973; Lenover & Seselj, 2019; Maresh, 1955) are common across biological anthropology. A description of such variation in relation to other traits is less common (see below). In the current study, I distinguish between the process or factors that cause variation in individual developmental components and instead, focus on the pattern of such variation in relation to the variation of other developmental components (Wagner, Booth, & Bagheri-Chaichian, 1997). The focus is not on a single growth or development process, but how such processes are related (or not) throughout ontogeny (Hallgrimsson et al., 2009; Hallgrimsson, Willmore, & Hall, 2002).

2.2 The Study of Phenotypic Integration

2.2.1 Definition

Phenotypic traits do not "vary independently, but instead reflect webs of developmental, physiological, and functional interactions" (Armbruster et al., 2014). The connections and relationships present within such complex webs of interaction represent the properties of integration broadly defined (Cheverud, 1996; Olson & Miller, 1958; Pigliucci, 2003). The idea that seemingly independent structures, like teeth or skeletal elements, vary in a coordinated manner has a long history in evolutionary biology and biological anthropology. This work extends from the principles of the correlation of parts (Rudwick, 2008), multi-trait correlations in domestic animals (Darwin, 1859), and the relative relationship between body size, shape, and form (Huxley, 1932; Olson & Miller, 1958; Thompson, 1917). While there are a series of complex quantitative descriptions underlying the statistical and biological properties of integration (e.g., Cheverud, 1982a; Lande, 2019; Mitteroecker & Bookstein, 2007; Raff, 1996; Wright, 1932), inherently integration is a study of covariation or correlation between phenotypic traits.

Covariance is a measure of joint variability between variables indicating the direction of the [linear] relationship between two variables. Covariance does not provide an indication of how strong the relationship between said variables may be. The value associated with the covariance is more reflective of the size of the variable than the size of the relationship. Statistically, a measure of covariance encapsulates both the standard deviation (variation) between a set of variables and the direction of association between

the variables (correlation). On the other hand, correlation is a standardized [unit-free] function of the covariance that measures both the strength and direction of a relationship.

Studies of integration often use both correlation and covariance interchangeably to describe how phenotypic traits may be related (Mitteroecker & Bookstein, 2007). Both metrics provide an estimate of the linear dependency between two variables, and neither metric implies causation between traits. Because covariance is influenced by the scale of the measurement and given the disparate measurement approaches between skeletal growth (continuous scale), skeletal development (ordered, discrete scale), and dental development (ordered, discrete-scale), the present study uses the standardized, unit-free measure of correlation to describe integration between traits. To paraphrase previous work, the interpretation of either correlations or covariances in the context of phenotypic integration will provide similar results (Mitteroecker & Bookstein, 2007).

2.2.2 The Modular Structure of Integration

Young and Hallgrimsson (2005) suggest that patterns of covariation between traits are hierarchically structured into discrete subunits. In other words, groups of traits may be more integrated to each other as compared to other traits. This process is known as modularity and each individual subunit is known as a module. The present study assumes that the growth and development components described in the introduction of this chapter are representative of growth and development modules. That is, there is a skeletal growth module, a skeletal development module, and a dental development module, where individual traits of each module may be more tightly integrated with each other in

comparison to traits from different modules. Properties of individual modules include: 1) an autonomous and discrete genetic organization, 2) composed of hierarchical units that themselves may be part of larger hierarchical units, 3) a specific "location" within the human body, 4) variable integration with other modules, and 5) a chronological component suggesting coordinated change through time (Raff, 1996). In the context of the present study, modularity may signify different (epi)genetic and/or embryological origins of skeletal growth versus that of tooth development, modules themselves may be further subdivided into other modules such as the difference between longitudinal and appositional growth, and the modular nature of human growth and development may be variable and dynamic across ontogeny (Hallgrimsson et al., 2002).

The processes of modularity and integration serve to pattern phenotypic variation within and between individual growth traits and broader growth modules. The tendency of a series of traits to covary or correlate is directly related to their levels of individual variation (Klingenberg, 2008). Therefore, because of the properties of modularity and integration, correlated variation is stronger with traits that are more tightly integrated – genetic and/or environmental factors that affect one trait of skeletal growth, may also be reflected in other traits of skeletal growth. Importantly, the tendency to vary or covary may act at different timescales and different spatial locations over the body leading to a series of flexible, overlapping, and dynamic processes that change throughout an individual's life course (Hallgrimsson et al., 2009). This is further evidenced by the age-specific covariance (and correlation) matrices that occur throughout studies of integration (Mitteroecker & Bookstein, 2009). As a result, the complex, hierarchical relationships described by the properties of integration and modularity are a palimpsest of dynamic,

ever-shifting processes acting during ontogeny to structure variation within and between developmental modules related to skeletal growth, dental development, and skeletal development (Hallgrimsson et al., 2009).

2.2.3 Implications

The presumption that phenotypic traits are necessarily related leads to several implications concerning phenotypic evolution, evolution of the human life history, the role of the environment in patterning human variation, and downstream practical applications that use integrated traits. In evolutionary biology, there are competing arguments related to the role of phenotypic integration in patterning phenotypic variation and broader evolutionary trends. On one hand, researchers view phenotypic integration and modularity as inherently a constraint on variation and evolution (Lewontin, 1978; Voje, Hansen, Egset, Bolstad, & Pélabon, 2014). Such work suggests that tightly integrated units (especially within modules) prevent large-scale changes that may impact evolvability or biological fitness. Traditional examples of constraint in relation to integration arise from studies of allometry whereby phenotypic diversity is often limited by a trait's relative relationship to body size (Huxley, 1932; Voje et al., 2014). On the other hand, integration may also be seen as adaptive whereas the tight relationships between traits may (co)evolve together and be modified by evolutionary forces together to survive in certain environments. An example may be the cranium and the relationship between brain size and cranial size and shape (Cheverud, 1982; Sardi & Rozzi, 2007). It is more likely than not that integration could be represented by either of these

circumstances depending on the traits in question. That is, modules could together be altered by environmental interactions signaling a plastic or adaptive response (Matesanz et al., 2021; Pigliucci, 2003; Schlichting, 1989), while at the same time, the integration between another set of traits may prevent a similar plastic response.

The above description is of the broad relevance of phenotypic integration in evolutionary contexts. At the individual level, developmental integration, the type of integration studied here, impacts the degree of (co)variation between traits. Instead of a constraint or adaptation in the broad evolutionary sense, developmental integration patterns the degree to which certain traits may or may not be related to similar embryological, hormonal, and (epi)genetic processes. Such linkages are tied to the genetic concept of pleiotropy whereby a single gene affects multiple elements, or linkage disequilibrium where two genes that affect a single trait tend to be inherited together (Cheverud, 1996). Thus, in the current study, developmental integration may speak to broader elements of the genetic origins of human growth and how the processes may or may not be related between separate growth modules. By extension, these genetic relationships and/or correlations may also be tied to the propensity of the environment to affect traits within each of the modules and how such interactions may influence an individual's life course (Duren, Seselj, Froehle, Nahhas, & Sherwood, 2013; Gluckman, Hanson, & Beedle, 2007; Matesanz et al., 2021).

In addition to the role of phenotypic integration in evolutionary timescales and in the patterning of individual levels of variation, the fact that growth and development traits may be correlated impacts the utility of such traits in downstream applications.

Variables associated with skeletal growth, skeletal development, and dental development are a crucial component of subadult chronological age estimation in forensic anthropology and bioarchaeology (Corron, Marchal, Condemi, & Adalian, 2018; Konigsberg & Frankenberg, 1992; Marquez-Grant, 2015; Ubelaker, 1987; Ubelaker & Khosrowshahi, 2019). This is because growth and development traits are correlated with an individual's age; for example, as one ages, the long bones get longer, and teeth become more developed. Contemporary methods of age estimation suggest the utility of more than one trait [multivariate methods] to capture as much information about age as possible given that the relationship between individual traits and chronological age is not uniform (Boldsen, Milner, Konigsberg, & Wood, 2002; De Tobel et al., 2020; Konigsberg, 2015; Navega, Costa, & Cunha, 2022; Stull & Armelli, 2021; Stull, L'Abbe, & Ousley, 2014). Crucial to multivariate age estimation is a characterization of the relationships or integration between traits, which is statistically known as conditional dependence. Essentially, regardless of an individual's age, there is a known relationship or correlation between individual traits, such as a long bone length or tooth score (Šešelj, 2013; Sgheiza, 2022; Stull, Corron, & Price, 2021). The broad definition of phenotypic integration corroborates the above cited studies – traits are in fact correlated to each other across development. The present study is thus an example characterizing developmental integration and as a result, conditional dependence between growth traits.

2.3 Previous Studies of Phenotypic Integration in Human Growth and Development

Phenotypic integration has a long history in developmental biology and biological anthropology (e.g., Armbruster et al., 2014; Huxley, 1932; Olson & Miller, 1958; Pigliucci, 2003; Thompson, 1917). However, most of these studies tend to focus on continuous-valued traits only and only analyze morphological trait interrelationships. That is, previous work tends to focus solely on the evolution and interrelationships between shape and form – i.e., the shape of upper limb bones versus that of the lower limb or the shape of the cranium with respect to the brain. No previous work explicitly uses the term "integration" to describe interrelationships between human growth and development traits. However, semantics aside, there are several previous studies whose work *does* address connections and/or relationships between traits commonly used to describe human growth and development.

There is a degree of contradiction and conflation of concepts across several of the earliest studies describing interrelationships between traits. Demisch and Wartmann (1956) suggest there is a high positive correlation between the degree of calcification of the mandibular third molar and skeletal age [termed chronological age in the study] as determined by carpal development (Greulich & Pyle, 1959). On the other hand, both Lamons and Gray (1958) and Lauterstein (1961) conclude that dental age as determined by contemporary dental charts (Schour & Massler, 1940) and skeletal age as determined by carpal development (Greulich & Pyle, 1959) are independent of each other. Additional work corroborates these early studies concluding that given an individual's skeletal and dental age, there is a fair degree of independence between skeletal development and

dental development (Demirjian et al., 1985). However, these early studies suffer from a conflation of terms by assuming the relationship between biological age(s) (i.e., skeletal age and dental age) or the relationship between a trait's development and chronological age (calendar age or age starting at birth) is the same as the relationship between the growth and/or development of separate traits (i.e., an increase in femur length leads to an increase in molar development). There are known differences between biological age and chronological age that are tissue-specific and result from a myriad of factors related to individual levels of plasticity, dynamic and variable growth processes that determine when a trait may start and/or stop developing, and underlying genetic and/or hormone-dependent processes that determine individual growth trajectories (Cameron, 2015; Cardoso, 2007; Cavallo, Mohn, Chiarelli, & Giannini, 2021). Further, the determination of skeletal age relies on statistical analyses with added layers of error that are also tissue-dependent and could mask *true* relationships between traits. Previous work discussed above (Section 2.2.3) confirms that there are known dependencies between traits independent of age. Therefore, questions about trait interactions should not focus on the strength of the trait's relationship with age, but instead, how the growth or development of one trait relates to that of another (Cameron, 2015).

Stanley Garn and colleagues provide the most well-known effort to elucidate relationships between individual growth traits (although, they do include few analyses of biological and chronological age) (Garn, Lewis, & Kerewsky, 1965; Lewis & Garn, 1960). The authors concluded that dental formation and dental eruption are weakly, but positively correlated to several measures of somatic growth and maturation. This includes weakly positive correlations to the number of hand and wrist centers, fusion of the

proximal epiphysis of the tibia, and appearance of the distal epiphysis of the fourth manual phalanx. However, when taking the correlation between dental development and additional factors of growth such as weight, height, and percentage of lower thoracic fat mass, the results were mixed with mostly weak correlations that range in characterization from negative to positive. Based on Garn and colleagues' initial studies, little information is available regarding the relationship between dental development and skeletal growth. Like the previous studies, those described here also suffer from methodological issues related to an inability to control statistical factors, such as conditional dependence between traits and the mixed continuous and discrete nature of the data.

Contemporary research has begun to control such statistical factors. There is general agreement that independent of age, there is a weak to moderately strong relationship between dental development and skeletal growth (Poulsen & Sonnesen, 2023; Šešelj, 2013). Typically analyzed using femoral growth and development of the first permanent molar, the suggestion is that as the femur gets longer, the molar increases towards a later stage of development. However, the authors caution that the relationship between both traits is not strong enough to suggest dental growth and/or skeletal growth may necessarily be a proxy for the other (Šešelj, 2013). But these analyses only focus on pairwise or bivariate relationships between two traits – the phenotype is multivariate and is made up of innumerable trait-by-trait relationships. Stull and colleagues present an information theoretic approach that does incorporate the multivariate nature of the phenotype using all of the growth and development traits from the current study (Stull et al., 2021). While the approach does corroborate known conditional dependence between growth traits, the analyses only focus on bivariate or pairwise relationships and do not

consider the joint relationship between the traits in a multivariate system. As such, while interrelationships between growth and development traits have been studied for three-quarters of a century, no previous study has done so through the lens of phenotypic integration, nor have they incorporated a full joint characterization of such relationships within the multivariate human growth and development phenotype.

2.4 Phenotypic Integration and Additional Variability Processes

Phenotypic integration can be thought of as part of a series of interrelated processes that structure biological and/or phenotypic variation in an organism. Additional processes include canalization and phenotypic plasticity. While traditionally thought of as independent processes that serve to enhance or suppress levels of overall phenotypic variation, it is the combination or combined effects of each of these processes in an integrated system that serve to structure how the human skeleton and human dentition may or may not be related in a growing human individual.

Canalization can be defined as the suppression of phenotypic variation (Wagner et al., 1997). The basic premise is that individual developmental pathways like that of individual skeletal elements or individual teeth, follow discrete, predefined trajectories toward an endpoint that is buffered against additional environmental influence (Waddington, 1942a). The endpoint in this case is twofold: the proximate expression of the trait at a certain age or the final expression of the trait once biological adulthood is reached. Aspects of canalization are intrinsically tied to variation at the individual trait or growth module level (i.e., dental development is thought to be more canalized than

skeletal growth) (Hermanussen, Largo, & Molinari, 2001). However, the tendency of a series of traits to covary is directly related to their individual levels of variation (Klingenberg, 2008). By extension, phenotypic integration may pattern how certain groups of traits may or may not be canalized. For example, if femoral growth is less canalized as compared to molar development, it is likely other skeletal traits in the same module are also less canalized. Interestingly, canalization, like integration, can be thought of as a constraint on phenotypic variability. That is, both processes tend to be related to more uniform levels of variability, while the lack of such constraints leads to increases in variability (Hallgrimsson et al., 2009, 2002). In fact, it is likely that more strongly integrated traits also show higher level of phenotypic stability and canalization (Hallgrimsson et al., 2002). Therefore, in reference to the current study, it may be likely that more canalized traits such as dentition, may also show stronger levels of integration as compared to elements of other modules such as skeletal growth and development.

A related yet distinct concept is that of phenotypic plasticity. Plasticity represents the capacity of a single genotype to produce any number of phenotypes in response to stimuli (Pigliucci, 2001; Wund, 2012). In comparison to canalization, plasticity of a trait leads to greater variability in expression. For example, heteroskedasticity in skeletal growth is directly related to the plastic nature of certain skeletal elements and the long-term interplay between the environment and growth processes that increases variability in trait expression as one gets older (Agarwal, 2016; Said-Mohamed, Pettifor, & Norris, 2018; Stearns & Koella, 1986). As it relates to integration, the relationship between processes can be thought of on two levels: 1) correlations or covariance between traits can be altered by certain environmental conditions (Schlichting, 1989), or 2) the degree

of plasticity is itself integrated (Matesanz et al., 2021; Pigliucci, 2003). In context, the above statements suggest that either correlation between traits may be stronger or weaker depending on the degree of plasticity between each, or the plasticity itself could be integrated such that plasticity of a single long bone may signify elements of the same module could also show similar degrees of plasticity. The opposite could also be true insomuch as traits that are less plastic may also show stronger levels of integration – this is directly comparable to the notion that more canalized traits tend to be more strongly integrated. However, it should be noted, that the ability for a trait to be more or less canalized could also be plastic in nature and as such, plasticity, canalization, and integration are not static processes that are necessarily uniform across human ontogeny.

The combined effects of phenotypic integration, canalization, and phenotypic plasticity serve to structure the human variation we study between growth and development traits. While there is consensus across disciplines that the human skeleton may be more plastic in comparison to the human dentition, no study has sought to characterize such assertions because growth and development cannot be distilled into single traits nor single modules. Are all skeletal elements equally plastic across ontogeny? Do all teeth show similar levels of canalization? Does a moderately strong correlation between the first molar and the femur suggest similar degrees of canalization and/or plasticity? An analysis of the multivariate human growth and development phenotype would clarify the patterns of variation that exist within and between skeletal growth, skeletal development, and dental development.

Chapter 3 – Modeling (Multivariate) Human Growth and Development

Any valid accounting of human growth and development requires two essential elements: 1) appropriate data sources to address the range of variation in traits, and 2) appropriate statistical methodologies to address specific research questions associated with growth and development. Traditional studies of human growth and development have typically focused on individual levels of variation within certain traits (e.g., height, femur length, molar score) to clarify "normal" levels of variation. However, traits associated with human growth and development can be utilized in a wide range of settings ranging from that of phenotypic integration described in the current study or to the utility of such traits in downstream applications such as chronological age estimation. The purpose of this chapter is to review the historic and contemporary approaches to the study of human growth and development. After this review, gaps in the current literature are discussed, followed by the introduction of the approach utilized in the current study to model the multivariate human growth and development phenotype.

3.1 Traditional Approaches to Human Growth and Development

The modern study of human growth and development dates back to the latter half of the 18th Century when Count Philibert de Montbeillard began plotting his son's height on six-month intervals from birth up until the age of 18 (Scammon, 1927). Since this time, researchers in human biology and auxology have sought to clarify the "normal" pace and sequence of individual elements of growth and development as an individual ages (Bogin, 1999; Cameron & Bogin, 2012; Eveleth & Tanner, 1990). The analysis of the growth and development process is typically done in reference to an individual's

chronological age and can be completed on either a scalar-valued trait, such as femoral growth-for-age (Figure 3.1), or on a discrete-valued trait, such as dental development score-for-age (Figure 3.2). Regardless, the goal of either set of analyses is to measure how individual growth traits vary and change across ontogeny. Such analyses are used to address sex differences in growth (e.g., Lampl & Jeanty, 2003; Noback, 1954; Smith & Buschang, 2004; Stinson, 1985; Tanner, Whitehouse, Marshall, Healy, & Goldstein, 1975), population differences in growth (e.g., Johnston, 1969; Pinhasi, Teschler-Nicola, & Shaw, 2005; Silventoinen, Kaprio, & Yokoyama, 2011), and the relationship between the environment and individual growth and development traits (e.g., Little, Malina, Buschang, DeMoss, & Little, 1986; Malina, Zavaleta, & Little, 1987; Moffat & Galloway, 2007; Schell, Gallo, & Ravenscroft, J., 2009; Wells, 2007).

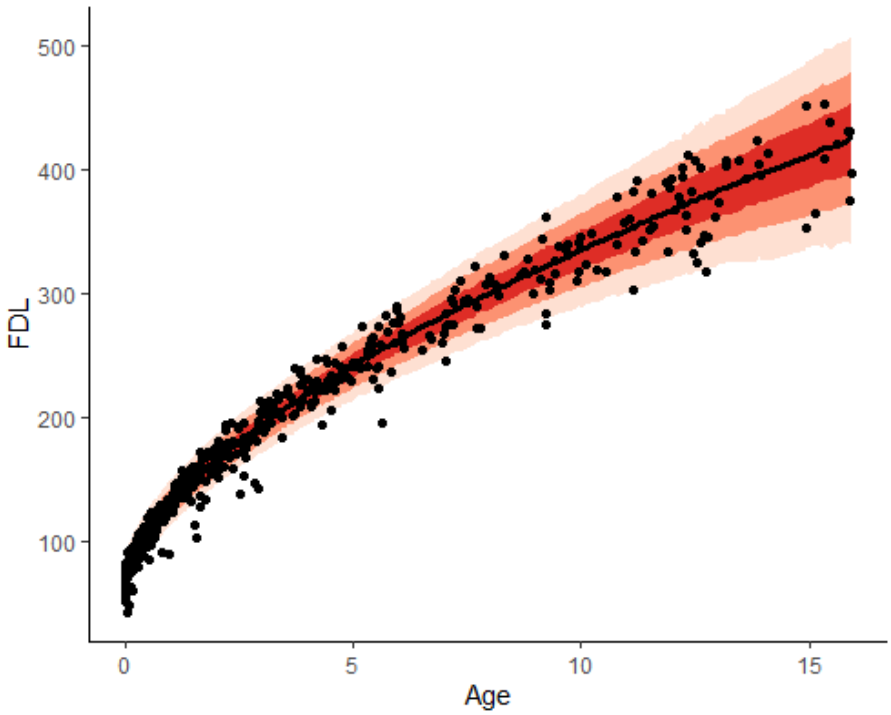

Figure 3.1. An example demonstrating the measurement of femoral diaphyseal growth-for-age – a traditional approach to analyzing the growth of individual scalar-valued elements.

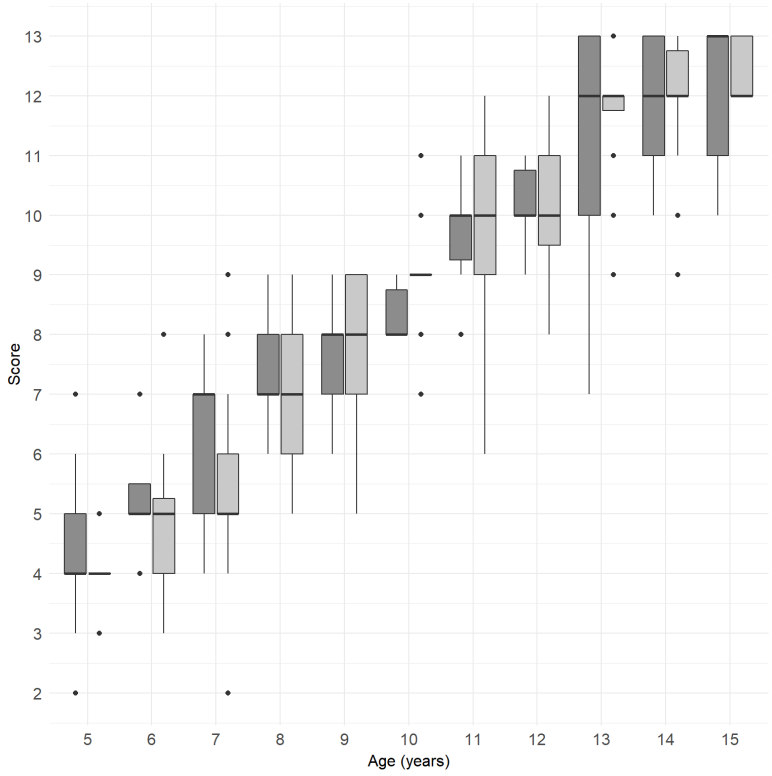

Figure 3. 2. An example demonstrating the measurement of second mandibular molar development-for-age - a traditional approach to analyzing the development of individual discrete-valued elements (dental development or skeletal development).

Whether a study of skeletal growth or development of individual teeth, historic studies of human growth and development relied upon longitudinal growth studies in specific locations across the United States. This includes the Fels Longitudinal Study in Ohio (Roche, 1992), the University of Iowa Child Welfare Station Study in Iowa (University of Iowa Child Welfare Research Station, 1924), the Harvard Growth Study in Massachusetts (Dearborn & Shuttleworth, 1938), the University of Colorado Child Research Council Study in Colorado (Maresh, 1972), the Brush Foundation Study in Ohio (Simmons & Greulich, 1944), and several studies in California at the University of California, Berkeley (Jones & Bayley, 1941). Each of these studies took a myriad of

anthropometric, maturational, and somatic measurements across mostly affluent, white children at each respective location across various periods throughout ontogeny. The goal of each study was to capture as much information about “normal” growth and development as possible in hopes of tracking and managing the welfare and health of the children at each location. Similar work has been conducted both across European countries such as the British Harpenden Studies (Tanner, 1981) and across Central America in the Institute of Nutrition of Central America and Panama (INCAP) studies (Martorell, 2020). In comparison to the United States, those in Europe and Central America tended to focus on “pathological growth” and how to remedy such pathologies in hopes of achieving “normal” growth. Regardless, each of these earlier studies are precursors to the modern World Health Organization’s approach to track “normal” human growth and development across global populations (de Onis, Garza, Victora, Bhan, & Norum, 2004).

However, there are issues related to the study of human growth in these traditional studies. This includes the lack of a definition for what constitutes “normal” human growth and development and given that contemporary work suggests the phenotype is multivariate and integrated (see Chapter 2), there is a lack of research that looks at growth beyond single trait approaches. The definition of normal human growth and development is context dependent. Not all childhood populations are breast-fed, white, or come from affluent socio-economic backgrounds (Cole, 2007). As a result, any accounting of the range of variation in normal human growth and development should encapsulate large, diverse samples of children that come from different growth environments. This is not apparent in the traditional longitudinal studies described above.

Further, while there are innumerable [multivariate] types of traits collected in each longitudinal study, the traits are neither analyzed in a multivariate capacity, nor do they necessarily contain the same suite of traits across diverse, large samples of children.

3.2 Contemporary Applications of Human Growth and Development

Traditional longitudinal approaches to the study of individual growth and development trajectories have given way to contemporary approaches that use growth and development traits to address questions beyond an accounting of "normal" human growth. This includes the use of such traits to investigate the evolutionary origins of the uniquely human growth and development process (e.g., Bogin & Smith, 1996; Brimacombe, 2017; Leigh & Park, 1998; Smith, 1992; Smith et al., 2007; Stearns, 1992; Stulp & Barrett, 2016), a comparison between human and non-human primate growth and development processes (Smith, Crummett, & Brandt, 1994; Robson & Wood, 2008; Schultz, 1923; Smith, 1994), the relationship between individual growth processes (Poulsen & Sonnesen, 2023; Šešelj, 2013; Stull et al., 2021), and the use of traits in chronological age estimation (e.g., De Tobel et al., 2020; Konigsberg, 2015; Stull, Chu, Corron, & Price, 2022; Stull, L'Abbe, & Ousley, 2014). In fact, much of the contemporary work related to growth and development traits stems from the fact that each trait displays varying levels of correlation with chronological age, and as a result, the relationship between chronological and biological age can be exploited to address how children grow, develop, and age across disparate populations. Therefore, while the traditional research tended to exist in the realm of human biology, auxology, and pediatric health, contemporary work is broader in nature and incorporates research questions

across developmental biology, human evolution and paleoanthropology, forensic anthropology, and human biology.

A necessary prerequisite for much of these contemporary studies into human growth and development is the availability of robust data sources to quantify as much information about the underlying growth and development phenotype as possible. Virtual anthropology provides the means to capture large [multivariate] amounts of phenotypic information across diverse settings (Weber, 2015). These virtual approaches are made possible by the measurement and digitization of growth and development traits across varied modern imaging modalities including ultrasound, radiography, magnetic resonance imaging (MRI), and computed tomography (CT). Of specific interest to the current study is the Subadult Virtual Anthropology Database (SVAD) (Stull & Corron, 2022). SVAD is a large digital repository that contains information on skeletal growth, skeletal development, and dental development (and other phenotypic characteristics), on a large, globally diverse sample of children. Thus, contemporary data sources make up for the lack of diverse data sources and the lack of multivariate data that hindered the historic longitudinal data sources.

An important distinction between the historic studies described in Section 3.1 and contemporary virtual approaches such as SVAD is the move away from longitudinal data sources to cross-sectional data sources. Longitudinal studies track the growth and development of individuals over time by taking a series of measurements at different ages (Low, 1970). These studies are best at capturing the pattern of growth in *individual* traits across a subset of the population. In other words, longitudinal growth is best at tracking

the growth of a limited number of traits and individuals. While longitudinal studies are preferred when tracking "normal" levels of childhood growth, they are financially expensive, limited to few traits of study, and not necessarily generalizable to other populations with different growth environments. In comparison, cross-sectional growth, like that captured in SVAD, is representative of a measurement taken at single time points across large sample sizes (Zangirolami-Raimundo, de Oliveira Echeimberg, & Leone, 2018). While not the best at tracking individual growth processes, cross-sectional analyses provide for the ability to make larger population-level comparisons between growth traits and allow for the measurement of innumerable traits at once. For this reason, virtual cross-sectional repositories such as the SVAD provide a unique opportunity to examine *multivariate* traits across large, diverse samples, allowing for comparisons between more traits than a traditional longitudinal study and between more diverse growth environments.

3.3 Multivariate Analyses and Human Growth and Development Traits

With the increasing availability of multivariate data sources comes a move away from traditional univariate approaches concerned with "normal" human growth and development. Instead, large data sources such as SVAD provide a means to investigate the multivariate human growth and development phenotype. Adams and Collyer (2019) explicitly define a multivariate phenotype as a set of "*continuously* measured trait values, which may be correlated with each other." Common multivariate techniques include factor analysis (e.g., Howells, 1951), principal components analysis (e.g., Relethford, Lees, & Byard, 1978), partial least squares analysis (e.g., Mitteroecker, Gunz, Neubauer,

& Muller, 2012), discriminant function analysis and the Generalized Distance (D^2) (e.g., Jantz & Ousley, 2005; Spradley, 2014; Walker, 2008), and some combination of shape analysis using Generalized Procrustes Analysis (GPA) with any of the above techniques (e.g., Slice, 2005). A commonality across each of the above methods is the use of a correlation and/or covariance matrix to distill patterns of (co)variation and/or similarity between groups of data. Further, each analytical approach provides a means to take a high-dimensional data vector and reduce the information to a set of "more meaningful" dimensions that best explain the patterns in the data. Additional approaches beyond the above dimensionality reduction techniques include linear causal models (Bollen, 1989; Pearl, 2000), biological network analysis (Junker, 2008), Bayesian network analysis (Friedman & Koller, 2003), Bayesian structural equation modelling (Kaplan & Depaoli, 2012), and the use of multivariate distributions in Bayesian inference, such as the multivariate Gaussian, multinomial, and Dirichlet distributions. While it may be possible to model a subset of growth and development relationships using any number of the above techniques or to generalize the relationships between traits using a known parametric form, no single technique above can take the complex set of data proposed and return an accurate representation of phenotypic relationships without violating any number of assumptions that may lead to invalid results.

Perhaps the most difficult hurdle in identifying biological relationships between skeletal growth, dental development, and skeletal development is the fact that not all data are measured on a continuous scale. As a result, assumptions related to Euclidean geometry are invalid. Euclidean geometry states that the axes of a multivariate data structure are orthogonal and as a result, more similar phenotypes are closer together in

space and dissimilar phenotypes are farther apart (Adams & Collyer, 2019). This notion of meaningfulness in biological space (Huttegger & Mitteroecker, 2011) and the assumption of Euclidean geometry all underlie the methods highlighted above. However, "meaningfulness" and relationships in Euclidean space are invalid when traits are scored differently as they are with long bone lengths, measured on a continuum and dental development, scored on an ordered-discrete scale. Therefore, to interpret and find biological meaning between growth traits, methods must be derived that account for the mixed nature of the data.

Researchers of chronological age estimation and forensic anthropological practitioners have long applied methods that allow the usage of discrete data types. This task is completed through the assumption that an ordinal trait can be represented as a latent continuous variable using ordinal regression techniques (univariate and multivariate) and either the probit link function (quantile function of the standard Gaussian distribution) or the logit link function (quantile function of the standard logistic distribution) (Kamnikar, Herrmann, & Plemons, 2018; Konigsberg, 2015; Konigsberg, Frankenberg, & Liversidge, 2016; Konigsberg & Hens, 1998; Shackelford, Harris, & Konigsberg, 2012; Stull & Armelli, 2021; Stull et al., 2022). An extension of this work is the ability to combine trait types in the same model using approaches known as multifactorial or multi-indicator models. Such approaches have proved particularly useful in age estimation in forensic contexts. De Tobel and colleagues (2020) show that by incorporating more than one anatomical location (i.e., dental development and skeletal ossification), age estimates were more valid. This coincides with the notion that there are known conditional dependencies between growth traits and that these dependencies

should be accounted for when designing age estimation models (Stull et al., 2021). These dependencies relate back to the discussion in Chapter 2 and corroborate the idea that growth and development traits are integrated both within and between modules.

Only Stull and colleagues (2022) and Milner and colleagues (2020) have devised methods that combine both continuous and discrete data types in the age estimation process. Of these, only Stull and colleagues estimate the age of subadult individuals and accommodate the integration of growth and development traits. Underlying this method is the covariance structure between the individual traits. However, because of the complexity of the statistical model and resulting computational inefficiency, several simplifying assumptions are made about the correlation/covariance structure. Specifically, the model groups or averages correlations across each trait module – i.e., all long bong dimensions are assumed to share the same correlation structure with all dental development scores. Such structure ignores the known within-indicator relationships between homologous limbs or between tooth classes, while simplifying the between-indicator relationships to assume all long bones must be equally correlated or less correlated with certain teeth. To clarify, the model by Stull and colleagues *can* learn the full correlation / covariance structure, but such an approach is impractical in application as it could take months to a year to fully optimize the model. As a result, while Stull and colleague provide the first known method in biological anthropology to combine disparate growth and development trait types, there are still gaps in our knowledge about the true relationship between the multivariate and multifactorial human growth and development phenotype.

3.4 A Way Forward: An Introduction to Copula Modeling

Stull and colleagues (2022) provide the only current method to incorporate the integrated, multivariate, multifactorial human growth and development phenotype in research or practice. However, their method makes several inflexible assumptions related to the structure of the data and is computationally inefficient. Further, at its core, the approach is mainly an age estimation technique – the goal is not to describe the underlying interrelationships between traits, but instead, to use knowledge of said relationships in a practical application. However, to incorporate such traits in practice, a full accounting of the entire integration structure should be completed first. This work introduces a novel statistical technique to biological anthropology known as a copula that provides an explicit method to explore the dependency structure underlying phenotypic traits.

Copulas are statistical models that provide tools for modeling complex relationships between a bivariate or multivariate dataset. The models allow a user to disentangle individual level variation (i.e., individual growth traits) based on each marginal probability distribution, and then capture the dependence between said variables in a second step with a copula function (Smith, 2013). Simply put, copula modeling provides a way to construct *flexible* multivariate probability distributions using each individual marginal distribution and a copula function to piece them together. These models are ubiquitous across several fields where multivariate data types are common including survival analysis (Othus & Li, 2010), actuarial science (Frees & Valdez, 1998; Herath & Herath, 2011), finance (Cherubini, Luciano, & Vecchiato, 2004; Dias &

Embrechts, 2004; Patton, 2009), marketing (Danaher & Smith, 2011), transportation studies (Ma, Luan, Ding, Liu, & Wang, 2019; Ma, Luan, Du, & Yu, 2017), health and medicine (Emura, Nakatochi, Murotani, & Rondeau, 2017; Zhao & Zhou, 2012), and econometrics (Fan & Patton, 2014; Patton, 2002).

The utility of copula models lies in the fact that the marginal distributions can be learned separately from the dependence structure. As a result, a bottom-up approach ensues where the modeler first learns something about each individual marginal distribution or growth trait and that information is bound together with the choice of copula function (Smith, 2013). Compare this with the top-down approach of assuming the data are multivariate Gaussian, which then assumes each marginal distribution must also follow a Gaussian distribution. As a result, copulas provide a flexible and robust means to model multi-indicator or multi-factorial problems, such as that with the human growth and development phenotype.

Copulas were first introduced by Skylar (1959) who showed that for any given series of marginal probability distributions, a joint multivariate probability distribution can be constructed based on a function that ties or links each marginal together. When the marginal distribution is strictly monotonically increasing or continuous in nature, then the copula function can be uniquely retrieved. This is not the case when one or more margins is discrete in nature (Genest & Nešlehová, 2007). As such, contemporary research in copula modeling presents methods to account for either discrete-only data or in mixed cases when there is a combination of discrete and continuous data. Such work focuses on data augmentation of the discrete variable to a latent continuous variable – an

augmentation procedure common across the statistical literature when modeling the relationship between ordinal categories and any number of covariates (Albert & Chib, 1993; Chib & Greenberg, 1998; Smith & Khaled, 2012). Regardless, whether in the strictly continuous case or when a latent continuous variable is introduced, the copula defined above is a well-defined joint distribution function for any parametric copula function (Joe, 1997, 2014; Skylar, 1959). Further it should be noted that the multivariate probit model utilized in chronological age estimation (Konigsberg, 2015) is a special case of a Gaussian copula with univariate probit marginals. Therefore, the approach put forth in this study is an extension of previous approaches in biological anthropology to mixed data applications.

A copula estimates two sets of parameters: those for each univariate marginal distribution coinciding with each column of the data (e.g., Gaussian, Beta, Gamma, Poisson, etc.), and those associated with the copula dependency term that relates each marginal distribution together. Specifics of this process are described in Chapter 5. Importantly, there are a myriad of parametric copula functions in the literature (Joe, 1997, 2014; Nelsen, 2006; Nelsen, 2005). While there are mathematical differences between each function, key differences lie in how the copula function defines the dependency structure between cumulative distribution functions of variables. Here dependence is defined simply as the association between variables. In general, while the structure for the dataset is learned jointly, dependence is presented as pairwise or bivariate measures between two traits or indicators. The two most popular measures are Kendall's τ and Spearman's ρ – both measures of rank correlations and the measuring of monotonic (unidirectional) relationships in the data. Another common dependence measure is that of

Pearson's product-moment correlation coefficient which measures the linear relationships between a set of variables (Joe, 2014; Smith, 2013; Song, 2000). For ease of interpretation, the current study has chosen an elliptical copula in the form of a Gaussian copula to bind together Gaussian marginals for each data type. As a result, the dependency term is presented as Pearson's *r* or a correlation coefficient. In the elliptical copula setting, Pearson's *r* and Spearman's ρ are similar and Kendall's τ is positively related to both terms (Song, 2000).

Traditional approaches to estimating the dependency parameter and individual marginal distribution parameters tend to rely on both maximum likelihood estimation (Joe, 2014; Nelsen, 2005) and methods of moments estimators (Genest & Rivest, 1993). While these approaches work well in low-dimensional settings with primarily continuous data, they are less efficient and valid in high dimensional settings or when discrete data are included (Smith & Khaled, 2012). For this reason, Bayesian data techniques are put forth as an alternative to maximum likelihood techniques. Smith and Khaled (2012) and Smith (2013) both demonstrate the applicability of Bayesian techniques and Markov Chain Monte Carlo sampling procedures in estimating the parameters of the marginal distribution and the copula function. Further, Bayesian data analysis provides a straightforward method to model missing data (an unavoidable occurrence in biological growth data) and to augment discrete data with latent continuous variables (Albert & Chib, 1993; Chib & Greenberg, 1998; Gelman, Carlin, Stern, & Rubin, 1995; Pitt, Chan, & Kohn, 2006).

In summary, each growth indicator is part of a larger multivariate data structure with inherent dependencies that must be accounted for either when making an inference related to phenotypic integration or when designing models that use traits in the estimation of chronological age. While multivariate methods are common across biological anthropology, no method has yet to account for the complexities inherent to biological growth data including mixed data types, heteroskedasticity with age, missing data, and the conditional dependence and relationships between *all* traits. The research presented below utilizes a Bayesian approach to bind together individual growth traits in a Gaussian copula whose dependency term is a correlation matrix describing the overall linear relationships between each variable. As a result, this study represents a novel approach in analyzing human phenotypic variation and integration across a common set of growth indicators used across biological anthropology.

Chapter 4 – Materials

All materials derive from the Subadult Virtual Anthropology Database (SVAD), which is a repository of phenotypic traits from contemporary (2010 – 2019) subadult (0 – 22 years old) individuals from around the world (N = 4,891) (Stull & Corron, 2022). The repository is composed of data collected from skeletal remains and medical imaging technologies, as well as associated demographic information (chronological age, biological sex). Available phenotypic derivatives from SVAD include: 1) skeletal and dental growth and development indicators, including diaphyseal dimensions, epiphyseal fusion stages, and dental development stages, 2) vertebral neural canal measurements, 3) craniometric landmarks, 4) cranial morphoscopic traits, and 5) metric and non-metric dental traits. The multivariate phenotype described in the current study focuses on a subset of the phenotypic derivatives in SVAD, which are the skeletal and dental growth and development indicators (M = 54). These indicators include diaphyseal dimensions (m = 18), skeletal fusion and ossification scores (m = 20), and dental development scores (m = 16). Information about each indicator is provided below and protocols about the collection of the data can be found at Stull and Corron (2021). Table 4.1 describes each variable abbreviation, name, and data type. Because of the inconsistent availability of the 54 growth traits across the entire SVAD repository, the United States (US) sample is chosen in this study to provide the largest sample size with the most complete set of traits (n = 1,316).

Table 4.1. SVAD abbreviations, variable names, and data types for all m = 54 indicators. If ordinal, the scoring system is also included. The column on the far left dental development scores, the middle columns show fusion and ossification scores, and the far right columns are long bone measurements.

SVAD Abbreviation	Variable Name	Data Type	SVAD Abbreviation	Variable Name	Data Type	SVAD Abbreviation	Variable Name	Data Type
max_M1_L	Maxillary M1	Ordinal (1-13)	FLT_EF_L	Femoral Lesser Trochanter	Ordinal (1-7)	FDL_L	Femur Diaphyseal Length	Continuous
max_M2_L	Maxillary M2	Ordinal (1-13)	FDE_EF_L	Femur Distal Epiphysis	Ordinal (1-7)	FMSB_L	Femur Midshaft Breadth	Continuous
max_M3_L	Maxillary M3	Ordinal (1-13)	TPE_EF_L	Tibia Proximal Epiphysis	Ordinal (1-7)	FDB_L	Femur Distal Breadth	Continuous
max_PM1_L	Maxillary PM1	Ordinal (1-13)	TDE_EF_L	Tibia Distal Epiphysis	Ordinal (1-7)	TDL_L	Tibia Diaphyseal Length	Continuous
max_PM2_L	Maxillary PM2	Ordinal (1-13)	FBPE_EF_L	Fibula Proximal Epiphysis	Ordinal (1-7)	TPB_L	Tibia Proximal Breadth	Continuous
max_C_L	Maxillary Canine	Ordinal (1-13)	FBDE_EF_L	Fibula Distal Epiphysis	Ordinal (1-7)	TMSB_L	Tibia Midshaft Breadth	Continuous
max_I1_L	Maxillary I1	Ordinal (1-13)	HPE_EF_L	Humerus Proximal Epiphysis	Ordinal (1-7)	TDB_L	Tibia Distal Breadth	Continuous
max_I2_L	Maxillary I2	Ordinal (1-13)	HDE_EF_L	Humerus Distal Epiphysis	Ordinal (1-7)	FBDL_L	Fibula Diaphyseal Length	Continuous
man_M1_L	Mandibular M1	Ordinal (1-13)	HME_EF_L	Humerus Medial Epicondyle	Ordinal (1-7)	HDL_L	Humerus Diaphyseal Length	Continuous
man_M2_L	Mandibular M2	Ordinal (1-13)	RPE_EF_L	Radius Proximal Epiphysis	Ordinal (1-7)	HPB_L	Humerus Proximal Breadth	Continuous
man_M3_L	Mandibular M3	Ordinal (1-13)	RDE_EF_L	Radius Distal Epiphysis	Ordinal (1-7)	HMSB_L	Humerus Midshaft Breadth	Continuous
man_PM1_L	Mandibular PM1	Ordinal (1-13)	UPE_EF_L	Ulna Proximal Epiphysis	Ordinal (1-7)	HDB_L	Humerus Distal Breadth	Continuous
man_PM2_L	Mandibular PM2	Ordinal (1-13)	UDE_EF_L	Ulna Distal Epiphysis	Ordinal (1-7)	RDL_L	Radius Diaphyseal Length	Continuous
man_C_L	Mandibular Canine	Ordinal (1-13)	CT_EF_L	Calcaneal Tuberosity	Ordinal (1-7)	RPB_L	Radius Proximal Breadth	Continuous
man_I1_L	Mandibular I1	Ordinal (1-13)	CC_Oss	Carpal Count	Ordinal (1-9)	RMSB_L	Radius Midshaft Breadth	Continuous
man_I2_L	Mandibular I2	Ordinal (1-13)	TC_Oss	Tarsal Count	Ordinal (1-8)	RDB_L	Radius Distal Breadth	Continuous
FH_EF_L	Femoral Head	Ordinal (1-7)	ISPR_EF_L	Ischio-Pubic Ramus	Ordinal (1-3)	UDL_L	Ulna Diaphyseal Length	Continuous
FGT_EF_L	Femoral Greater Trochanter	Ordinal (1-7)	ILIS_EF_L	Iliac-Ischio Fusion	Ordinal (1-3)	UMSB_L	Ulna Midshaft Breadth	Continuous

4.1 Sample Information

The US sample derives from a medico-legal context from two institutions: 1) the Office of the Chief Medical Examiner, Baltimore, Maryland (OCME, *n* = 244), and 2) the University of New Mexico Health Sciences Center, Office of the Medical Investigator, Albuquerque, New Mexico (UNM, *n* = 1072). The UNM and OCME sample are pooled for the analyses, resulting in a total sample size of *n* = 1,316, which is comprised of slightly more males (n=783) than females (n= 583) (Figure 4.1).

All indicators are collected from post-mortem full-body CT scans at each institution from individuals aged 0 – 21 years old, which is primarily why the US has the largest sample of growth and development data. The images from both samples were generated between 2011 to 2018 – suggesting that the birth dates for all individuals would range from the mid-1990s up until 2018. The OCME data was generated with a General Electric (GE) Light Speed RT-16-slice multi-detector scanner, and slice thickness is specified at 0.625 mm for the skull and 1.25 mm for the postcrania. UNM data were generated with a Phillips Brilliance Big Bore 16-slice multi-detector scanner, with a 512 x 512 image matrix, 0.5 mm slice thickness and 1 mm overlap. Further, the individuals from UNM are part of the New Mexico Decedent Image Database (NMDID) with additional information provided at https://nmdid.unm.edu/ (Berry & Edgar, 2017).

All data associated with SVAD was funded by the National Institute of Justice Awards 2015-DN-BX-K409 and National Science Foundation BCS-1551913. All data types were collected either on a series of segmented virtual bones surfaces (diaphyseal dimensions) or directly from CT slices (dental development and skeletal fusion /

ossification) based on standardized protocols within the Amira™ (Amira™ v.6.5.0, Thermo Fisher Scientific, Waltham, MA, USA) image visualization software (Stock et al., 2020; Stull & Corron, 2021b, 2021a). The standardized protocol (Stull & Corron, 2021b) and associated measurements (Stull & Corron, 2021) are openly available at https://zenodo.org/communities/svad/.

The demographic profile of the sample separated according to biological sex and chronological age is described in Figure 4.1. Because the period of human growth and development is dynamic and variable across individuals within a population, the data are explored at numerous grouping levels to capture the possibility of nuanced differences within the United States sample. This includes subsetting the data by biological sex (males n =783; females n = 583) and developmental stage (infancy, childhood, juvenile + adolescence) (Table 4.2). The developmental stages correspond to known life history periods used across biological anthropology but are subset based on the age of an individual and not broader markers of maturation, such as peak height velocity, age at menarche, or weaning age (Bogin, 1999; Bogin & Smith, 1996; Cameron & Bogin, 2012). Furthermore, the juvenile and adolescence stages are collapsed in order to increase data availability across older age individuals.

Table 4.2. Count of individuals (pooled sex) across each developmental stage.

Developmental Stage	Age Range (years)	Count
Infancy	0 - 2.99	426
Childhood	3.0 - 6.99	128
Juvenile + Adolescence	7.0 - 21.0	762

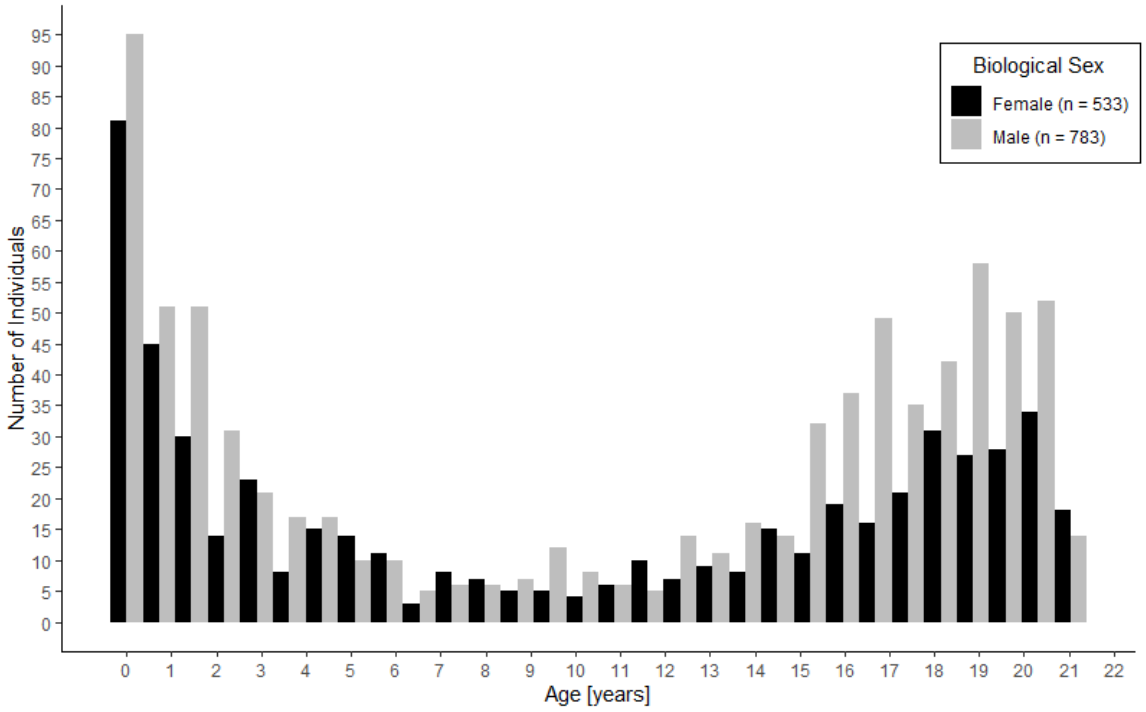

Figure 4.1. Age and Biological Sex Distribution of the study sample.

4.2 Indicator-Specific Information

4.2.1 Diaphyseal Dimensions

The current study utilizes 18 continuous diaphyseal length and breadth measurements of the six long bones (femur, tibia, fibula, humerus, radius, and ulna) collected for each individual and measured on segmented bone surfaces (Figure 4.2). Measurements were collected per definitions described in Stull, L'Abbe, & Ousley (2014), which are based on previous definitions from Fazekas & Kosa (1978) and Moore-Jansen, Ousley, & Jantz (1994). Left-sided elements are included in the current study with right antimeres used if the left is missing or damaged. Length measurements are only taken on unfused diaphyseal elements; therefore, after approximately 13 years of

age (element dependent), most diaphyseal metrics are unavailable as the element has completed growth. The age and percentage of data available is dependent on the element – for example, the earlier fusion of the distal humerus leads to less data availability for younger individuals compared to the femur. In contrast, breadth measurements are available as these were able to be collected until complete fusion commenced. Previous studies demonstrate the high precision, accuracy, repeatability, and reproducibility of measurements collected on virtually reconstructed skeletal elements (Colman, Dobbe, Stull, & Ruijter, 2017; Colman et al., 2019; Corron, Condemi, & Chaumoitre, 2017; Stull, Tise, Ali, & Fowler, 2014). Observer error and agreement for all long bones corroborate the validity and repeatability of all measurements with all technical error of measurement (TEM) and relative TEM (%TEM) metrics available at Stull & Corron (2021b).

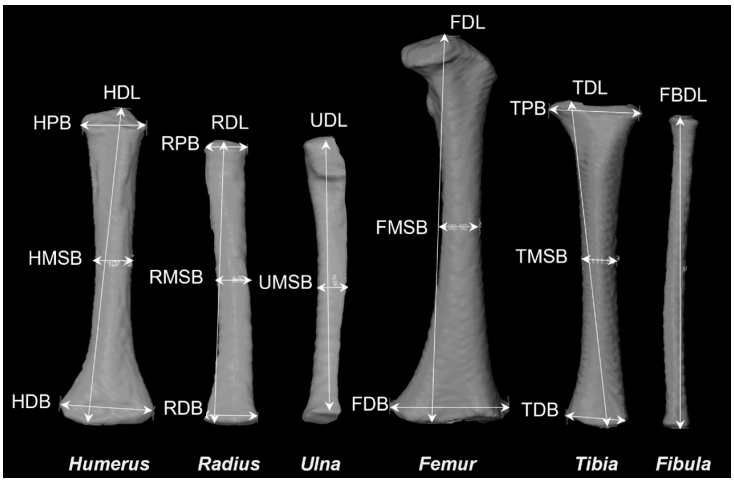

Figure 4.2. Diaphyseal dimensions utilized in the current study. Image adapted from Stull & Corron (2022).

4.2.2 Dental Development

Within SVAD, dental development was collected for all 32 permanent teeth following AlQahtani, Hector, & Liversidge (2010) (Table 4.3). AlQahtani and colleagues'

13-stage system is a revision of the original Moorrees, Fanning, & Hunt, (1963) mineralization stages for mono- and pluri-radicular teeth. Data were scored on an ordinal scale (1-13) based on a numeric adaptation of the original stage names from the publication (Table 4.3). Note, in all analyses stages 12 and 13 are collapsed because of the difficulty in ascertaining apex width / closure on CT scans. The current study utilizes only left-sided maxillary and mandibular dentition, including upper and lower first, second, and third molars, canines, first and second premolars, and first and second incisors (m = 16). Teeth were scored directly from CT slices within Amira™. Recent work demonstrates high inter- and intra-observer agreement across dental development data collected from CT scans and in comparison to dry-bone and radiographic modalities (Corron et al., 2021).

4.2.3 Skeletal Fusion and Ossification

Epiphyseal fusion stages for proximal and distal long bone epiphyses, the calcaneal tuberosity, the ischiopubic ramus, the ilium and ischium, ossification of the patella, and ossification of the carpals and tarsals were given ordinal scores based on stage of development on left-sided elements. Three different staging systems were employed: a seven-stage system was used of the long bone epiphyses and the calcaneal tuberosity, a three-stage system was used for pelvic epiphyses, tarsals and carpals were scored based on the number ossified (eight or nine, respectively), and binary absent / present was used for individual elements of the humeral epiphyses and the patella. Because previous research demonstrates the overall lack of information associated with

binary variables in human growth and development (Stull, Corron, & Price, 2021), only polychotomous variables (> 2 stages) are included in the present analyses (Figure 4.3). This includes 16 variables of epiphyseal fusion from long bones, two variables of pelvic epiphyseal fusion, and two ossification variables from the carpals and tarsals, for a total of $m = 20$ skeletal fusion and ossification variables. All variables were scored by scrolling through individual CT slices on Amira™. Recent work demonstrates high inter- and intra-observer agreement across skeletal fusion and ossification data collected from CT scans and in comparison to dry-bone and radiographic modalities (Corron et al., 2021).

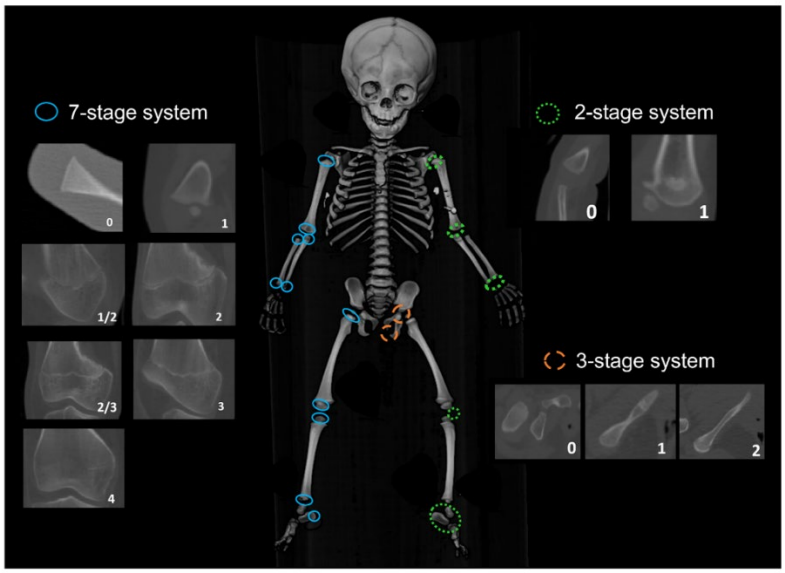

Figure 4.3. Three staging systems used to skeletal fusion and ossification. Fusion of long bone epiphyses and the calcaneal tuberosity is 7-stages, pelvic fusion is 3-stages, and individual carpals or tarsals are translated from single binary elements to a total count of number present. Note, binary ossification centers associated with the humerus are not included. Image adapted from Stull & Corron (2022).

Table 4.3. Stages used to score development of the permanent dentition.

Stage	Description
1	Initial cusp formation
2	Coalescence of cusps
3	Cusp outline complete
4	Crown half completed with dentine formation
5	Crown three-quarters completed
6	Crown completed with defined pulp root
7	Initial root formation with divergent edges
8	Root length less than crown length
9	Root length equals crown length
10	Three-quarters of root length developed with divergent ends
11	Root length completed with parallel ends
12	Apex closed (root ends converge) with wide periodontal ligament
13	Apex closed with normal periodontal ligament width

Note, stages 12 and 13 are collapsed in analyses.

Chapter 5 – Methodology

The purpose of this dissertation is to apply a novel statistical method that quantifies the complex, multivariate relationships among human growth and development traits. The observed traits derive from n = 1,316 individuals from the US sample within the SVAD repository. Each individual is made up of a multivariate data vector of length M = 54 traits with a mixture of continuous and discrete responses. To determine the relationship between traits a statistical approach known as a Gaussian copula is fit to the data. A copula is chosen because of its capability to model the mixed data structure in the current study. Further, the copula is selected to be Gaussian because of its intuitive dependency parameter in the form of a correlation matrix. The correlation matrix is conditional upon an individual's chronological age. Continuous response variables are assumed to follow a Gaussian distribution with both a mean and standard deviation conditional on an individual's age. The resulting copula samples from a continuous variable follow a standard Gaussian distribution with each response standardized by subtracting the mean from the observed value and dividing by the standard deviation. Ordinal responses are augmented via the probit link function to a latent continuous value. The model is fit using Bayesian inference with the Hamiltonian Monte Carlo sampling algorithm within the Stan programming environment (Stan Development Team, 2022). Bayesian techniques provide robust quantification of uncertainty, principled approaches to missing data, and tractable solutions to copulas with mixed data types (Smith, 2013).

In total, six Gaussian copula models are fit to subsets of the data. First, the full dataset is fit to model the dependency structure underlying all of ontogeny. Next, the

dependency structure is analyzed across ontogeny with three separate models fit to the infancy stage (0-2.99 years old), childhood stage (3-6.99 years old), and the juvenile-adolescence stage (7-21 years of age). Last, sex-specific models are fit to the entire age range (0-21 years old) for both biological males and biological females. Combined, the results facilitate the interpretation of the dependency structure across ontogeny, between the sexes, and when considering the entire / full dataset. The results are presented based on a series of bivariate relationships to allow for ease of interpretation. Therefore, all results in the present study focus on the dependence structure or the bivariate relationships between all traits described on the scale -1 to 1. Because the model learns the structure across 54 growth traits, this leads to a total of 1,431 unique bivariate relationships.

The remainder of this chapter provides the statistical definitions of copulas, the Gaussian copula, and specifies the exact statistical model in the current study: a mixed discrete-continuous Gaussian copula. At the end, I specify the model construction in Stan and describe relevant parameters related to prior choice, missing data specification, and data augmentation in the discrete case. Last, I present how results are obtained within a copula setting and discuss model checking and validation.

5.1 Copula Framework

A copula is a specification of a multivariate joint distribution of random variables where each marginal distribution u is uniformly distributed [0,1]. An M-dimensional copula $C(\boldsymbol{u}) = C(u_1, \dots, u_m)$ for $u \in (0,1)^M$ is the cumulative distribution function

(cdf) over the *M*-dimensional unit cube $(0, 1)^M$ with standard uniform marginals [0, 1]. Following Skylar (1959), I define a joint cumulative distribution function *F* with marginal distribution functions $F_1, \dots, F_M$ as:

$$F(\boldsymbol{y}) = C(F_1(y_1), \dots, F_M(y_M)). \quad (1)$$

Here, *F* is the joint cdf of $(y_1, \dots, y_M)$ with marginal cdfs $(F_1, \dots, F_M)$. Simply, a copula is a function that links a multivariate distribution function to each of its one-dimensional marginal distribution functions (Nelsen, 2005). When the marginal distribution is strictly monotonically increasing or continuous in nature, then the copula *C* can be uniquely retrieved. This is not the case when one or more margins is discrete in nature (Genest & Nešlehová, 2007). As such, contemporary research in copula modeling presents methods to account for either discrete-only data or mixed data, when there is a combination of discrete and continuous data. Such work focuses on data augmentation of the discrete variable to a latent continuous variable – an augmentation procedure common across the statistical literature when modeling the relationship between ordinal categories and any number of covariates (Albert & Chib, 1993; Chib & Greenberg, 1998; Smith & Khaled, 2012). Regardless, whether in the strictly continuous case or when a latent continuous variable is introduced, the copula defined in equation 1 is a well-defined cumulative distribution function *F* for any parametric copula function *C* (Joe, 1997, 2014; Skylar, 1959).

Much like traditional parametric modeling, the user defines both the copula function that parameterizes the multivariate distribution as well as the associated

marginal distributions that are linked within the copula function. The uniformly distributed marginals described above are achieved by applying the probability integral transform to each individual marginal distribution. For example, the user may define a single marginal distribution to be distributed standard Gaussian $N(0,1)$ and by the probability integral transform, this can be represented as $U(0,1)$. The choice of individual marginal distributions in the current study are described below. There are numerous types of copulas currently defined in the literature. Differences between types of copula functions manifest in the characterization of the dependence structure underlying the data (Joe, 2014).

5.2 Gaussian Copula Framework

This dissertation utilizes a Gaussian copula with the dependency structure parameterized as a correlation matrix $\boldsymbol{R}$. Historically, studies of integration and interrelationship between traits relied upon linear correlations and/or covariances to measure the strength and direction of relationships. The Gaussian copula provides a flexible alternative to previous integration analyses with less statistical assumptions and the ability to capture valid relationships between mixed data types. A Gaussian copula is constructed from the multivariate Gaussian distribution:

$$C_R^G(\boldsymbol{u}) = \phi_{\boldsymbol{R}}\left(\phi^{-1}(u_1), \dots, \phi^{-1}(u_M)\right), \quad (2)$$

where $\boldsymbol{R}$ is a correlation matrix, ϕ_R is the cdf of $N_M(\mathbf{0}, \boldsymbol{R})$, the M-dimensional multivariate Gaussian distribution with mean 0 and covariance matrix **R**, u_m is each individual marginal cdf, and ϕ and ϕ^{-1} are the cdf and inverse cdf of the standard Gaussian distribution $N(0,1)$, respectively.

The vector of discrete and/or continuous responses is defined as $\boldsymbol{y} = [y_1, \dots, y_M]$ where M = 54. Each can be defined by a marginal distribution F_m. Assuming each marginal distribution can be linked based on a Gaussian copula function, I write the joint cumulative distribution of $\boldsymbol{y}$ as follows:

$$\begin{aligned} F(y_1, \dots, y_M) &= C_{\boldsymbol{R}}^{G}\left(F_1(y_1), \dots, F_M(y_M)\right) \\ &= \phi_{\boldsymbol{R}}\left(\phi^{-1}\left(F_1(y_1)\right), \dots, \phi^{-1}\left(F_M(y_M)\right)\right). \end{aligned} \tag{3}$$

Each marginal can be further decomposed to $z_m = \phi^{-1}(F_m(y_m))$ where $\boldsymbol{z} = (z_1, \dots, z_M)$ are the transformed set of observations following the probability integral transform (and resulting inverse). Taking the derivative of each side with respect to each z yields

$$\begin{aligned} f(y_1, \dots, y_M) &= \left[\phi_R(z_1, \dots, z_M) / \prod_{m=1}^{M} \phi(z_m)\right] \prod_{m=1}^{M} f_m(y_m) \\ &= \frac{1}{\sqrt{|R|}} \exp\left[-\frac{1}{2}\boldsymbol{z}(R^{-1} - I)\boldsymbol{z}'\right] \prod_{m=1}^{M} f_m(y_m). \end{aligned} \tag{4}$$

In equation 4, f is the joint probability density function (pdf) of $\boldsymbol{y}$, $\phi_{\boldsymbol{R}}$ is the pdf of a multivariate Gaussian distribution $N_M(\mathbf{0}, \boldsymbol{R})$, ϕ is the pdf of a standard Gaussian

distribution $N(0,1)$, and f_m is each marginal pdf parameterizing each individual growth indicator (Park, Oh, Ahn, & Oh, 2021). The exponential function described in equation 4 says that the joint pdf of $\boldsymbol{y}$ can be decomposed into a term related to the dependence $\boldsymbol{R}$ and terms associated with each individual marginal distribution.

5.3 The Mixed Discrete Continuous Gaussian Copula

Let $y_i = (y_i^{\{1\}}, y_i^{\{2\}}, \dots, y_i^{\{M\}})$ denote a multivariate observation consisting of *M* growth indicators for individual *i* ($i = 1, \dots, N$). The superscript $y^{\{m\}}$ denotes the m-th response variable. *M* can be further reduced to *J* continuous observations and *K* ordinal observations where $M = J + K$. To be more precise, the marginal cdf of $y^{\{m\}}$ is given by $F^{\{m\}}(y^{\{m\}};\ \boldsymbol{\theta}^{\{m\}}, x)$, where $\boldsymbol{\theta}^{\{m\}}$ is a parameter vector associated with each $F^{\{m\}}$, $y^{\{m\}}$ is either a continuous or ordinal response variable, and *x* is an individual's chronological age. The full cumulative distribution of **y** is

$$F_{\boldsymbol{Y}}\left(y^{\{m\}};\ \boldsymbol{\theta}^{\{m\}}, x, \boldsymbol{R}\right) = \phi_{\boldsymbol{R}}\left(\phi^{-1}\left(F^{\{1\}}\left(y^{\{1\}};\ \boldsymbol{\theta}^{\{1\}}, x\right)\right), \dots, \phi^{-1}\left(F^{\{m\}}\left(y^{\{m\}};\ \boldsymbol{\theta}^{\{m\}}, x\right)\right)\right). \quad (5)$$

5.3.1 Continuous Marginal Distribution

Let x_i be a scalar independent variable (chronological age) and let $y_i^{\{j\}}$ be an observed scalar response for each *j* continuous variable (*J = 18*). $y_i^{\{j\}}$ is distributed as univariate Gaussian distribution with mean $\mu_i^{\{j\}}$ and standard deviation $\sigma_i^{\{j\}}$ that are both

conditional upon an individual's chronological age x_i. This can be specified as $y_i^{\{j\}} \sim normal(\mu_i^{\{j\}}, \sigma_i^{\{j\}})$. The mean and standard deviation are specified as a function of x_i with $\mu_i^{\{j\}} = a^{\{j\}} x_i^{r^{\{j\}}} + b^{\{j\}}$ and $\sigma_i^{\{j\}} = \kappa_1^{\{j\}}[1 + \kappa_2^{\{j\}}]$ where each parameter are part of the Bayesian fit. In the mean function, *a* is a constant that defines the magnitude of the response variable, *r* is the exponent determining the scaling relationship, and *b* is an offset determining the location of the curve on the y-axis. The noise function suggests a heteroskedastic relationship where the standard deviation changes as a linear function of x_i. Stull and colleagues (2022) demonstrate the validity and fit of the above mean and standard deviation functions when applied to scalar human growth and development data. Further, preliminary testing of additional mathematical growth models corroborated the fit of the above specifications as compared to related parametric functions (Lampl, 2012). Following transformation in the copula (See equations 3 and 4), the random variable associated with scalar valued response data can be precisely written as $z^{\{j\}} \sim normal(0,1)$. Here, $z^{\{j\}} = \phi^{-1}(F^{\{j\}}(y^{\{j\}}))$ where each value is the inverse of the cdf of the standard Gaussian distribution. To be precise, $z^{\{j\}}$ is a scalar value distributed as a standard Gaussian distribution, while **z** is a vector of the multivariate copula function $\boldsymbol{z} \sim N(0, \boldsymbol{R})$, where **R** is the correlation matrix. This standardization occurs in the Bayesian model by subtracting the conditional mean $\mu_i^{\{j\}}$ and dividing by the conditional standard deviation $\sigma_i^{\{j\}}$. Steps associated with parameterizing the continuous marginal distributions include:

1. Calculate mean μ_i^j and standard deviation σ_i^j conditional on age x_i

2. Standardize each individual response where $\widehat{z_i^j} = \frac{\left(y_i^j - \mu_i^j\right)}{\sigma_i^j}$.

5.3.2 Ordered Probit Marginal Distribution

Let x_i be a scalar independent variable (chronological age) and let $y_i^{\{k\}}$ be an observed discrete response for each *k* ordinal variable (*K* = 36) of either dental development or skeletal fusion and ossification. The superscript $y^{\{k\}}$ relates to the k-th ordinal response variable. Considering previous research, the discrete-valued responses are augmented based on the latent variable transformation that is a scalar value distributed as a standard Gaussian distribution with a mean of $\eta_i^{\{k\}}$ and standard deviation of 1 via the probit link function or the cdf of the standard Gaussian distribution. The latent continuous response $v_i^{\{k\}}$ can be expressed as $v_i^{\{k\}} \sim N(\eta_i^{\{k\}}, 1)$. The truncation results from the presence of *T* ordered boundary parameters or thresholds where $t = 1, 2, \ldots, T$, make up the thresholds between ordinal categories *C*. Thresholds *t* define the boundary between two different ordinal categories and as such, the number of thresholds per ordinal variable is *C – 1*. For example, if there are 13 total ordinal categories, there are 12 threshold parameters. Given the data collection described above for dental development and skeletal fusion and ossification, there are five different ordinal category classifications where *C* = 12 categories for dental development (*k = 16*), $C = 7$ categories for epiphyseal fusion (*k = 16*), $C = 3$ categories for pelvic fusion (*k = 2*), *C* $= 9$ categories for carpal ossification and count (*k = 1*), and $C = 8$ categories for tarsal ossification and count (*k = 1*).

The relationship between the observed response variable $y_i^{\{k\}}$ and latent response variable $v_i^{\{k\}}$ can be expressed as follows:

$$p(v_i^{\{k\}}|\eta_i^{\{k\}}, t^{\{k\}}) = \begin{cases} 1 - \phi\left(\eta_i^{\{k\}} - t_1^{\{k\}}\right) & if\ c = 1, \\ \phi\left(\eta_i^{\{k\}} - t_{c-1}^{\{k\}}\right) - \phi\left(\eta_i^{\{k\}} - t_c^{\{k\}}\right) & if\ 1 < c < C, \\ \phi\left(\eta_i^{\{k\}} - t_{C-1}^{\{k\}}\right) & if\ c = C. \end{cases} \quad (6)$$

This expression can be found at https://mc-stan.org/docs/functions-reference/ordered-probit-distribution.html. Above, $\phi(\cdot)$ is the cdf for the standard Gaussian distribution with a mean of 0 and standard deviation of 1, t is the ordered vector of threshold parameters, and η is the conditional mean function specifying the relationship between age and latent response $\eta_i^{\{k\}} = a^{\{k\}}x_i$, where a defines the slope of the linear relationship between age and latent response. Because of identifiability concerns, the standard deviation is held constant. Note, a final component of the model construction (see Appendix) is the inclusion of an additional nuisance parameter $u_i^{\{k\}}$, a standard uniform variate that accounts for the inequality constraints resulting from the augmentation $y_i^{\{k\}} \Rightarrow v_i^{\{k\}}$.

5.3.3 Missing Data Specification

The model presented here allows for missing values across all scalar and discrete-valued responses. In both cases, missing values are incorporated as an additional random

variable that the model learns as a component of each marginal predictive distribution. In the scalar response, I introduce an additional parameter *ymiss* into the model and fill in all missing values with this parameter. As such, the missing data is learned alongside the parameters associated with the mean and noise functions. In the discrete setting, the nuisance parameter *u* described in Section 5.3.2 is utilized much in the same way as *ymiss*. That is, the missing data is again learned as an additional parameter in the model. However, because missing discrete data are unconstrained (either lower or upper bounded) the latent variable *v* is defined as $\phi(u_i^{\{k\}})$ where $u_i^{\{k\}}$ is standard uniform with a density of 1. This approach is described in detail in Goodrich (2017). See Appendix 1 for a description of this step in the Stan model.

5.3.4 Full Mixed Model

The joint cdf of the multivariate vector of growth outcomes $\boldsymbol{y}$ can be generalized as follows:

$$F_{\boldsymbol{Y}}(\boldsymbol{y}, \boldsymbol{v};\ \boldsymbol{\theta}^{\{J\}}, \boldsymbol{\theta}^{\{K\}}, \boldsymbol{R}, x) = \ \phi_{\boldsymbol{R}}\left(\phi^{-1}\left[F^{\{J\}}\left(\boldsymbol{y}^{\{J\}};\ \boldsymbol{\theta}^{\{J\}}, x\right)\right], \phi^{-1}\left[F^{\{K\}}\left(\boldsymbol{v}^{\{K\}};\ \boldsymbol{\theta}^{\{K\}}, x\right)\right]\right), \quad (7)$$

where **y** is a scalar response vector, $\boldsymbol{\nu}$ is a latent continuous variable resulting from the transform $y_i^{\{K\}} \ \Rightarrow \ v_i^{\{K\}}$ associated with the discrete-valued response, $\boldsymbol{\theta}^{\{J\}}$ is a parameter vector associated with all continuous response variable, $\boldsymbol{\theta}^{\{K\}}$ is a parameter vector associated with all latent continuous variable, $\boldsymbol{R}$ is a symmetric positive semidefinite

correlation matrix specifying the dependency structure, and *x* is chronological age. The full parameterization of the continuous marginals is

$\boldsymbol{\theta}^{\{J\}} = [a^{\{J\}}\ r^{\{J\}}\ b^{\{J\}}\ \kappa_1^{\{J\}}\ \kappa_2^{\{J\}}\ ymiss_l^{\{J\}}]^T$. *a*, *r*, and *b* parameterize the mean function, κ_1 and κ_2 parameterize the noise function, and *ymiss* is the missing data parameter. The subscript *l* associated with each *ymiss* references individual missing elements where $l = 1, \ldots, L$. The length of L varies depending on each response $y^{\{J\}}$. The full parameterization of the ordinal marginals is $\boldsymbol{\theta}^{\{K\}} = [a^{\{K\}}\ \boldsymbol{t}^{\{K\}}\ \boldsymbol{u}^{\{K\}}]^T$. *a* parameterizes the mean function, *t* is an ordered vector parameter representing the thresholds between each ordinal category, and $\boldsymbol{u}$ are standard uniform variates the same size of the ordinal data (*N x K*) introduced to alleviate inequality constraints and help with parameterizing missing ordinal data. Finally, the full parameterization of the joint model is $F_{\boldsymbol{Y}} = [a^{\{J\}}\ r^{\{J\}}\ b^{\{J\}}\ \kappa_1^{\{J\}}\ \kappa_2^{\{J\}}\ ymiss_l^{\{J\}}\ a^{\{K\}}\ \boldsymbol{t}^{\{K\}}\ \boldsymbol{u}^{\{K\}}\ \boldsymbol{R}]^T$ where $\boldsymbol{R}$ is the copula parameter defining the dependency structure between the marginal cdfs.

The correlation matrix $\boldsymbol{R}$ can be defined as follows:

$$\boldsymbol{R} = \begin{pmatrix} 1 & r_{12} & \cdots & r_{14} \\ r_{12} & 1 & \cdots & r_{24} \\ \vdots & \vdots & \ddots & \vdots \\ r_{14} & r_{24} & \cdots & 1 \end{pmatrix}, \quad (8)$$

where r_{12} is the correlation coefficient between variable 1 and variable 2. Because the outcomes of the model are based on Gaussian marginal distributions, r is the Pearson correlation between pairs of traits Y_{ij}. Here, r_{12} is a value along the interval -1 to 1, with values closer to 1 strongly positively correlated and values closer to -1 strongly

negatively correlated. Values near 0 suggest weak dependence between each bivariate relationship. This can be generalized as

$$r_{12} = corr\left[\phi^{-1}\left\{F^{\{1\}}\left(y^{\{1\}}\right)\right\}, \phi^{-1}\left\{F^{\{2\}}\left(y^{\{2\}}\right)\right\}\right] \stackrel{\text{def}}{=} r(y^{\{1\}}, y^{\{2\}}). \quad (9)$$

For numerical stability, modeling efficiency, and the assurance of positive semi-definiteness, the $M \times M$ correlation matrix R undergoes Cholesky factorization to an $M \times M$ lower triangle matrix L with positive diagonal elements such that $R = LL^T$. To recover the posterior distribution of each correlation term, I compute the product of the lower triangle portion L times its own transpose as a generated quantity in the model.

5.3.5 Prior Specification

Bayesian statistics require prior specification for all unknown parameters in the model. I assume a generic weakly informative standard Gaussian prior $N(0,1)$ for all parameters associated with the mean and noise functions across each data type $\left(a^{\{j\}}\ r^{\{j\}}\ b^{\{j\}}\ \kappa_1^{\{j\}}\ \kappa_2^{\{j\}}\ a^{\{k\}}\right)$. This assumption coincides with the scale and magnitude associated with the standard Gaussian marginal distribution for continuous data and the ordered probit marginal distribution associated with the latent continuous data that augments each ordinal trait. Except for the offset parameter *b*, each of the above parameters is constrained to be positive (> 0) – this is akin to defining the prior on each parameter as a half-normal distribution with support on $x \in [0, \infty)$. The assumption of positivity on each parameter is reinforced by two notions: 1) growth is always positive,

and 2) growth is monotonically increasing until final size / development is reached. The offset b is left unconstrained to allow variability in where the growth "curve" falls along the y-axis.

Each ordinal variable k with $C^{\{k\}}$ ordered categories is defined by threshold parameters $t^{\{k\}}$ equal to $C^{\{k\}} - 1$. Each successive threshold is increasing in nature, meaning any prior specification should account for the ordered nature of the parameters. Following previous prior choice recommendations (https://github.com/stan-dev/stan/wiki/Prior-Choice-Recommendations#prior-for-cutpoints-in-ordered-logit-or-probit-regression), priors are placed on the differences between thresholds rather than the thresholds themselves. To be precise, the prior on each threshold parameter $t = 1, 2, \dots, T$ can be expressed as $t_{C-1} \sim normal(t_{C-1} + 1, 1)$. This construction ensures that the ordered vector is continually increasing, while keeping the threshold parameters of similar magnitude to the data at hand. Additionally, the parameter u associated with missing data and inequality constraints is implicitly defined as $u \sim uniform(0,1)$.

A final prior specification is necessary for the correlation matrix ***R***. Here, ***R*** is a symmetric positive semidefinite matrix that is decomposed for efficiency to its $M \times M$ Cholesky factors. I specify ***R*** as being distributed according to the Lewandowski-Kurowicka-Joe (LKJ) distribution (Lewandowski, Kurowicka, & Joe, 2009). $R \sim LKJ(\eta)$, where η is a shape parameter that can be interpretated much like the shape parameter of a symmetric beta distribution. η tunes the strength of the correlations. If $\eta = 1$, then the density is uniform over all correlation matrices of size M suggesting the correlation values are uniform on the interval [-1,1]. If $\eta > 1$, matrices with a stronger diagonal

(weaker correlations) are more likely. As η approaches ∞, the correlation matrix resembles the identity matrix with 0 correlation. If $0 < \eta < 1$ stronger correlations are favored (positive or negative). The current model specifies the prior as $R \sim LKJ(8)$ suggesting the probability mass is centered at 0 with the highest density falling in a range approximately from -0.8 to 0.8.

5.4 Sampling and Parameter Estimation

Parameter estimation is completed in Stan, a probabilistic programming language written in C++ that computes the joint log probability density of a set of continuous parameters up to a proportional constant. The log probability density of a Gaussian copula is

$$c(\boldsymbol{u}) = |L|^{-N} \exp\left\{-\frac{1}{2}\sum_{m=1}^{M}\sum_{i=1}^{N}([L^{-T}L^{-1} - I] \odot Q'Q)\right\}, \quad (10)$$

$$Q_{N\,x\,M} = \begin{pmatrix} \phi^{-1}(u_1) \\ \vdots \\ \phi^{-1}(u_M) \end{pmatrix}. \quad (11)$$

Above, *u* is each marginal cdf, *L* is the *M x M* Cholesky factorization, *I* is the identity matrix, and $\odot$ is the elementwise multiplication operator or the Hadamard product. This construction of the likelihood is identical to that in (Stull, Chu, Corron, & Price, 2023). However, these models do have subtle differences related to the mean and noise construction of the ordinal marginal distributions. Further, that by Stull and colleagues is a maximum likelihood approach, while that used here is full Bayesian inference.

Bayesian inference is carried out using Stan's No U-Turn Sampler (NUTS), which uses Hamiltonian Monte Carlo (HMC) to draw from the posterior (Betancourt, 2017; Carpenter et al., 2017; Hoffman & Gelman, 2014; Stan Development Team, 2022). HMC is more efficient (statistically) than traditional MCMC techniques, such as Gibbs Sampling and Metropolis-Hastings samplers, allowing for better estimates in fewer iterations of the sampler. The efficiency is an important contribution when the posterior is complex, such as that associated with Gaussian copulas. The model is fit in R (R Core Team, 2022) via the package CmdStanR (Gabry & Cesnovar, 2022). CmdStanR is a lightweight interface to Stan that relies on Stan's backend interface to the command line CmdStan to compile, sample, and write results to output files. The use of CmdStanR alleviates the memory overhead incurred using R's traditional Stan interface Rstan.

Stan code for the full model can be found in Appendix 1. The code is adapted from initial code written for a Mixed Discrete-Continuous Gaussian copula by Stan Developers Sean Pinkney, Ethan Alt, and Andrew Johnson found at https://spinkney.github.io/helpful_stan_functions/group__gaussian__copula.html. The code found here is based on the method described in Smith and Khaled (2012). Code for the ordinal margin is modified from the ordered_probit_lpmf function found in Stan's math library at https://github.com/stan-dev/math/blob/develop/stan/math/prim/prob/ordered_probit_lpmf.hpp. All Stan and R code are provided at https://github.com/ChristopherAWolfe/Mixed-Discrete-Continuous-Gaussian-Copula.

All models are run using four chains in parallel with 3000 warmup iterations and 6000 sampling iterations. Tuning parameters associated with total number of simulation steps (max_treedepth) and step size within the Hamiltonian system (adapt_delta) are adjusted to account for the complex posterior. Max_treedepth is set to 12 (default is 10) and adapt_delta is set to 0.99 (default is 0.95). While the adjustment of these parameters leads to increased overall sampling time, the result is a more reliable and valid set of samples (Stan Development Team, 2022). Parameters across all models show a split R-hat statistic less than 1.05 and appropriate effective sample size statistics (> 400) suggesting convergence of the Markov chains and validity of the estimates. Finally, all models have no divergent transitions and no E-FMI warnings (> 0.2), suggesting geometric ergodicity – the sampler efficiently explores the whole parameter space. All these values are standard diagnostic features obtained from CmdStanR and provide evidence that the model described here is statistically valid and provides reliable parameter estimates.

5.5 Copula Output Information

Results from HMC and the Mixed Discrete-Continuous Gaussian copula consist of posterior samples for all parameters, which includes samples associated with each mean and noise function, threshold parameters, and the Cholesky factors (as well as generated correlation parameters). However, the main parameter of interest associated with the use of copula modeling is the dependence term or the $\boldsymbol{R}$ correlation matrix in the present study. Therefore, all results in the present study focus on the dependence structure

or the bivariate relationships between all traits described with a correlation from -1 to 1. Because the model learns the structure across 54 growth traits, this leads to a total of 1,431 relationships.

The most common way to visualize the dependence structure of a set of data or the correlation structure, especially when the data is >2 variables, is either through examination of a scatter plot or the use of correlograms. Both approaches are utilized to present the results. However, to visualize the results of the dependence learned via a copula, we must present the results based on how the copula is constructed. Described in Section 5.1, a copula can be described in stages. First, by definition the multivariate cumulative distribution functions that represents as copula has uniform cdfs such that $u_m \sim (0,1)$, where such transformation result from the probability integral transform. The probability integral transform says that any continuous random variable can be converted to a standard uniform variate. In the r programming language, the cdf of the standard Gaussian is *pnorm*. However, this initial step does not contain any information on the designation given to each margin. Therefore, after making each marginal distribution uniform, the inverse probability integral transform is applied giving the "observed values" of the copula dependence distributed according to a standard Gaussian distribution such that $z_m \sim normal(0,1)$. Known as *pseudo-observations* these can be specified precisely as $z_m = F_m^{-1}(U_m) \sim F_m(\cdot)$, where each marginal *m* is made up of simulated values achieved using the quantile function associated with each marginal distribution. The quantile function is the inverse of the cdf function and is designated

using *qnorm* in r. These transformed pseudo-observations are then used to visualize each bivariate relationship (Erdely & Rubio-Sanchez, 2022; Hughes, 2022).

In practice, the specific steps are as follows:

1. Fit a Mixed-Discrete Continuous Gaussian copula in Stan
2. Using the mean posterior correlation matrix $\boldsymbol{R}$ learned above, simulate observations from a Multivariate Gaussian Distribution with mean equal to 0 and correlation matrix equal to $\boldsymbol{R}$ ($\mathbf{z} \sim Normal(0, \boldsymbol{R})$)
    a. MASS package (Venables & Ripley, 2002) and *mvrnorm*
3. Uniformize each individual marginal using the standard normal cdf - *pnorm(mean = 0, sd= 1)*
4. Translate to each specified marginal using the quantile function *qnorm*
    a. Both marginals are specified as *qnorm(mean = 0, sd = 1)*

Following the above steps results in a dataset with rows the size of the number of simulations in *mvrnorm* and columns the size of the number of marginals (*M = 54)*. This dataset encapsulates the dependence structure conditional on age that is learned by the copula model. Figure 5.1 demonstrates visually how we move from observed data to pseudo-observations. Note, because the marginal cdfs are Gaussian, Steps 2 and 4 above yield identical results. The purpose here is to show the exact steps involved if we assumed a different marginal construction (*i.e.,* if we assumed a beta distribution it would be the quantile function of the beta distribution or *qbeta*).

In addition to the visual analysis of correlations, this study tests the rank association or similarity between each posterior correlation matrix. Similarity is

measured with Spearman's ρ rank correlation value that assesses monotonic relationships. In other words, two matrices with similar correlation values will have either a strong positive or negative association closer to +1 or -1. Matrices that are dissimilar will have values closer to 0. In correlation tests, the null hypothesis is no relationship or complete dissimilarity between each matrix ($\rho = 0$). The p-value in correlation tests is the probability of observing non-zero correlations when in fact the null is true. A p-value less than 0.001 ($\alpha < 0.001$) and a correlation that is non-zero (e.g., $\rho = 0.85$) suggests the null hypothesis is rejected and the alternate is accepted – there is a true non-zero association or similarity between two matrices. However, a traditional p-value is inappropriate because the data are non-independent such that each correlation value cannot be taken out without affecting other values within the same structure (Chen et al., 2016). As such, a non-parametric permutation test is completed. Across 5,000 iterations, the order of the rows and columns from one of the correlation matrices is re-shuffled. Each time, Spearman's ρ is recalculated between the re-shuffled matrix and another matrix whose rows and columns are unchanged. The p-value is estimated based on the number of values that fall above the true correlation. This process is modified from the following code: https://gist.github.com/jcheong0428/4e11b983ac1d24b967321332fc281ef5#file-sim_mat4-py. Permuted p-values less than 0.001 are considered statistically significant. Tests are run between each pair of developmental stage models (infancy x childhood, infancy x juvenile and adolescence, child x juvenile and adolescence) and between biological sex models (male x female).

5.6 Model Check and Validation

Each model fit in the current study demonstrates convergence of the Markov chains, geometric ergodicity, and resulting reliable posterior estimates for all parameters (Figure 5.2). However, an additional check is necessary to ensure the process described in the statistical model fits the true characterization of the data. That is, if we assume that each marginal distribution follows a standard Gaussian distribution, does this assumption match reality if we scale our observed data by the posterior mean and standard deviation from the model. This is known as the posterior predictive distribution where the learned model is used to predict a new value that, if valid, should be similar to the observed data in the study (Gelman et al., 2014; Hobbs & Hooten, 2015).

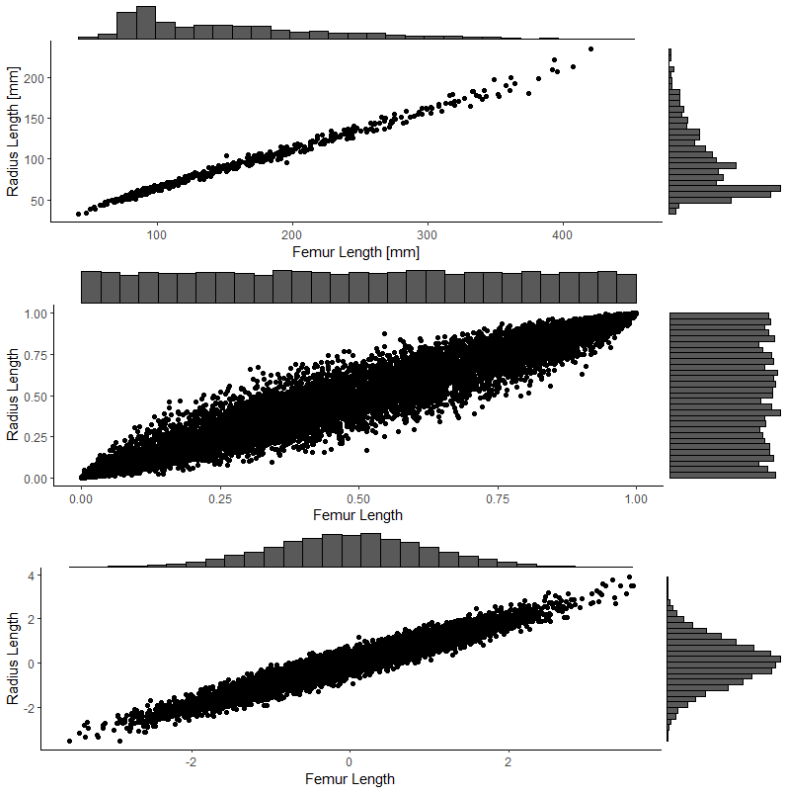

Figure 5.1. Top: Observed Femur length by Radius Length (response variable y), Middle: Uniform transform of Femur length by Radius length following copula model (pnorm) (the cdf u or $F^{\{m\}}(y^{\{m\}})$), Bottom: Application of inverse probability transform based on arbitrary marginal designation (qnorm) (the transformed random variable z).

Recall above in Figure 5.1, I have simulated correlated values from a standard multivariate Gaussian distribution based on the correlation matrix $\boldsymbol{R}$ learned from the model and then through a series of transformations, applied the standard Gaussian distribution chosen to represent each margin. To replicate this process on the observed continuous data I repeat the same standardization procedure where $z_i^{\{j\}} = \frac{\left(y_i^{\{j\}} - \mu_i^{\{j\}}\right)}{\sigma_i^{\{j\}}}$ such that z is random sample related to simulating data from the copula, μ is the posterior mean of that response, and σ is the posterior standard deviation. To check the fit of the model, I can either show the relationship between the observed and predicted values (Figure 5.3, top) or I can use the above transformation to show the bivariate relationship resulting from the posterior predictive distribution (Figure 5.3, bottom). On the top panel, the predictive density of femur diaphyseal length overlaps the true observations of the data indicating the model estimates plausible results. Further, when comparing the bivariate relationship between femoral and radial diaphyseal lengths after standardizing based on the posterior mean and standard deviation, the bottom panel shows that the model recovers the true relationship between radial and femoral growth when the marginal distributions are standard Gaussian. To be clear, in Figure 5.3 the blue values result from drawing random samples from the copula function ($\boldsymbol{z} \sim MVN(\boldsymbol{0}, \boldsymbol{R})$) and the red values result from standardizing the observed response variable y using the conditional mean and standard deviation from the model.

Similar posterior predictive relationships can be demonstrated with individual ordinal variables as well as using bivariate relationships between ordinal and continuous variables. There are two ways to complete this task: 1) discretize the pseudo-observations

learned from the copula model based on the threshold parameters (effectively the inverse of the initial steps), or 2) augment the observed discrete values with the same procedure highlighted in the model code to achieve latent continuous values. Below, I describe the steps taken to both augment the observed data to latent continuous values for the maxillary first molar and to transform the predicted values to ordinal stages. First, I extract the posterior samples associated with the ordinal mean function (a_M1), as well as samples associated with the threshold parameters ($t = 11$), and the nuisance parameters u. Next, using the steps highlighted in the ordered probit function in the Stan code in Appendix 1, I use *pnorm* (the cumulative distribution function of standard normal) to quantify the relationship between threshold parameters and mean values, followed by the inverse *qnorm* (the quantile function of the standard normal) to translate the value to the latent scale. Figure 5.4, top visualizes the predictive density of M1 in both the observed and predicted latent values, while the bottom panel visualizes the bivariate relationship between the observed and predicted femoral lengths and M1 latent values. Like the continuous results above, both panels demonstrate agreement between the observed and predicted values, suggesting the Gaussian copula described here recovers the *true* relationship between both data types. To transform the predicted values to ordinal categories, I use *pnorm* to get the probability of each category and then predict ordinal values using the function *rmultinom.* Figure 5.5 demonstrates the correspondence between the observed and predicted ordinal scores, again corroborating the fit of the model.

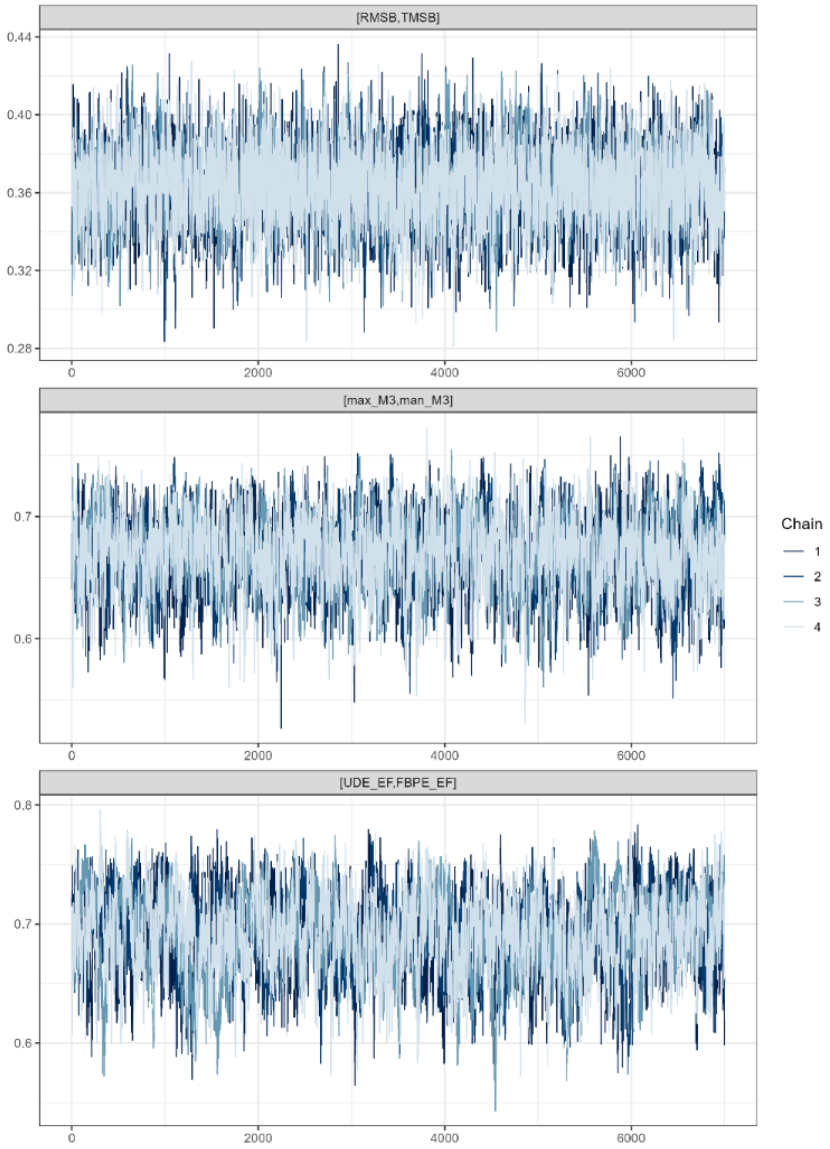

Figure 5.2. Trace plots demonstrating convergence of chains for a subset of comparisons (correlation parameters; r_{ij}).

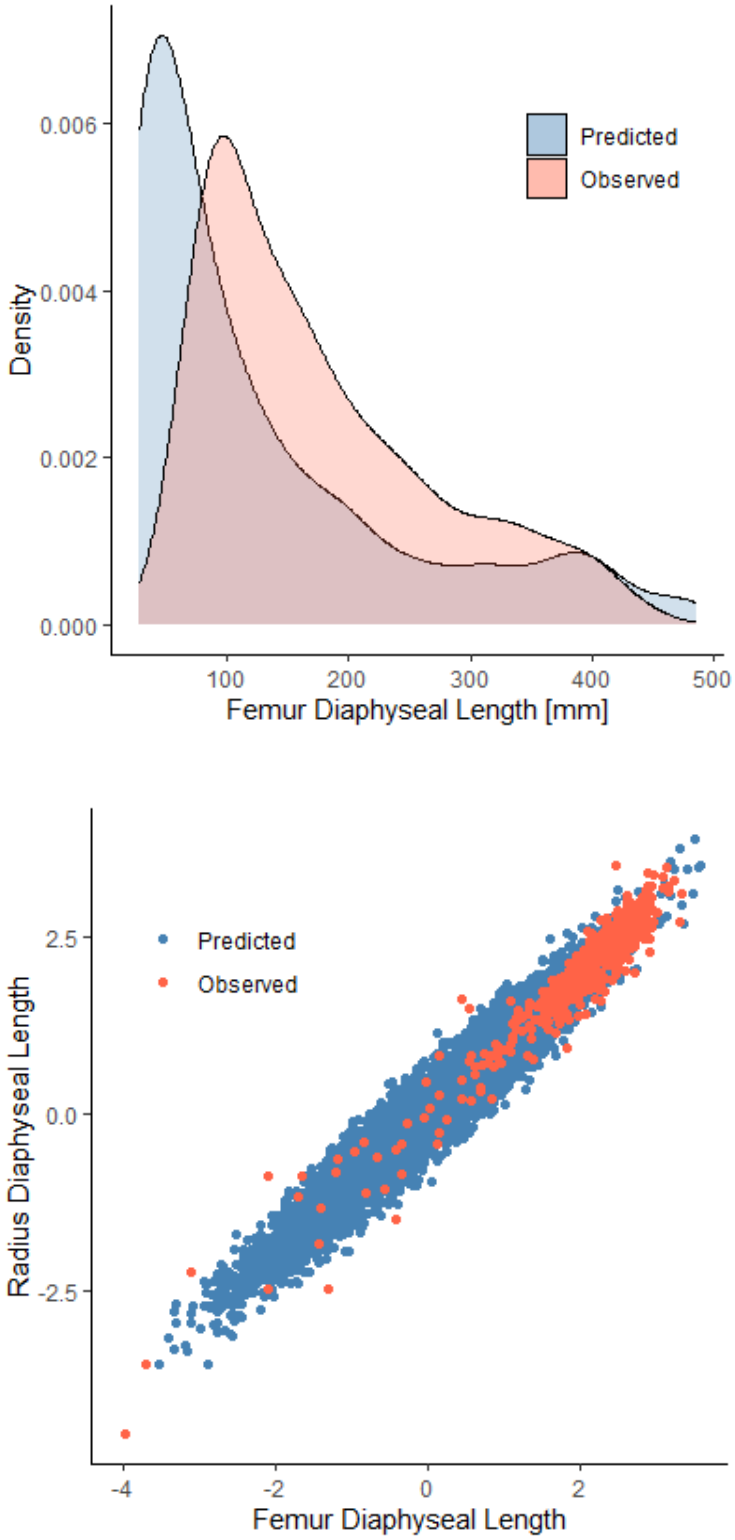

Figure 5.3. Top: Posterior predictive distribution of the observed femur diaphyseal length against the predicted length, Bottom: The pseudo-observations plotted against the standardized true observations demonstrating a similar relationship.

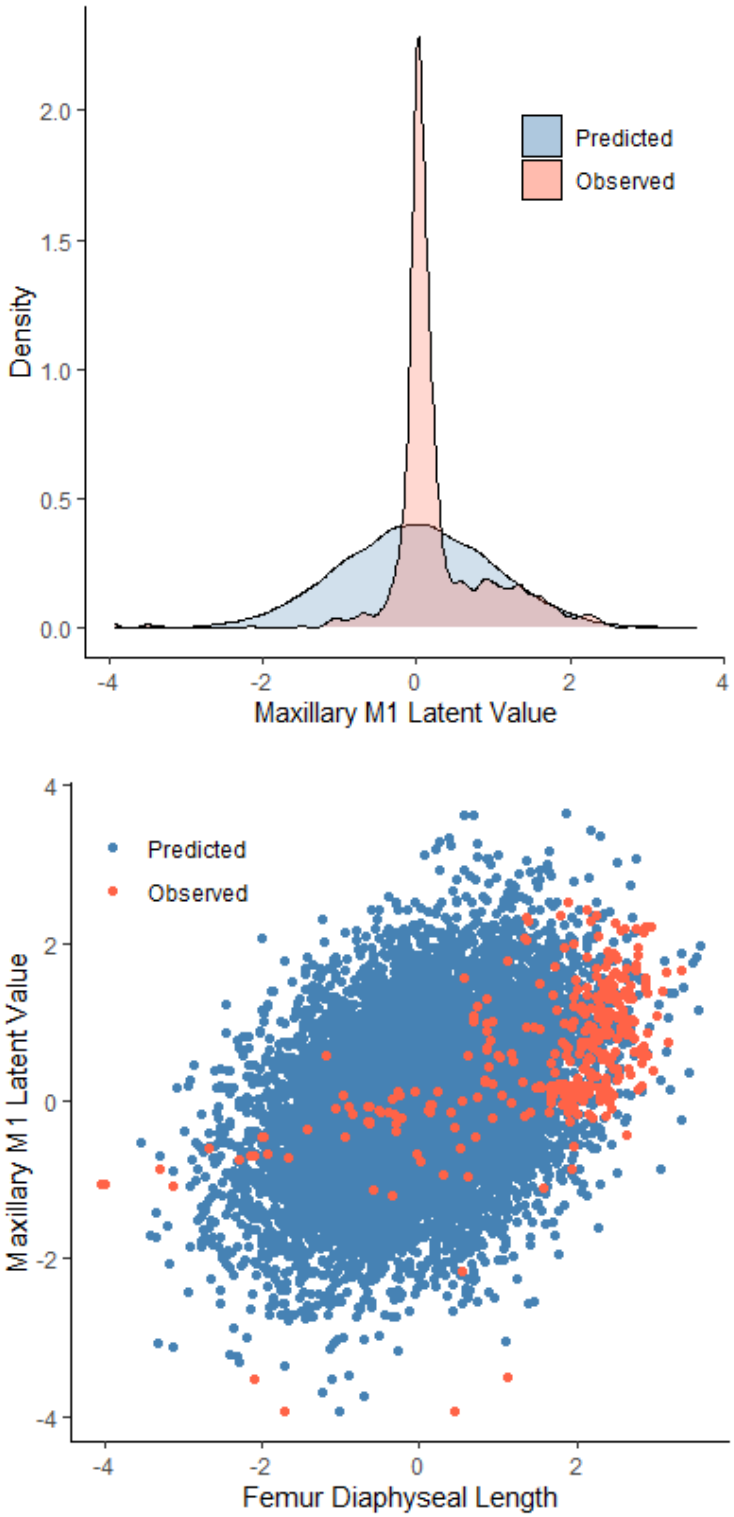

Figure 5.4. Top: Posterior predictive distribution of the observed M1 latent score against the predicted score, Bottom: The pseudo-observations plotted against the latent true observations demonstrating a similar relationship.

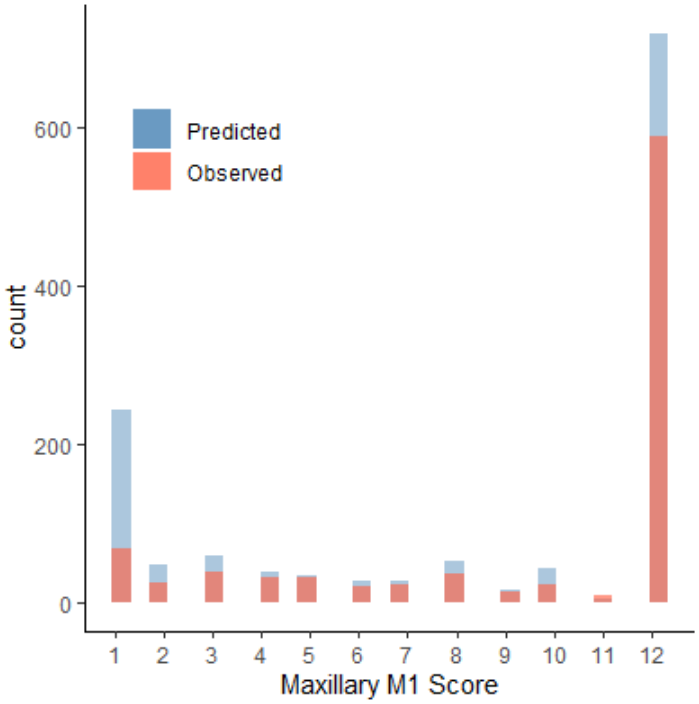

Figure 5.5. PPD of the predicted M1 scores against the observed. Overlap demonstrates good model fit.

Chapter 6 – Results

A total of six Mixed Discrete-Continuous Gaussian copula models were fit. The models are: 1) the full dataset, 2) the infancy subset (0 – 2.99 years old), 3) the childhood subset (3.0 – 6.99 years old), 4) the juvenile and adolescence subset (> 7 years old), 5) the male subset, and 6) the female subset. The output of each model includes 24,000 random samples (6,000 iterations x 4 chains) for all model parameters including mean function, standard deviation function, threshold parameters, missing values, and the correlation terms. All downstream analyses extend from these samples including generated quantities related to transforming the Cholesky factors back to a symmetric positive semidefinite correlation matrix (Chapter 5.3.4) and related summary statistics and expectations. While there are thousands of parameters to be explored across each model, the present study focuses on the copula parameter describing the dependency structure of the data: the correlation matrix $\boldsymbol{R}$.

All results are presented according to bivariate and/or pairwise relationships between either individual phenotypic traits (e.g., FDL and TDL) or between larger growth modules. Growth modules are defined as broad growth and development processes: 1) long bone length (LBL; longitudinal growth), 2) long bone breadth (LBB; appositional growth), 3) dental development (DD), 4) skeletal ossification (OSS), and 5) skeletal fusion (EF). Bivariate pairs describing relationships between individual traits (e.g., FDL and TDL) present the mean posterior correlation r, while the growth module relationships average across all mean posterior correlation values that define each relationship type. For example, the relationship between FDL x HMSB and TDL x HPB are both indicative

of growth module relationships between LBL and LBB. In total, there are 72 of these types of relationship across the dataset. Results are averaged across all relationship types (e.g., LBL x LBB) and presented as an average correlation between different growth modules.

The remainder of this chapter describes the results in detail according to the dependency structure (correlations) that underlie both individual growth traits and averaged across larger growth modules. A broad summary is presented first followed by a description of each of the six models. In section 6.1, a parallel coordinates plot is used to summarize the growth module relationships across all six models. The parallel coordinates plot is broken up into more-specific point plots to focus on patterns across the developmental stages and between biological sexes. In the remainder of the sections, two other visualizations are consistently used to display the large number of numeric results. The first is a correlogram, or correlation plot, which displays mean posterior correlations between individual traits – red tiles indicate positive relationships and blue tiles indicate negative relationships. Values close to 0 are lighter in color and a 0.00 correlation (no linear relationship) is represented by a white tile. Axis labels are organized and shaded by growth module. The second common plot is that of a copula scatterplot first introduced in Chapter 5.5. The purpose of the scatterplots is to provide an example of traditional copula visualizations (Erdely & Rubio-Sanchez, 2022), while recognizing that displaying 1,431 unique relationships in such a manner may be burdensome and not the most meaningful. Here, I present only the strongest and weakest relationships across each model. To corroborate the visualizations, a Spearman's ρ rank correlation test and a non-parametric permutation of the p-value are completed to test similarity between correlation matrices.

6.1 Summary of All Models

All models are summarized according to the average correlations between growth modules. Figure 6.1 displays a parallel coordinates plot where growth module pairs are on the horizontal axis and the average correlation value is on the vertical axis. The lines are colored according to each of the six models. In general, within-module relationships ([DD,DD], [EF,EF], [LBB,LBB], [LBL,LBL], [OSS,OSS]) are stronger as compared to between-module relationships (e.g., [DD,LBL] or [LBB,OSS]). These relationships are dynamic and variable across ontogeny but are relatively stable between males and females. Long bone growth is most active early, followed by dental development, and ending with fusion of the epiphyseal surfaces; activity is indicated by larger numbers in both negative and positive directions. By adolescence, the patterning of three broad growth modules is visible in the form of skeletal growth/diaphyseal dimensions (LBL and LBB are collapsed), dental development, and skeletal ossification and fusion (OSS and EF are collapsed). Figure 6.2 displays a point plot of each developmental stage with the correlation value on the horizontal axis and the module pairs on the vertical axis. This figure corroborates the above information showing how relationships between module pairs vary according to developmental stage. Table 6.1 reinforces this information and shows statistically significant ($\alpha < 0.001$) weak to moderate association between each developmental stage correlation matrix. This result corroborates the overall pattern of differential correlation structures across ontogeny. Males and females display similar correlation structures. Figure 6.3 and Table 6.1 support this similarity with a statistically significant Spearman's ρ of 0.84 suggesting strong association between male and female correlations. The full model corroborates the results from all previous subsets with

distinct growth modules present within each trait type. The strongest between-trait relationships exist between those elements with similar developmental schedules, such as early forming dentition and the growth of long bones (Figure 6.4). However, in general, traits in the same module are more strongly correlated as compared to traits between two different modules. Across all models, an additional level of modularity exists whereby an examination of inter-module relationships reveals an additional hierarchy in the strength of relationships (e.g., Figure 6.5-6.7). This includes stronger correlations between pairs of length variables (e.g., FDL x HDL) versus that of breadth variables (e.g., HPB vs UMSB). Similar structure arises in the dentition whereby tooth isomeres (e.g., man_M1 and max_M1) are more strongly correlated with each other as compared to the remainder of the dentition. There is less evidence to suggest similar hierarchical modularity structures are present across variables of fusion and ossification.

Table 6.1. Spearman's ρ and associated permuted p-values to measure the similarity between correlation matrices from each model. Higher positive values indicate strong rank association and similarity.

Model Correlation Matrix Pair	**Spearman's ρ**	**Permuted P-Value**
[Biological Male, Biological Female]	0.84	0.0002
[Infancy Stage, Childhood Stage]	0.48	0.0002
[Infancy Stage, Juvenile & Adolescence Stage]	0.39	0.0002
[Childhood Stage, Juvenile & Adolescence Stage]	0.42	0.0002

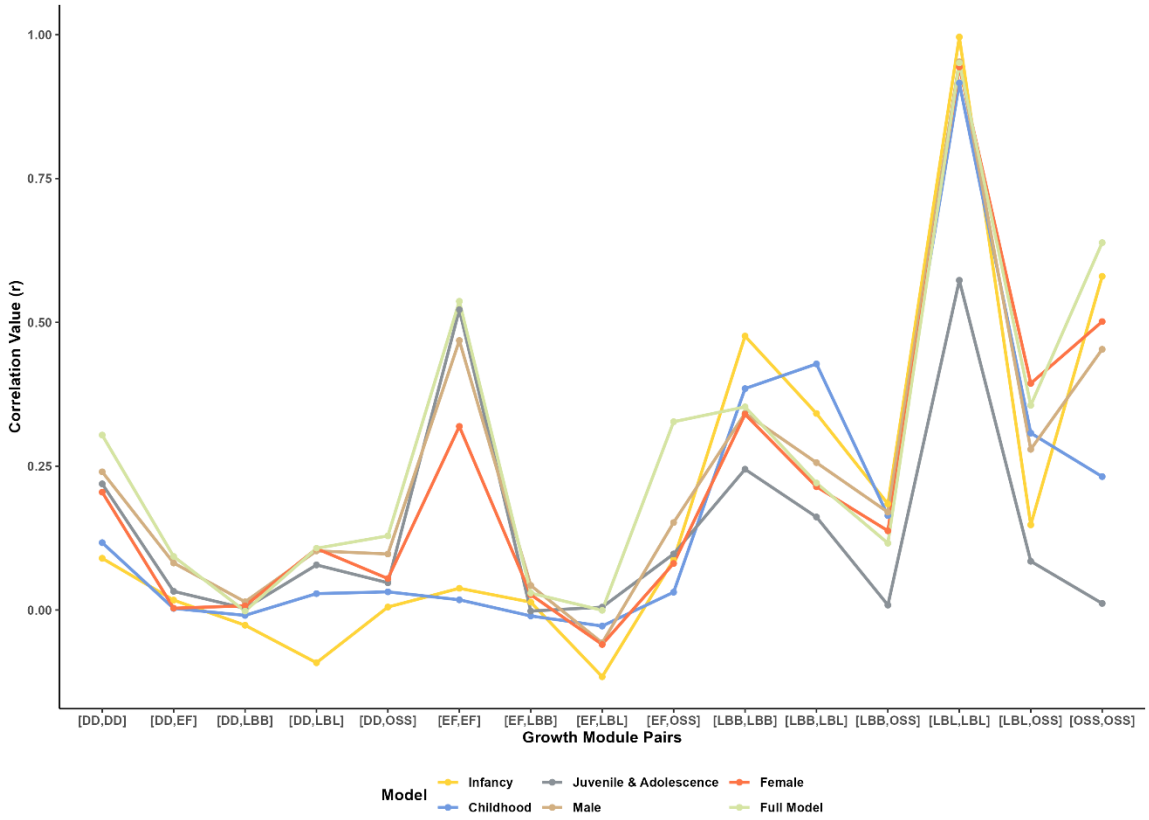

Figure 6.1. Parallel coordinates plot of the average posterior correlations between growth modules across all six models. The lines are colored by model. DD = Dental Development, LBL = Long Bone Growth, LBB = Long Bone Breadth, EF = Epiphyseal Fusion, and OSS = Skeletal Ossification.

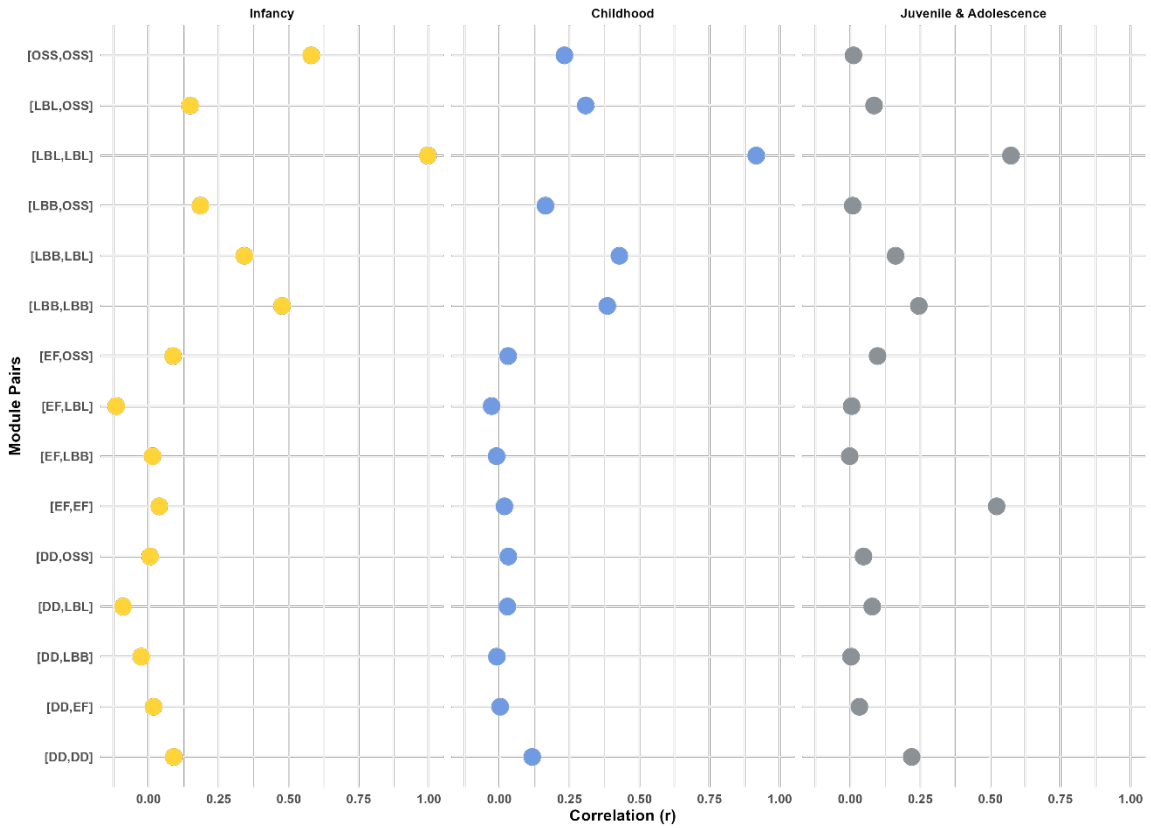

Figure 6.2. Point plot of the average correlation between module pairs across each developmental stage. The correlation value is on the horizontal axis and the module pairs are on the vertical axis. Infancy is in yellow on the left, childhood in blue in the middle, and juvenile and adolescence in grey on the right.

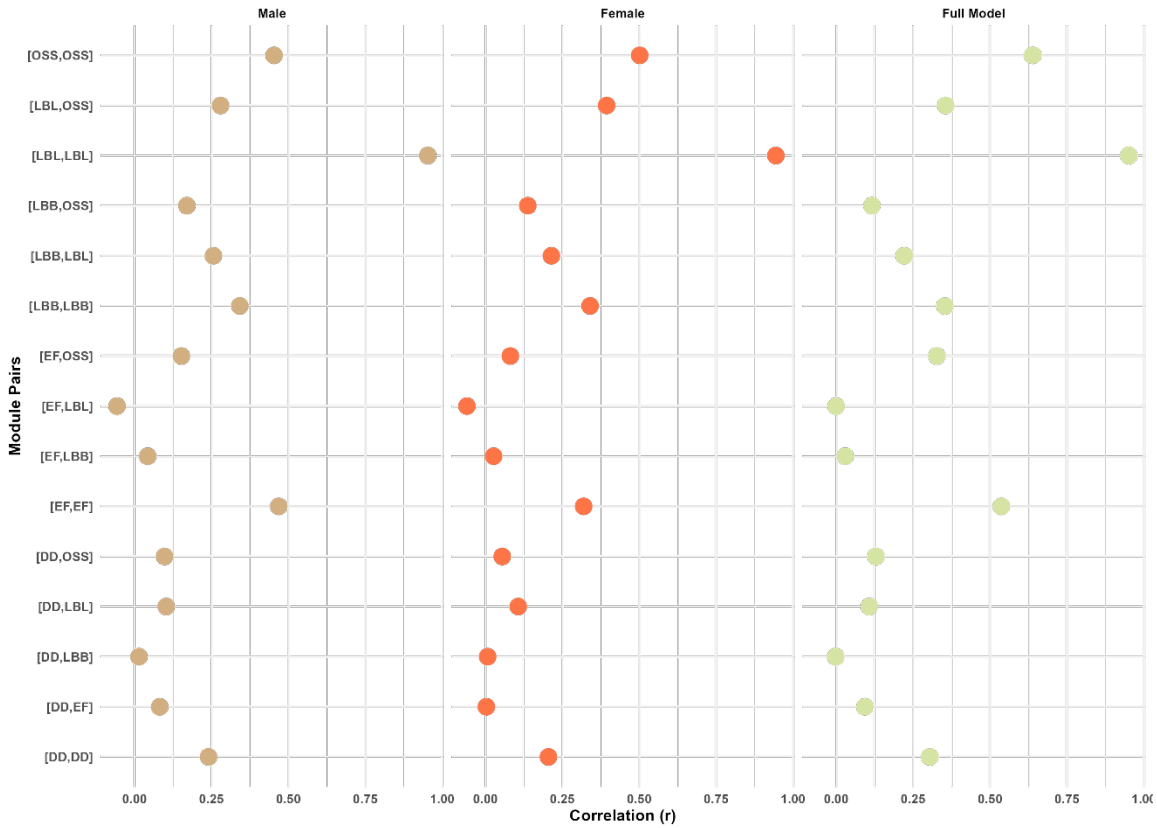

Figure 6.3. Point plot of the average correlation between module pairs across biological sex and the full model. The correlation value is on the horizontal axis and the module pairs are on the vertical axis. The male model is in tan on the left, female model in reddish orange in the middle, and the full model in light green on the right.

6.2 Full Model

6.2.1 All Variables

Figure 6.4 displays a correlogram of the posterior mean correlations for all 54 growth and development traits. The strongest relationships are between traits of the same growth module as compared to between traits of different modules. This is appreciated by the triangle shaped areas that are darker red as compared to other areas of the plot. The lower left is the diaphyseal dimensions (skeletal growth) module, the middle is the dental

development module, and the top right is the skeletal fusion and ossification module. Table 6.2 corroborates the strength of these within-module relationships by displaying the average correlations between and within modules whereby the strongest correlations exist within the long bone length module ([LBL,LBL]) and skeletal ossification module ([OSS,OSS]). When examining individual traits in Figure 6.4, radius diaphyseal length (RDL) and ulna diaphyseal length (UDL) show the strongest correlations among all bivariate trait relationships (r = 0.9862). The weakest correlation across all traits is between the proximal epiphysis of the ulna (UPE_EF) and the diaphyseal length of the radius (RDL) (r = -0.2205). The copula scatterplot in Figure 6.5 visualizes the differences between the strongest and weakest bivariate relationships.

Early developing dentition including first molars (M1), canines (C), and first and second incisors (I1 and I2) are moderately correlated to all LBLs. Similarly, early developing skeletal elements, such as tarsal ossification (TC_Oss) and carpal ossification (CC_Oss), are also moderately correlated to all LBLs. These patterns suggest that traits that grow within the same time frame and with relatively the same developmental speed have stronger positive correlations, while those on opposite trajectories (i.e., later forming versus earlier forming) have weaker positive correlations. An example includes the correlation between diaphyseal length of the femur (FDL) and maxillary M1 development (max_M1) as compared to FDL and UPE_EF. Both FDL and the M1 are active in infancy and complete growth in adolescence. In comparison, while FDL is active from infancy to early adolescence, the ossification center associated with UPE_EF does not appear until approximately 8 to 10 years old and fuses shortly after in adolescence at approximately 12 to 18 years old. As a numerical comparison, the

correlation between FDL and M1 is $r = 0.2914$, while the relationship between FDL and UPE_EF is $r = -0.1527$.

Table 6.2. The average posterior correlation within and between growth modules for the full model. Displayed in descending order with the strongest relationship at top. DD = Dental Development; EF = Epiphyseal Fusion; LBB = Long Bone Breadth; LBL = Long Bone Length; OSS = Skeletal Ossification.

Growth Module Pairs	Mean Posterior Correlations
[LBL,LBL]	0.9510
[OSS,OSS]	0.6386
[EF,EF]	0.5366
[LBL,OSS]	0.3559
[LBB,LBB]	0.3531
[EF,OSS]	0.3273
[DD,DD]	0.3041
[LBB,LBL]	0.2208
[DD,OSS]	0.1289
[LBB,OSS]	0.1162
[DD,LBL]	0.1073
[DD,EF]	0.0931
[EF,LBB]	0.0294
[EF,LBL]	-0.0004
[DD,LBB]	-0.0018

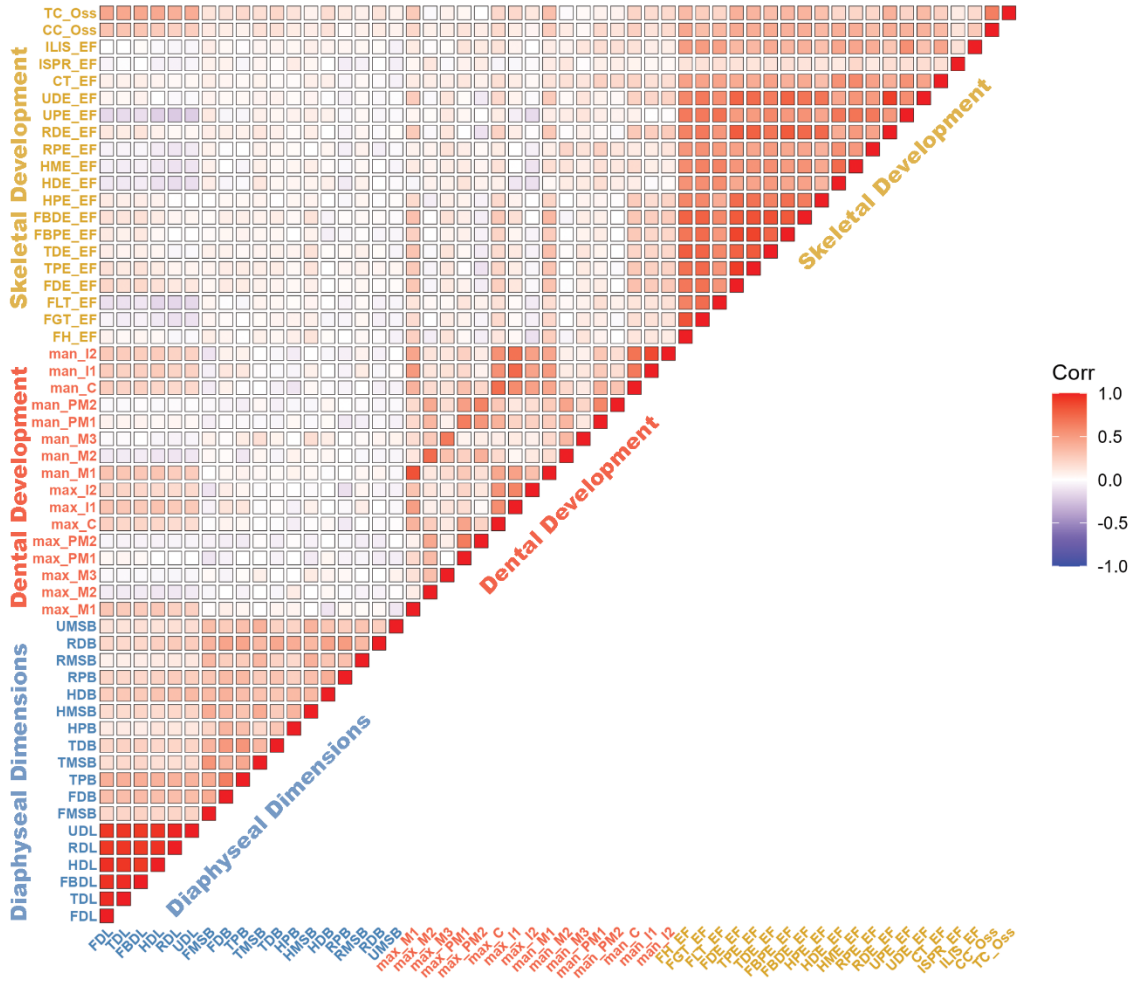

Figure 6.4. Correlogram showing relationship between 54 growth and development indicators from the full model. Labels are colored by growth module. Red = positive correlation, Blue = negative correlation, White = no correlation.

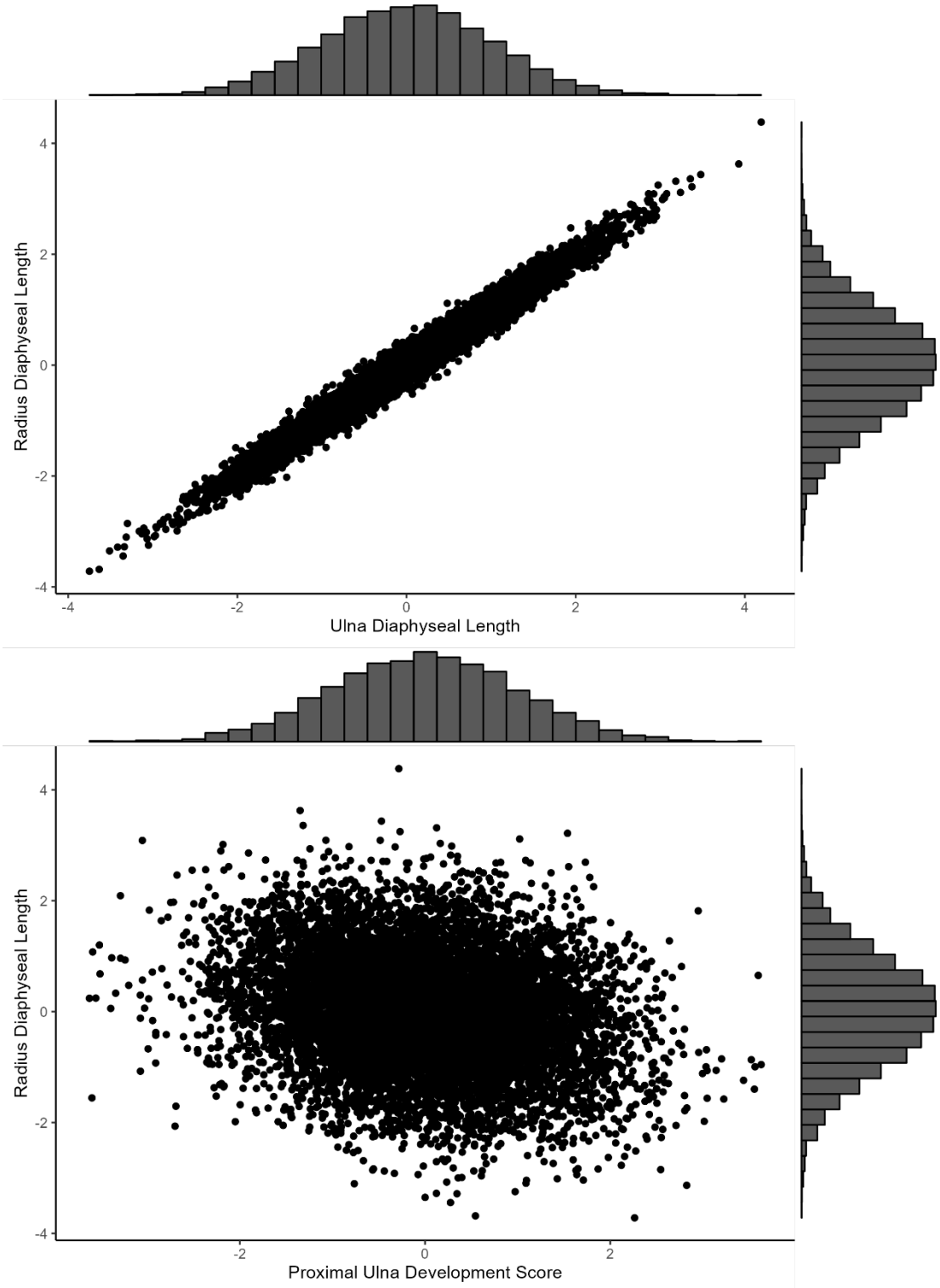

Figure 6. 5. Copula scatterplot displaying the strongest (UDL x RDL, top) and weakest (UPE_EF x RDL, bottom) correlations. The variables are standardized with each marginal distribution shown as a standard Gaussian distribution along the right and top axis. This is *z* in the equations described in Chapter 5.

6.2.2 Skeletal Growth Module: Diaphyseal Dimensions

Diaphyseal lengths are strongly correlated with each other, while diaphyseal breadths are weak to moderately correlated with all other variables associated with skeletal growth (Figure 6.6). In general, intervariable correlations of the lower limb (FDL, TDL, FBDL) are stronger than intervariable correlations within the upper limb (HDL, RDL, UDL). However, the strongest relationship across the skeletal growth module is between the length of the radius and the ulna (RDL and UDL) indicative of the close developmental, anatomical, and functional relationships between both elements (r = 0.986). In comparison, intervariable relationships associated with breadth measurements (-PB, -DB, -MSB) are weaker than those associated with length measurements. The weakest relationships result from bivariate pairs that include midshaft measurements (e.g., FDL x RMSB, r = 0.074). The difference in strength associated with length measurements versus that of breadth measurements suggests an additional level of organization whereby the skeletal growth module can be further subdivided into a longitudinal growth module (e.g., FDL and TDL) and an appositional growth module (e.g., HMSB and RPB). Figure 6.6 depicts how length variables are more strongly correlated to other length variables, and breadth variables are more strongly correlated to other breadth variables.

6.2.3 Dental Development Module

Isomeres, or similar teeth between both arcades (e.g., max_M1 and man_M1), are most strongly correlated in the dental development module (Figure 6.7). There are no

uniform patterns associated with tooth classes. For example, within-class relationships, like max_M1 and max_M2, show weak correlations as compared to that between isomeres. The lack of tooth class relationships is likely because the strongest relationships are patterned by developmental timing, and tooth classes do not always share the same developmental timing. Teeth that form and develop within similar developmental periods (*e.g.*, I1, I2, C, M1) are more strongly correlated with each other as compared to teeth that form and develop at different periods (*e.g.,* max_M1 and max_M3). The strong correlations between teeth that develop during similar times are present both within the same arcade and across isomeres in the opposing arcade.

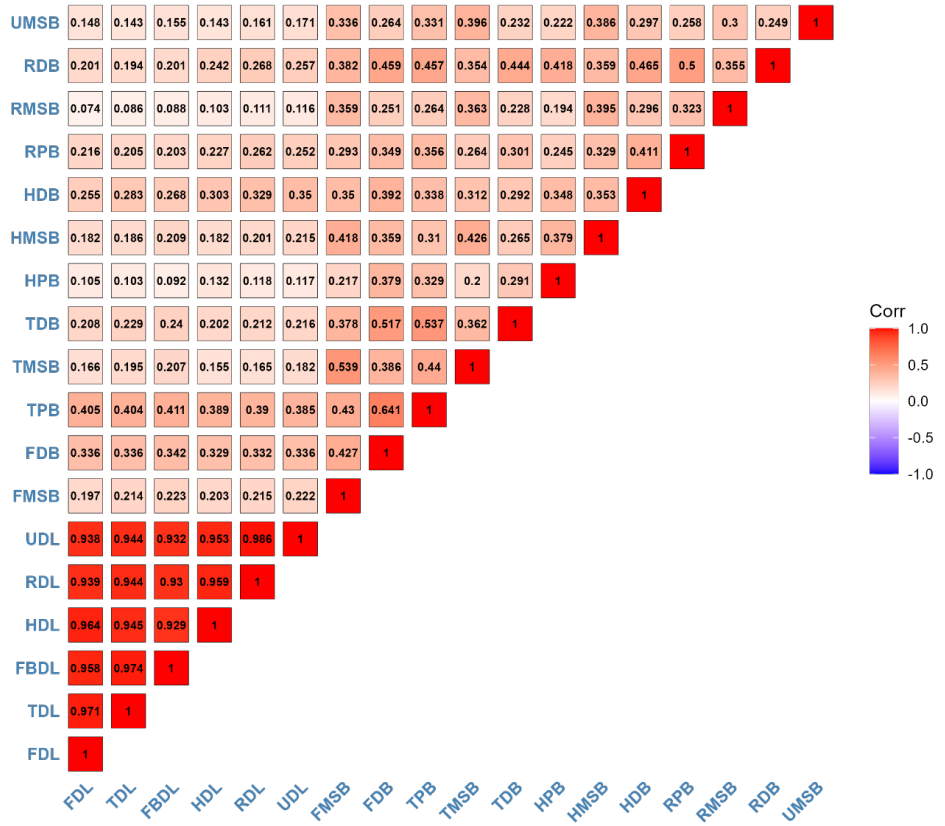

Figure 6.6. Correlogram showing relationships between traits associated with the skeletal growth module from the full model. Red = positive correlation, Blue = negative correlation, White = no correlation.

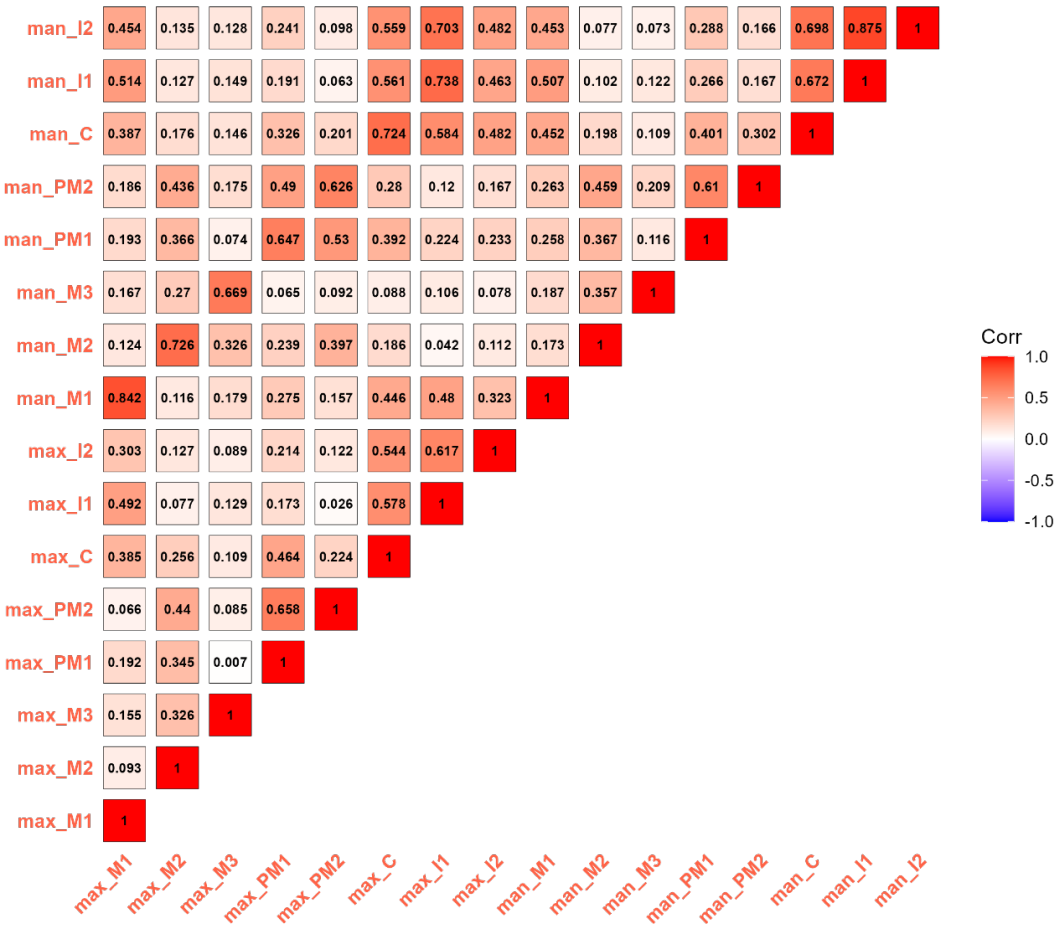

Figure 6.7. Correlogram showing relationships between traits associated with the dental development module from the full model. Red = positive correlation, Blue = negative correlation, White = no correlation.

6.2.4 Skeletal Development Module: Epiphyseal Fusion and Skeletal Ossification

Correlations between all fusion locations on the long bones are moderate to strong (Figure 6.8). Ossification of the carpals (CC_Oss) and tarsals (TC_Oss), calcaneal tuberosity (CT_EF), and fusion at the ischium (ISPR_EF) and ilium (ILIS_EF) all display weak correlations with other variables. Notably, the weakest relationships are between ISPR_EF and all other variables – possibly related to the earlier fusion of ISPR_EF during childhood (approximately 5 to 8 years old) compared to the fusion timing of other

elements much later in childhood and adolescence. Elements with close anatomical and developmental relationships are most strongly correlated including the femoral head (FH_EF) and greater trochanter (FGT_EF) (r = 0.839), distal epiphysis of the femur (FDE_EF) and proximal epiphysis of the tibia (TPE_EF) (r = 0.925), and the distal epiphysis of the radius (RDE_EF) and distal epiphysis of the ulna (UDE_EF) (r = 0.908). Similar to the dentition and long bones, developmental timing plays an outsized role in the patterning of correlations between individual traits of fusion and ossification.

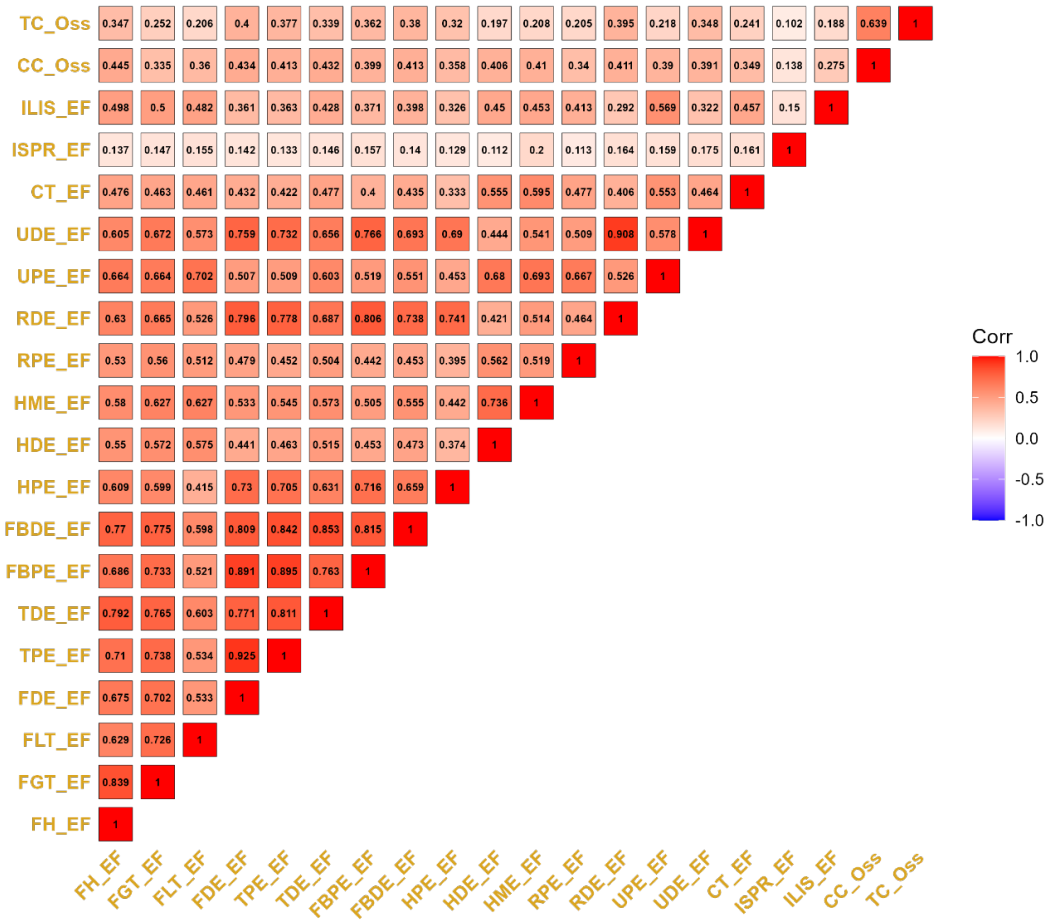

Figure 6.8. Correlogram showing relationships between traits associated with the skeletal development module from the full model. Red = positive correlation, Blue = negative correlation, White = no correlation.

6.3 Infancy Model

6.3.1 All Variables

Figure 6.9 shows the correlogram for all variables in the infancy model. The strongest relationships are between diaphyseal length and breadth measurements. Weaker, yet still positive, relationships are visualized between diaphyseal lengths and early forming dentition (I1, I2, C, M1), diaphyseal lengths and the carpals (CC_Oss) and tarsals (TC_Oss), and diaphyseal lengths and development at the distal femur (FDE_EF) and proximal tibia (TPE_EF). Combined, the elements described above all display active levels of growth and development (either increasing in size or increasing in ordinal score) during the infancy period. The strongest correlation is between diaphyseal length of the ulna (UDL) and radius (RDL) (r = 0.998), while the weakest is between diaphyseal length of the radius (RDL) and epiphyseal fusion of the distal tibia (TDE_EF) (r = -0.366) (Figure 6.10). Table 6.3 presents the average correlations within and between each growth module. The strongest relationships are within each module (e.g., [LBL, LBL]) as compared to between (e.g., [LBL, EF]).

6.3.2 Skeletal Growth Module: Diaphyseal Dimensions

During infancy, the correlation between all variables associated with diaphyseal length is strong (r is greater than 0.99) (Figure 6.11). All breadth measurements display positive correlations of varying strength. The weakest relationships associated with breadths is between midshaft breadth of the radius (RMSB) and diaphyseal length of the

femur (FDL) (r = 0.081). The strongest breadth-associated relationship is between distal breadth of the femur and all diaphyseal lengths except for the fibula (FBDL) (r >= 0.95). Lengths are more strongly correlated with other lengths and breadths are more strongly correlated with other breadths.

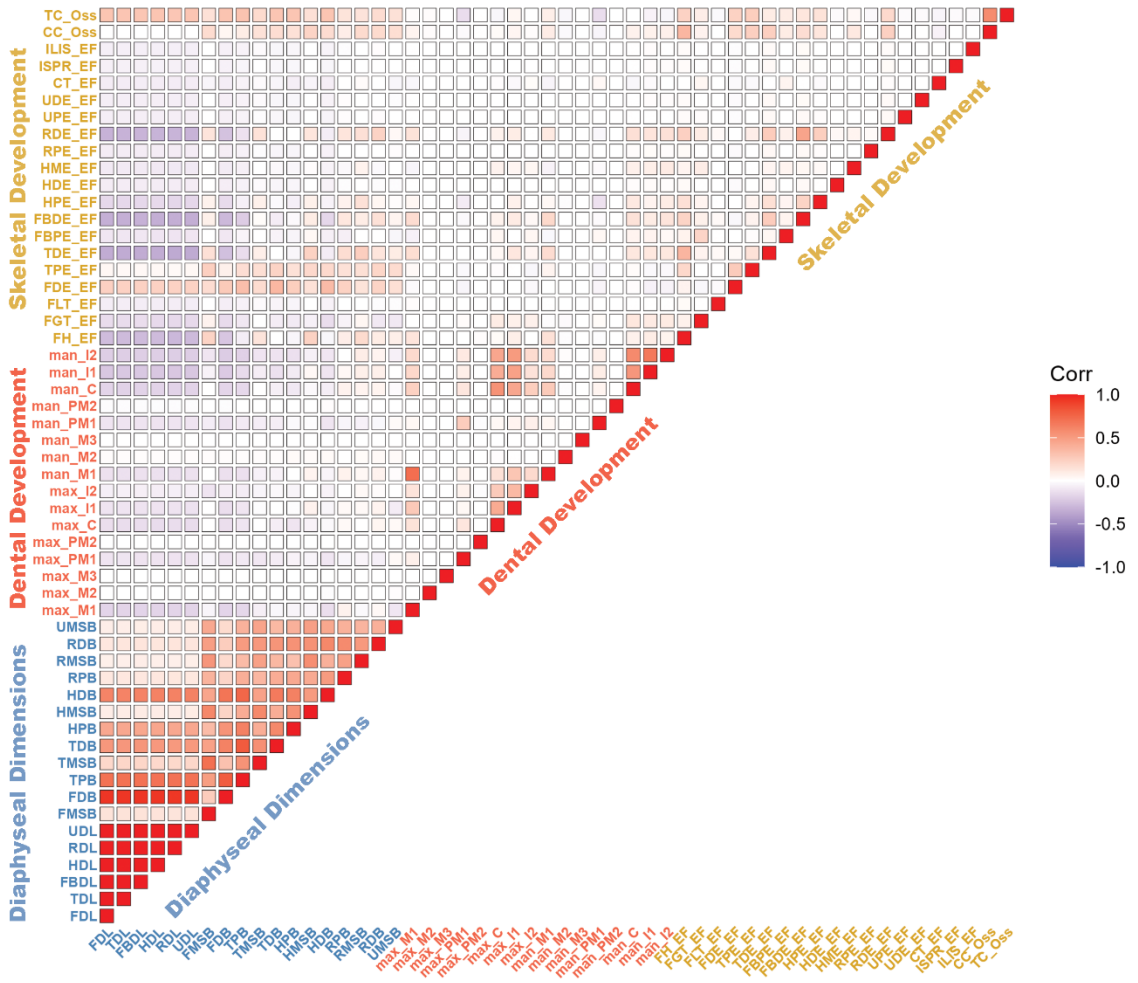

Figure 6.9. Correlogram showing relationship between 54 growth and development indicators from the infancy model. Labels are colored by growth module. Red = positive correlation, Blue = negative correlation, White = no correlation.

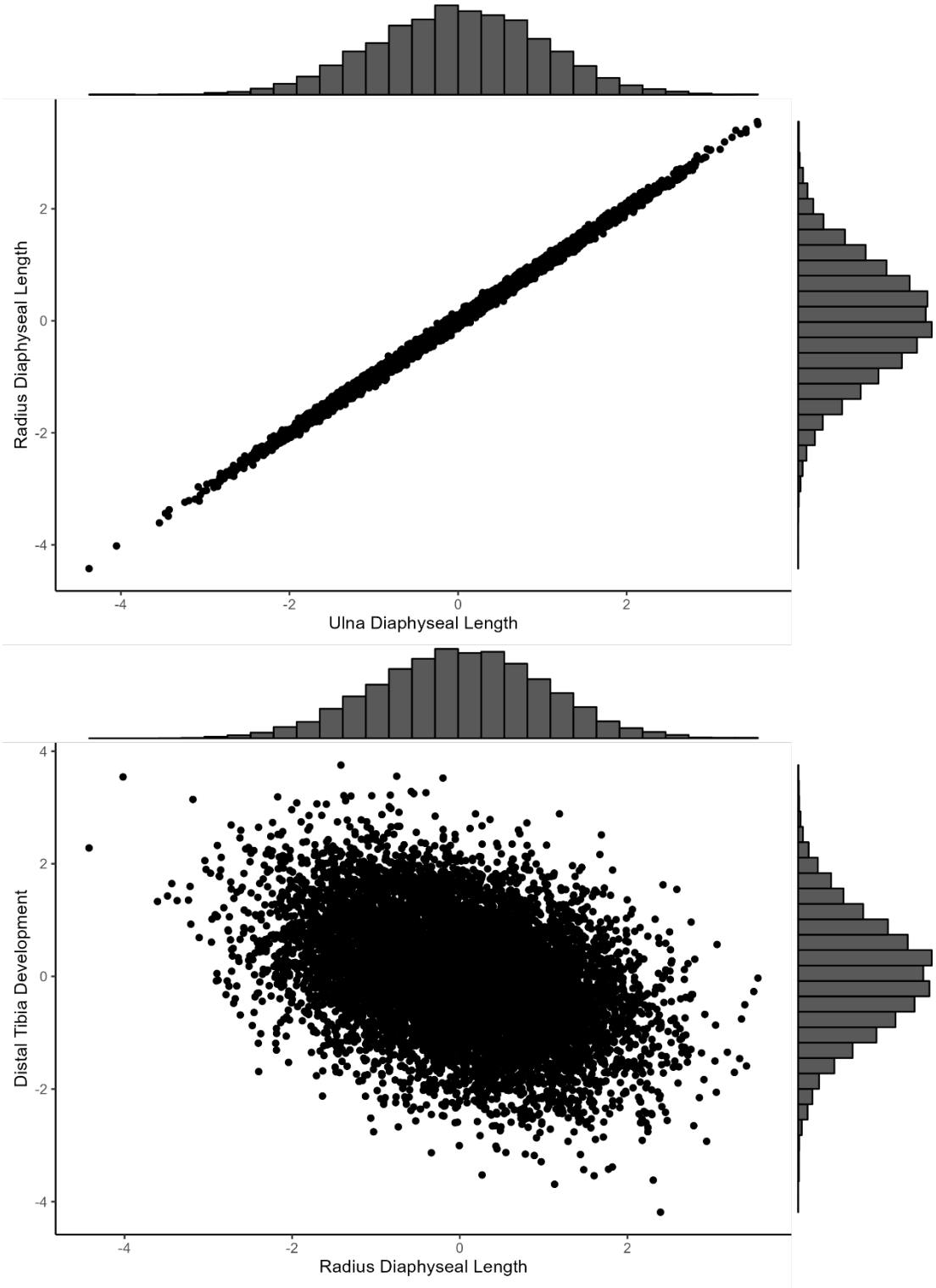

Figure 6.10. Copula scatterplot displaying the strongest (UDL x RDL, top) and weakest (RDL x TDE_EF, bottom) correlations. The variables are standardized with each marginal distribution shown as a standard Gaussian distribution along the right and top axis. This is *z* in the equations described in Chapter 5.

Table 6.3. The average posterior correlation within and between growth modules for the infancy model. Displayed in descending order with the strongest relationship at top. DD = Dental Development; EF = Epiphyseal Fusion; LBB = Long Bone Breadth; LBL = Long Bone Length, OSS = Skeletal Ossification.

Variable Pairs	Mean Posterior Correlations
[LBL,LBL]	0.996127
[OSS,OSS]	0.580047
[LBB,LBB]	0.476192
[LBB,LBL]	0.341635
[LBB,OSS]	0.184484
[LBL,OSS]	0.148125
[DD,DD]	0.089884
[EF,OSS]	0.08733
[EF,EF]	0.037797
[DD,EF]	0.017198
[EF,LBB]	0.013673
[DD,OSS]	0.005216
[DD,LBB]	-0.02637
[DD,LBL]	-0.09155
[EF,LBL]	-0.11591

6.3.3 Dental Development Module

The strongest correlations in the dentition are between isomeres that are actively developing during the infancy period and between different teeth also developing during the infancy period (Figure 6.12). This includes development of the mandibular and maxillary first molar (man_M1 x max_M1, $r = 0.720$) and between the first and second mandibular incisor (man_I1 x man_I2, $r = 0.672$). Besides teeth that actively develop during infancy, the majority of bivariate relationships between teeth (~95% of bivariate relationships) have correlations less than 0.5, indiciating weak within-module

relationships overall during the infancy period. This corroborates previous sections suggesting that correlation strength is related to active growth and development patterns.

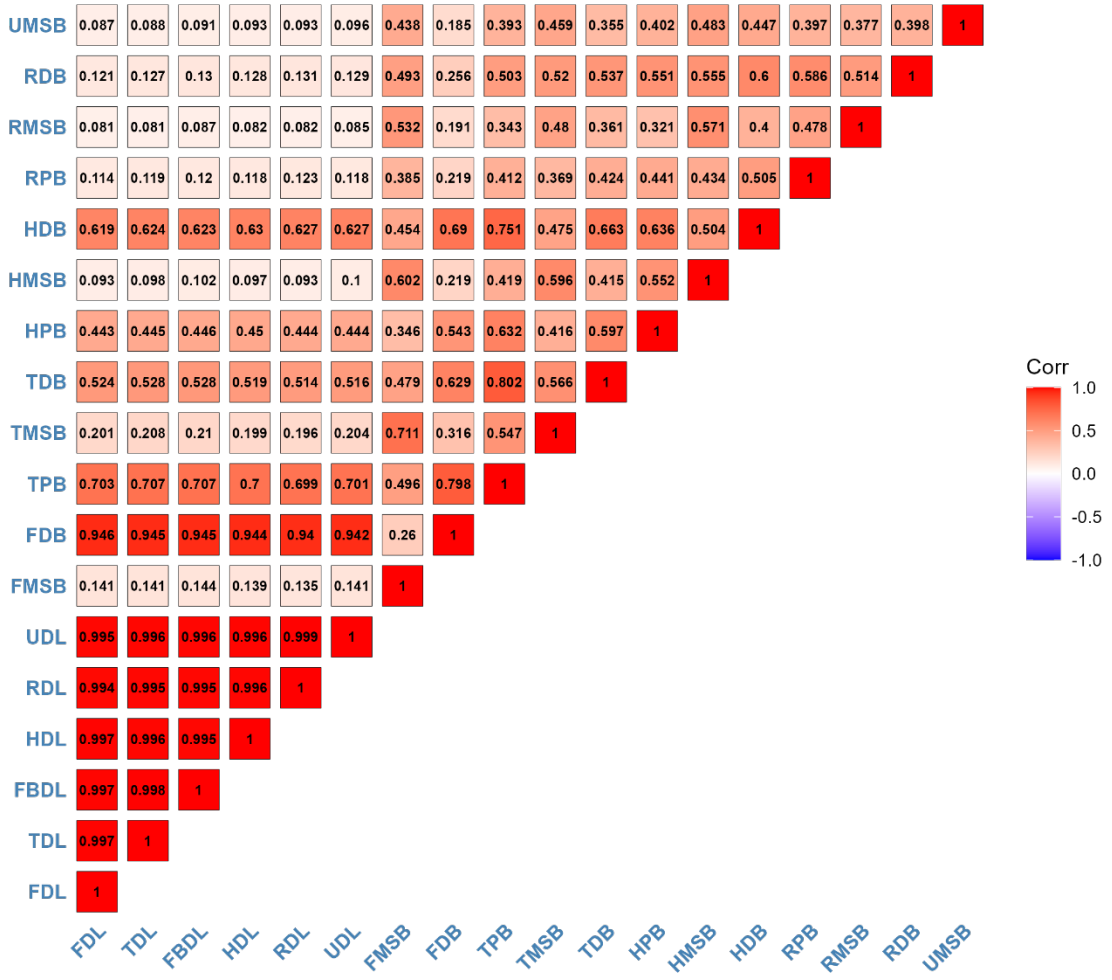

Figure 6. 11. Correlogram showing relationships between traits associated with the skeletal growth module from the infancy model. Red = positive correlation, Blue = negative correlation, White = no correlation.

6.3.4 Skeletal Development Module: Epiphyseal Fusion and Skeletal Ossification

All correlations between traits associated with epiphyseal fusion and skeletal ossification are moderate to weak ($r < 0.58$) (Figure 6.13). The strongest correlation is

between carpal ossification (CC_Oss) and tarsal ossification (TC_Oss) ($r = 0.58$). The strength of this relationship most likely results from similar ossification timing and the homologous origin of the wrist and ankle. Other correlations that are greater than 0, such as that between appearance of the distal epiphysis in the fibula (FBDE_EF) and appearance of the distal epiphysis of the radius (RDE_EF), are also related to similar developmental timing as appearance of both ossification centers occurs during infancy and specifically within the first 24 months of life.

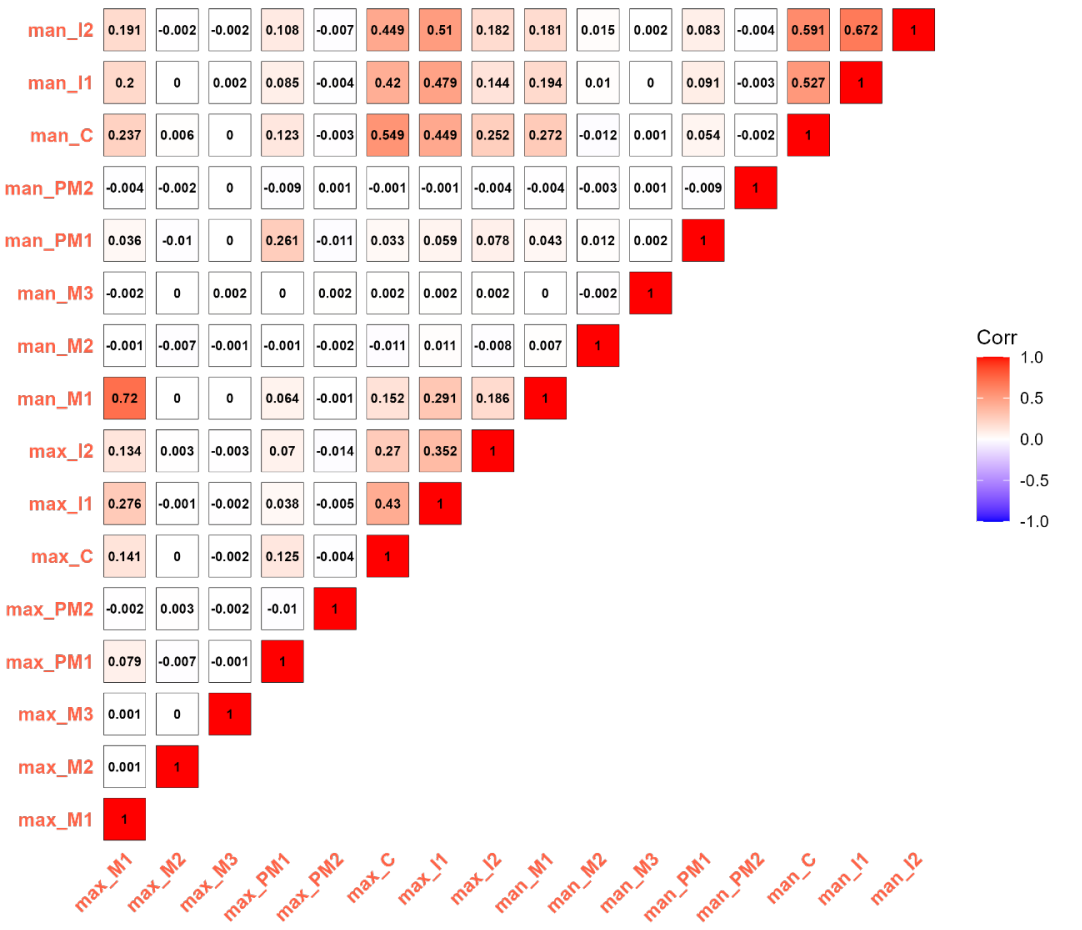

Figure 6.12. Correlogram showing relationships between traits associated with the dental development module from the infancy model. Red = positive correlation, Blue = negative correlation, White = no correlation.

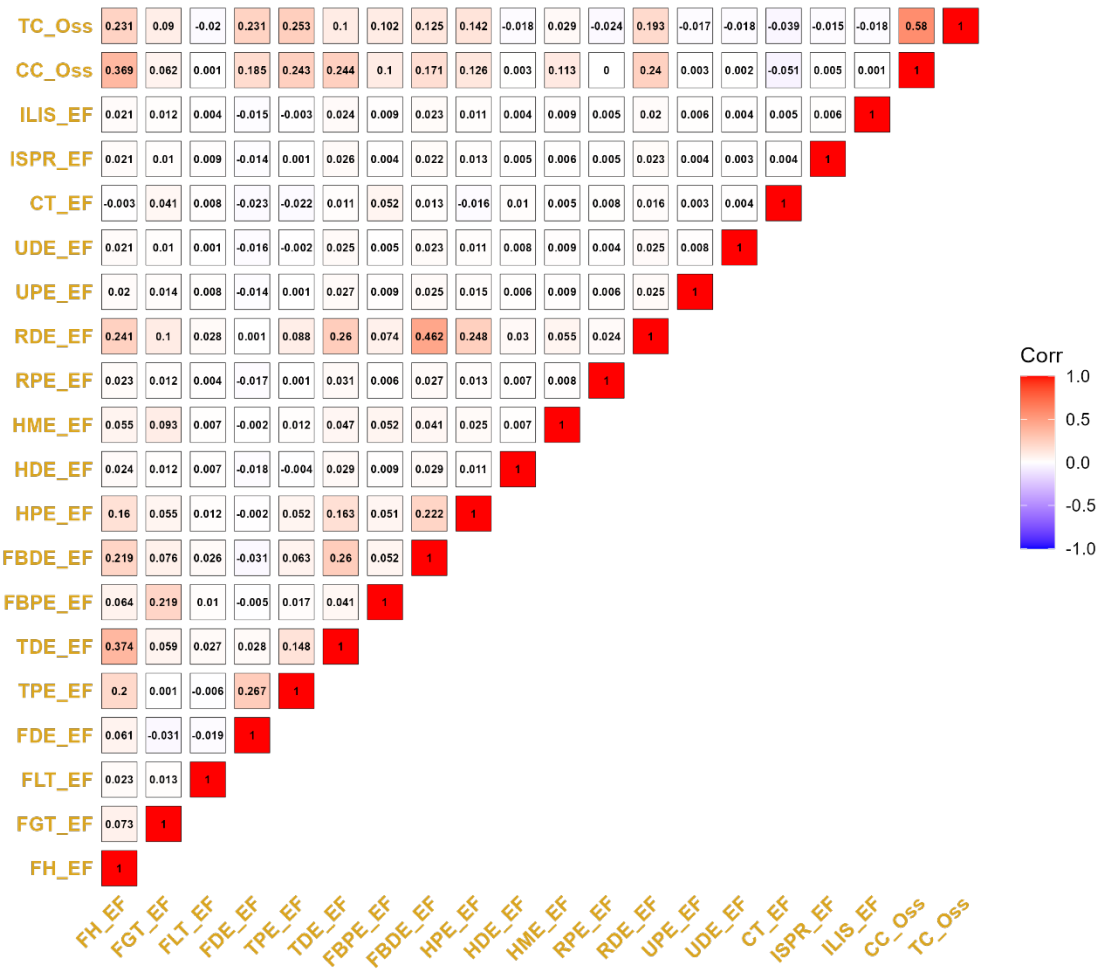

Figure 6.13. Correlogram showing relationships between traits associated with the skeletal development module from the infancy model. Red = positive correlation, Blue = negative correlation, White = no correlation.

6.4 Childhood Model

6.4.1 All Variables

Figure 6.14 displays the correlogram for all variables in the childhood model. Similar to the results in Section 6.2.1 and 6.3.1, the strongest correlations are presented between variables within the skeletal growth / diaphyseal dimension module. The weakest correlations across all variables are between those associated with dental development and long bone breadth and epiphyseal fusion and long bone length (Table

6.4). An example of this includes development of the maxillary second premolar (max_PM2) and proximal breadth of the tibia (TPB) (r = -0.226). In fact, the weakest bivariate relationship is between development of the mandibular second premolar (man_PM2) and diaphyseal length of the tibia (TDL) (r = -0.227). The strongest bivariate relationship matches that seen in the infancy period between length of the ulna (UDL) and radius (RDL) (r = 0.979) (Figure 6.15). Additional similarities to the infancy model include the moderately strong correlations seen between either carpal ossification and all elements of skeletal growth or between tarsal ossification and all elements of skeletal growth. Combined, the results corroborate the continued pattern that the strongest between-module values coincide with traits that are actively growing during childhood.

Table 6.4. The average posterior correlation within and between growth modules for the childhood model. Displayed in descending order with the strongest relationship at top. DD = Dental Development; EF = Epiphyseal Fusion; LBB = Long Bone Breadth; LBL = Long Bone Length, OSS = Skeletal Ossification.

Variable Pairs	Mean Posterior Correlations
[LBL,LBL]	0.9161
[LBB,LBL]	0.4278
[LBB,LBB]	0.3849
[LBL,OSS]	0.3076
[OSS,OSS]	0.2319
[LBB,OSS]	0.1642
[DD,DD]	0.1171
[DD,OSS]	0.0316
[EF,OSS]	0.0310
[DD,LBL]	0.0285
[EF,EF]	0.0178
[DD,EF]	0.0028
[DD,LBB]	-0.0093
[EF,LBB]	-0.0103
[EF,LBL]	-0.0278

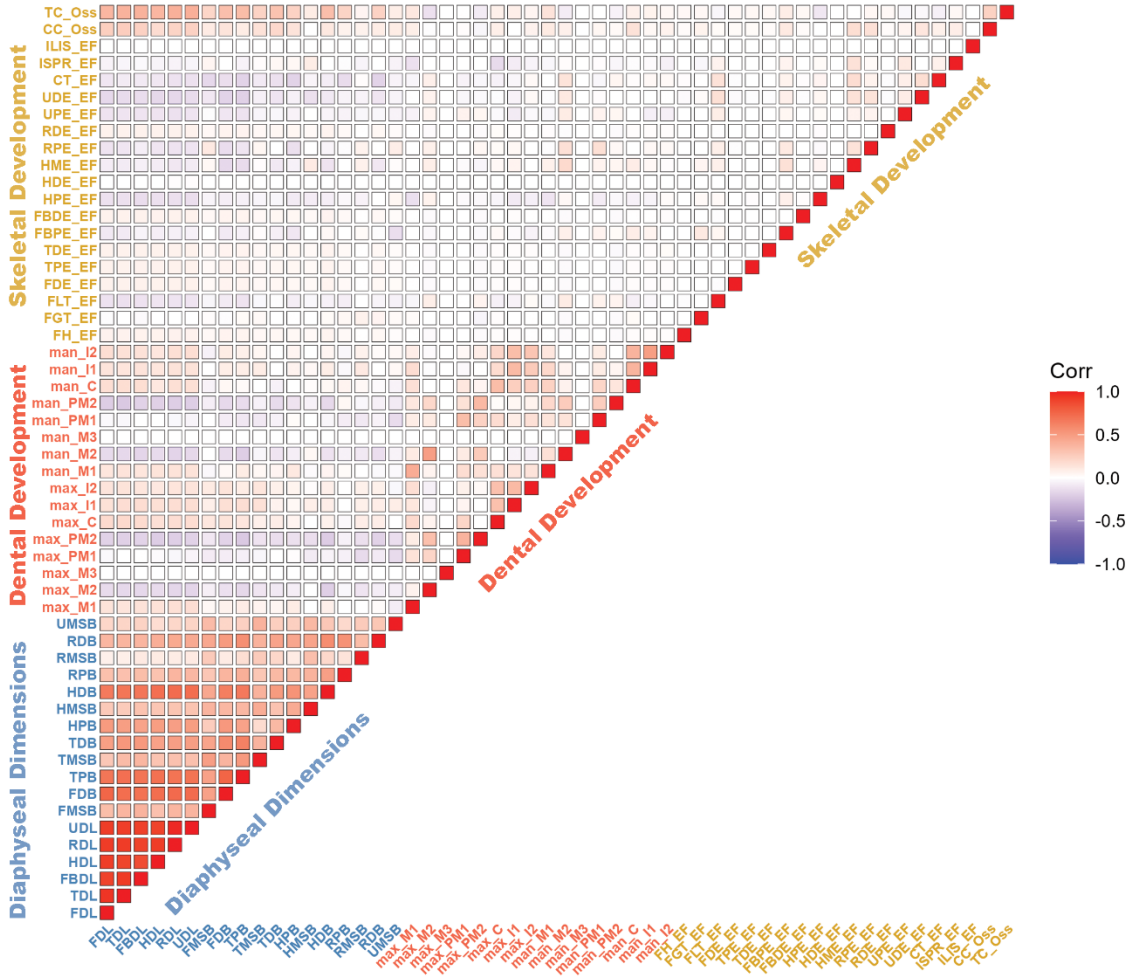

Figure 6.14. Correlogram showing relationship between 54 growth and development indicators from the childhood model. Labels are colored by growth module. Red = positive correlation, Blue = negative correlation, White = no correlation.

6.4.2 Skeletal Growth Module: Diaphyseal Dimensions

During childhood, the correlations between all length variables remains strongly positive ($r > 0.90$) (Figure 6.16). Overall, and in comparison to the infancy results (Section 6.3.2), the relationships are marginally weaker, but the same module pattern

exists whereby intervariable correlations between breadths and intervariable correlations between lengths are strongest.

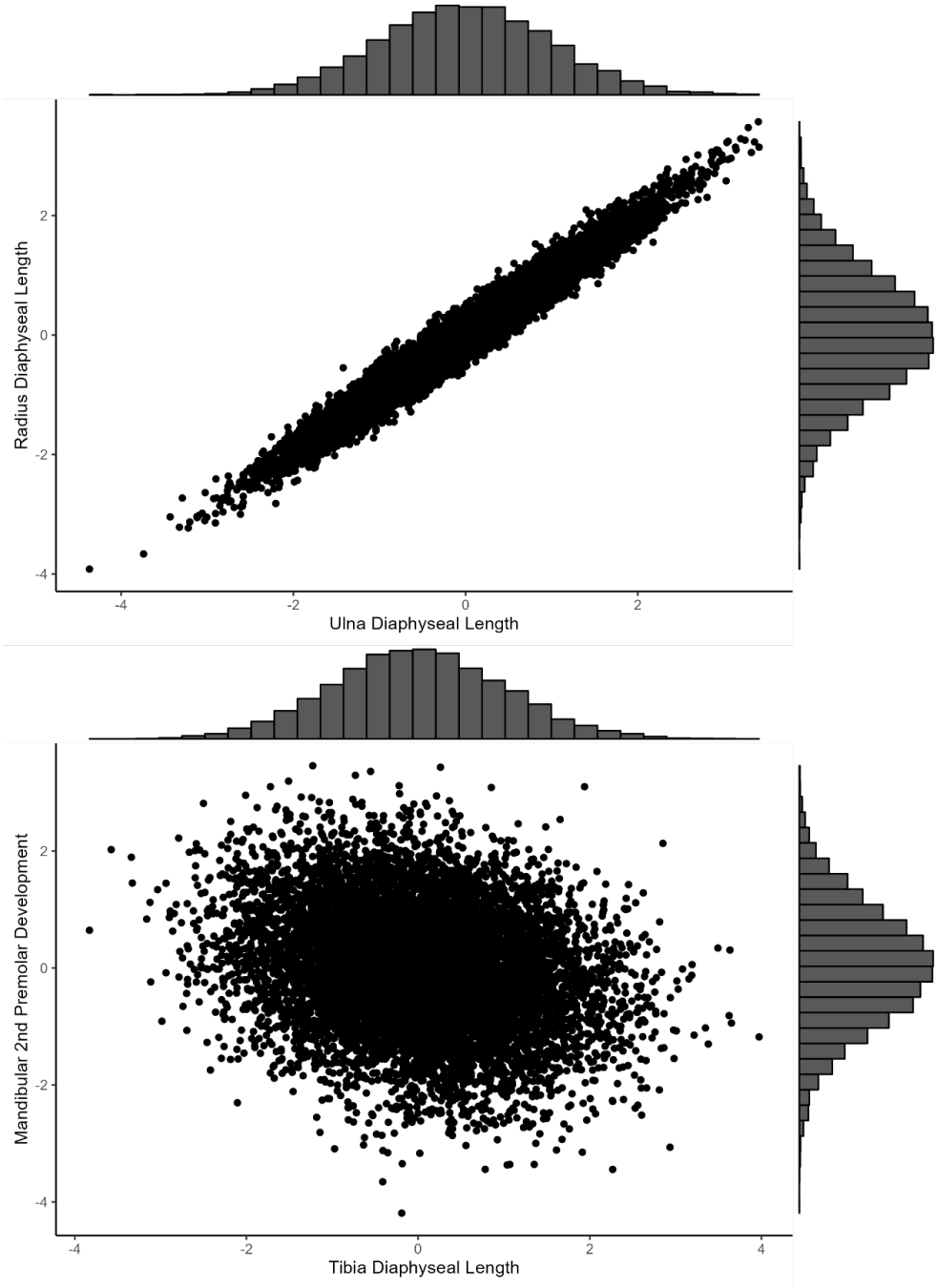

Figure 6.15. Copula scatterplot displaying the strongest (UDL x RDL, top) and weakest (TDL x man_PM2, bottom) correlations. The variables are standardized with each marginal distribution shown as a standard Gaussian distribution along the right and top axis. This is *z* in the equations described in Chapter 5.

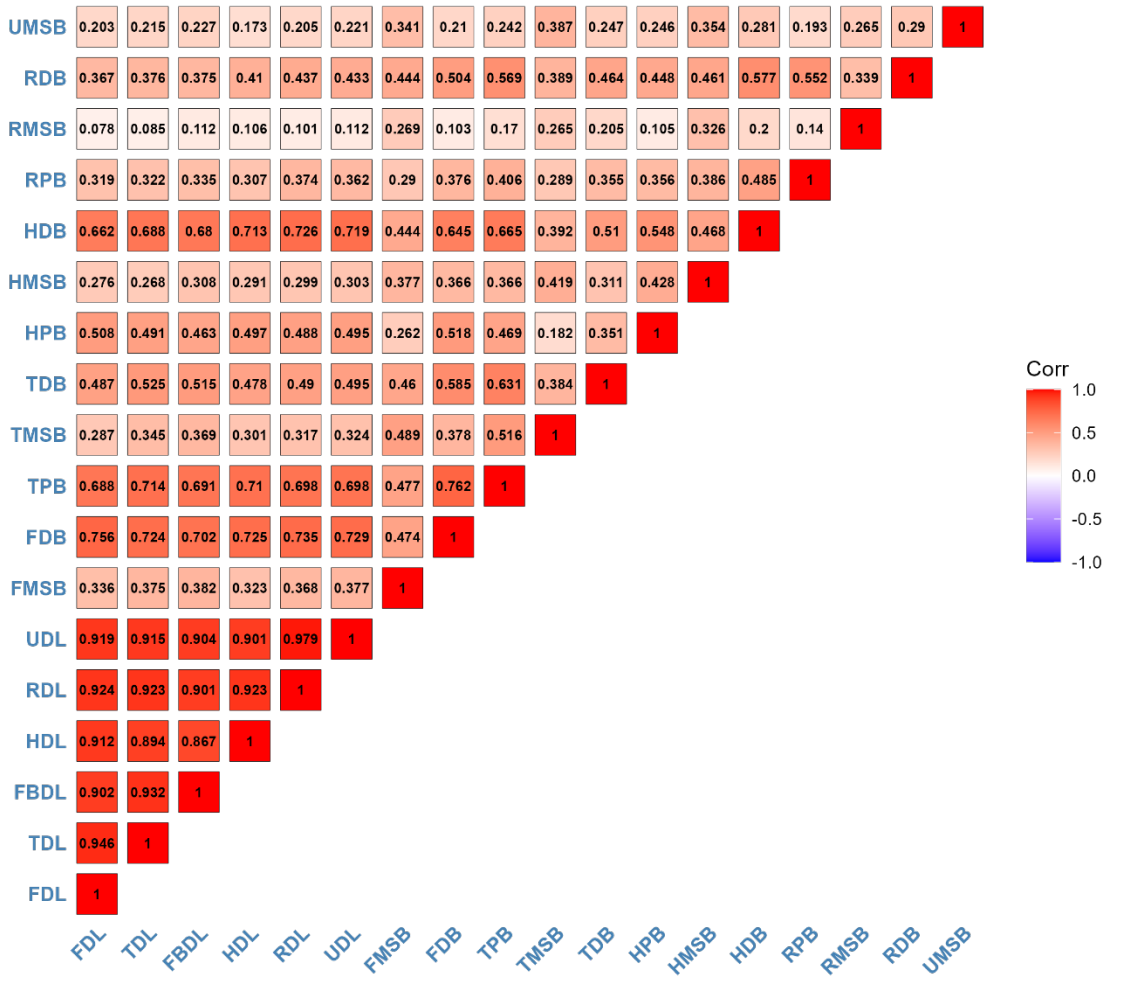

Figure 6. 16. Correlogram showing relationships between traits associated with the skeletal growth module from the childhood model. Red = positive correlation, Blue = negative correlation, White = no correlation.

6.4.3 Dental Development Module

Correlations between most dental traits increase from infancy to childhood (Figure 6.17). The increase in strength is especially prevalent between isomeres in the upper and lower dentition. For example, the correlation between upper and lower incisors (I1 and I2), canines (C), and upper and lower premolars (PM1 and PM2) all increase in strength in a positive direction from infancy to childhood. On the contrary, there is a

slight reduction in positive strength between teeth that were most active during infancy (e.g., max_I1 and man_I2) suggesting reduced activity or stasis during the childhood period in teeth whose development begins in infancy.

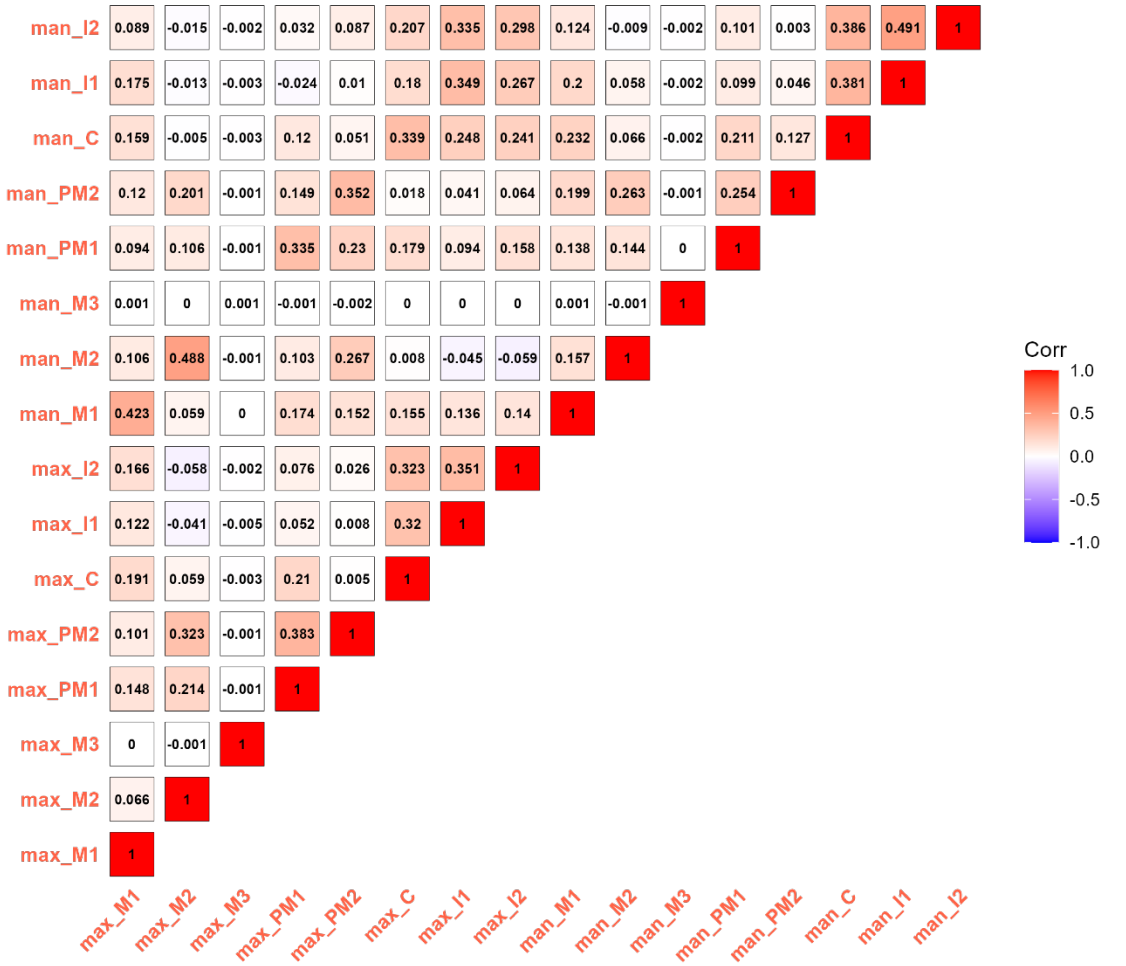

Figure 6.17. Correlogram showing relationships between traits associated with the dental development module from the childhood model. Red = positive correlation, Blue = negative correlation, White = no correlation.

6.4.4 Skeletal Development Module: Epiphyseal Fusion and Skeletal Ossification

During childhood, all traits associated with skeletal ossification and epiphyseal fusion show weak correlations ($r < 0.232$) (Figure 6.18). The strongest correlation is between carpal and tarsal ossification with $r = 0.232$. The weak relationships described here are likely related to the ordinal nature of the data resulting in a lack of variation in scores. In other words, if epiphyseal fusion is scored on a scale from 1-7, then during childhood, most traits are most likely at stage 1 with little to no variation across traits.

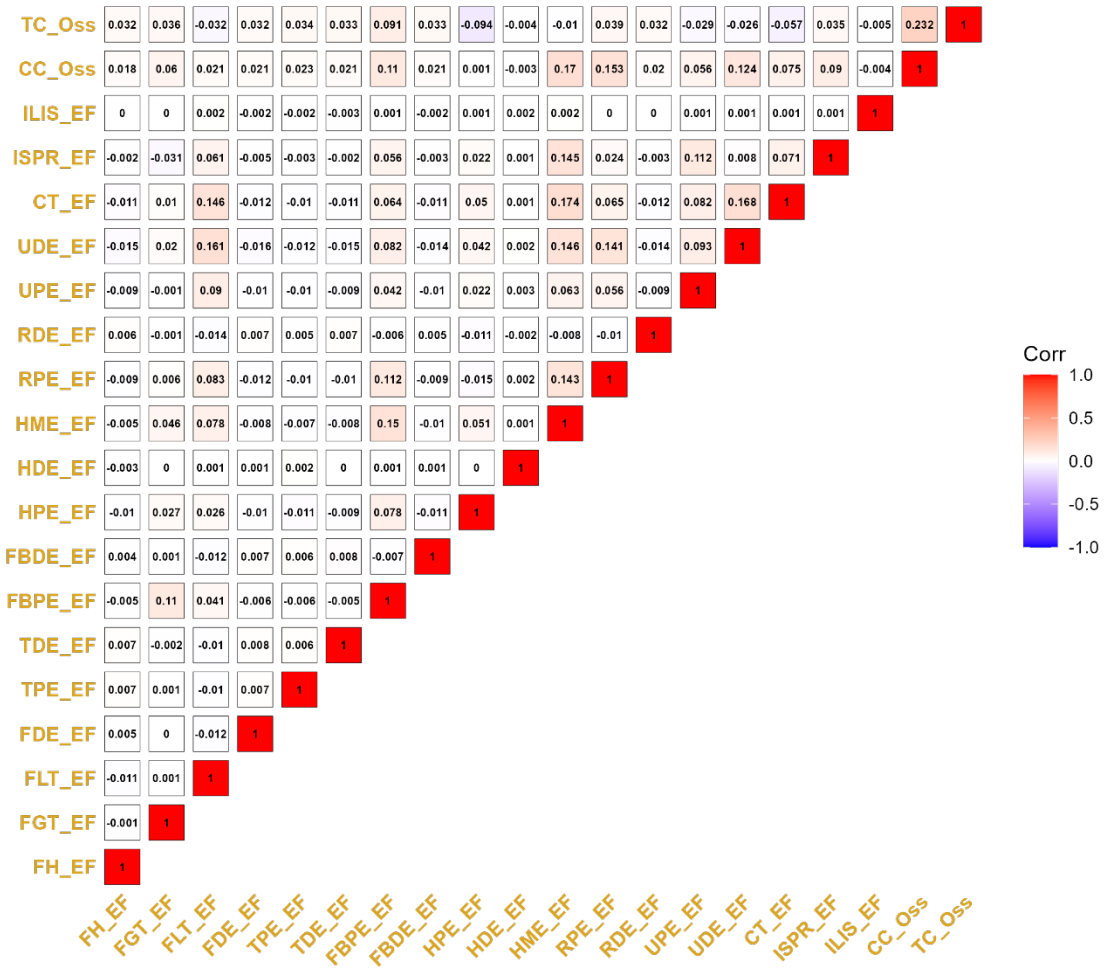

Figure 6. 18. Correlogram showing relationships between traits associated with the skeletal development module from the childhood model. Red = positive correlation, Blue = negative correlation, White = no correlation.

6.5 Juvenile & Adolescence Model

6.5.1 All Variables

Figure 6.19 displays the correlogram for all variables in the juvenile and adolescence model. During the juvenile and adolescence period, the growth modules first highlighted in Figure 6.4 (where the data are not subset by developmental stage) are recognizable in the dependency structure. That is, within-module relationships are stronger than between module relationships. This can be seen in Figure 6.19 in the lower left of the plot (skeletal growth module), center of the plot (dental development module) and top right of the plot (skeletal development module). This result is corroborated by the average correlations presented in Table 6.5. In contrast to infancy and childhood, relationships between pairs of epiphyseal fusion variables are moderate to strongly positive ([EF, EF], $r = 0.5221$). In fact, the strongest positive relationship overall is between fusion of the proximal tibia (TPE_EF) and distal femur (FDE_EF) ($r = 0.9203$). The weakest relationship is between fusion of the femoral head (FH_EF) and development of the maxillary second incisor (max_I2) ($r = -0.1733$) (Figure 6.20). Further, there is an overall reduction in positive strength of all intervariable relationships in the skeletal growth modules (e.g., FDL x HDL or HMSB x HPB). This is most likely because skeletal growth ceases during adolescence. Alternatively, epiphyseal fusion across all long bones is most active during this period. Combined, correlations across the juvenile and adolescence period corroborate the information in other stages whereby stronger correlations are tied to active growth and development.

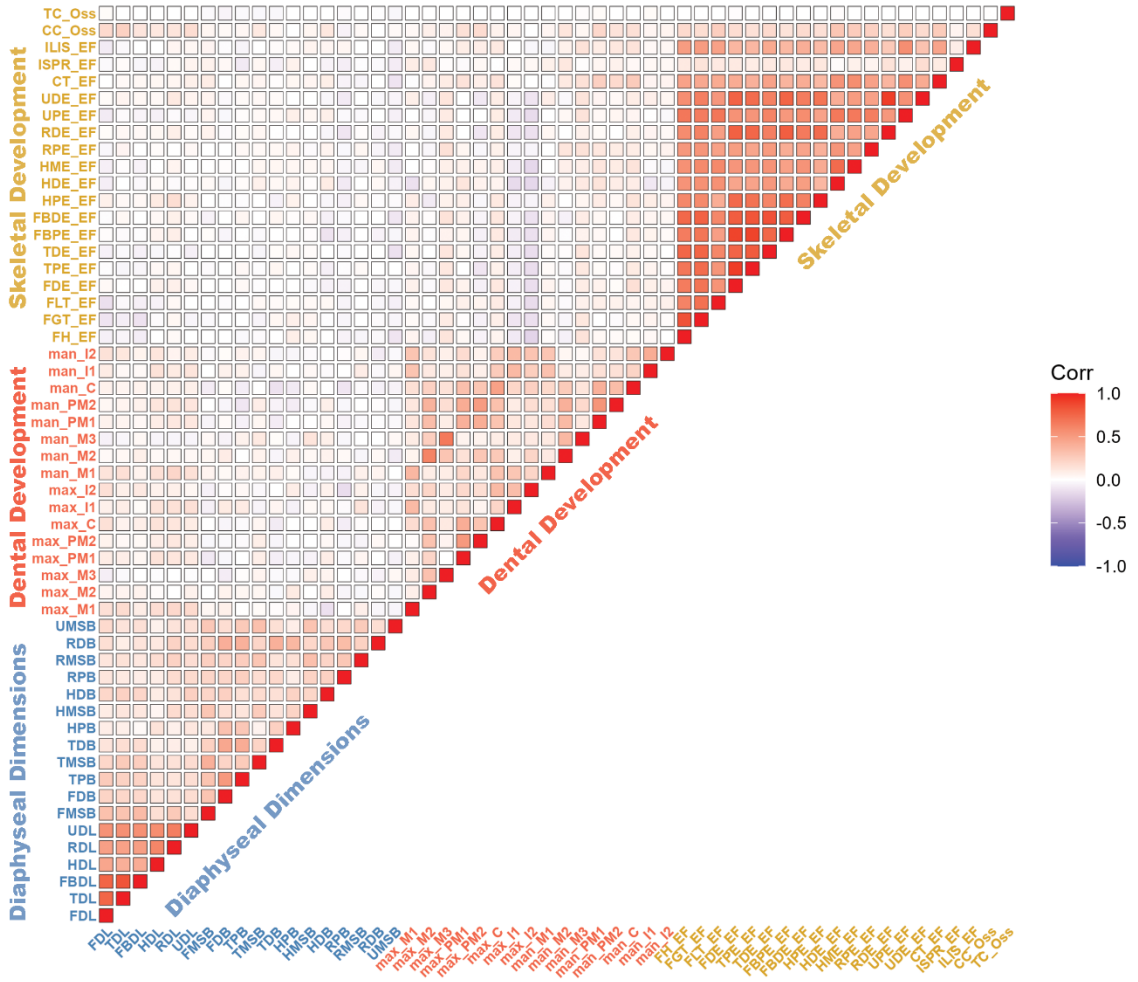

Figure 6.19. Correlogram showing relationship between 54 growth and development indicators from the juvenile and adolescence model. Labels are colored by growth module. Red = positive correlation, Blue = negative correlation, White = no correlation.

6.5.2 Skeletal Growth Module: Diaphyseal Dimensions

During juvenile and adolescence, correlations associated with all diaphyseal length variables are weaker and less positive than at any other point during ontogeny (Figure 6.21). Modules associated with appositional growth (breadths) and longitudinal growth (lengths) are still present during this developmental stage. Appositional growth at the distal radius (RDB) and at the proximal humerus (HPB) tends to occur slightly longer

than growth at other dimensions and may explain why a correlation associated with either measurement is stronger than the remainder of the bivariate relationships. Regardless, reduction in overall strength of the relationships (particularly in longitudinal growth) relates to the cessation of growth as fusion commences at the proximal and distal ends of each long bone.

Table 6.5. The average posterior correlation within and between growth modules for the juvenile and adolescence model. Displayed in descending order with the strongest relationship at top. DD = Dental Development; EF = Epiphyseal Fusion; LBB = Long Bone Breadth; LBL = Long Bone Length, OSS = Skeletal Ossification.

Variable Pairs	**Mean Posterior Correlations**
[LBL,LBL]	0.5731
[EF,EF]	0.5221
[LBB,LBB]	0.2447
[DD,DD]	0.2193
[LBB,LBL]	0.1617
[EF,OSS]	0.0975
[LBL,OSS]	0.0848
[DD,LBL]	0.0784
[DD,OSS]	0.0474
[DD,EF]	0.0325
[OSS,OSS]	0.0115
[LBB,OSS]	0.0086
[EF,LBL]	0.0050
[DD,LBB]	0.0029
[EF,LBB]	-0.0018

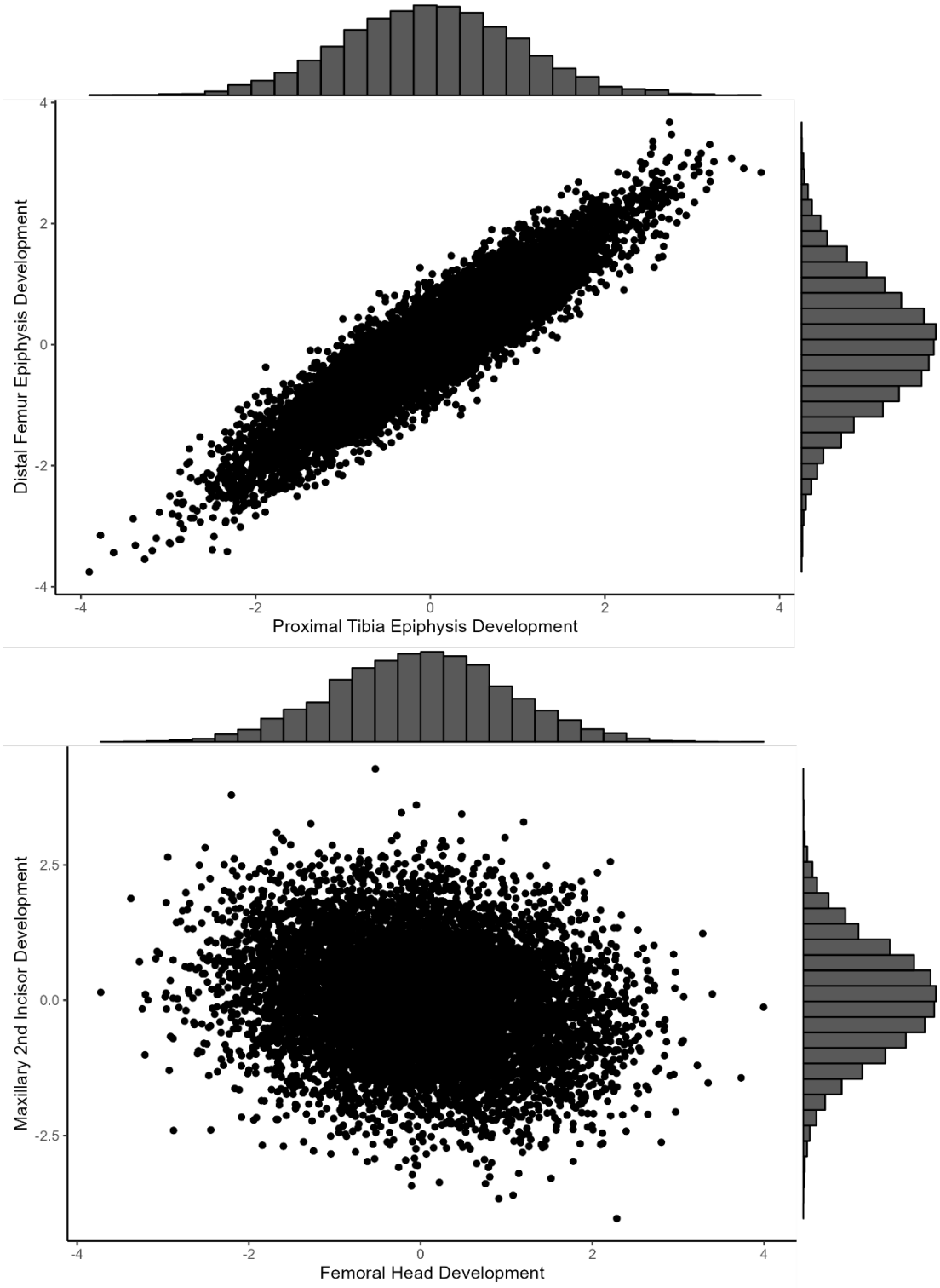

Figure 6. 20. Copula scatterplot displaying the strongest (TPE_EF x FDE_EF, top) and weakest (FH_EF x max_I2, bottom) correlations. The variables are standardized with each marginal distribution shown as a standard Gaussian distribution along the right and top axis. This is *z* in the equations described in Chapter 5.

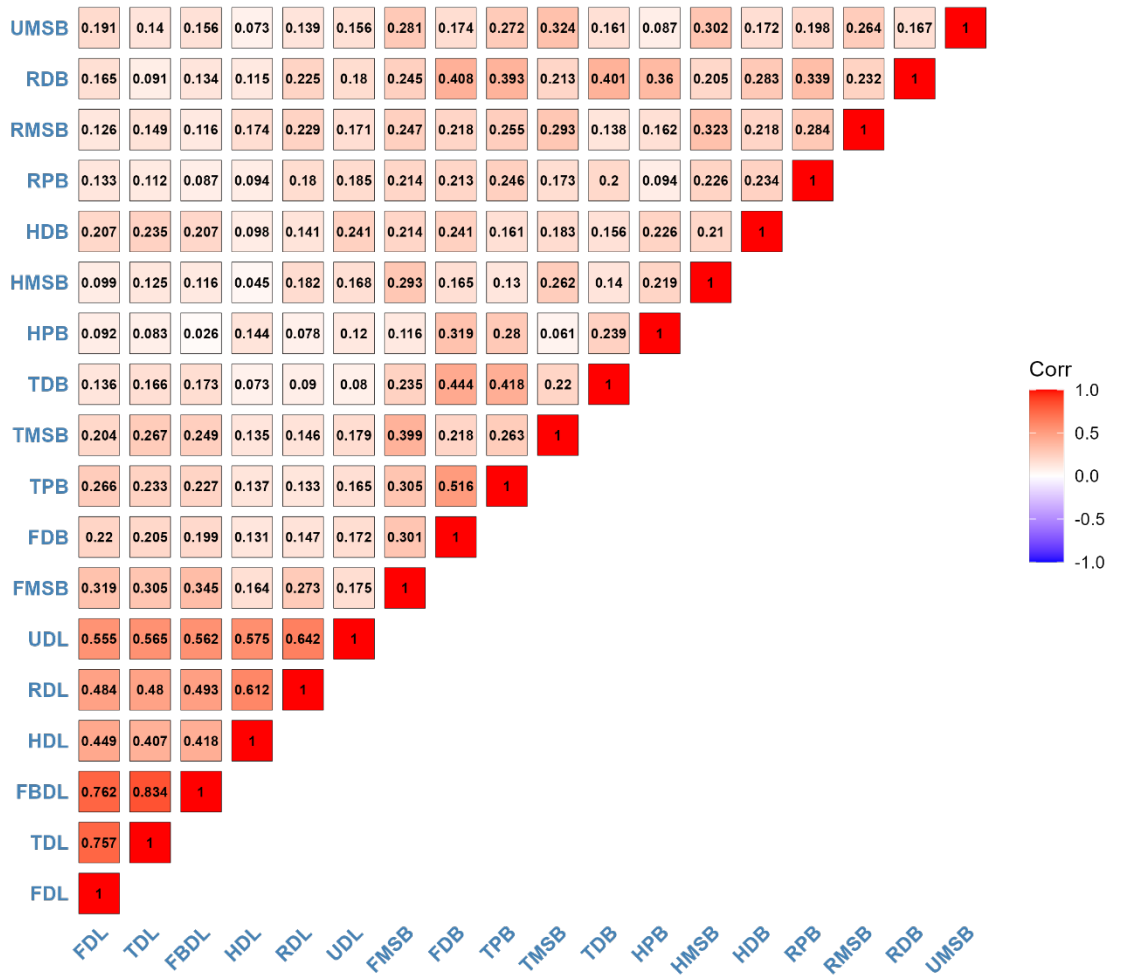

Figure 6. 21. Correlogram showing relationships between traits associated with the skeletal growth module from the juvenile and adolescnece model. Red = positive correlation, Blue = negative correlation, White = no correlation.

6.5.3 Dental Development Module

Correlations between dental traits have marginally increased in positive strength from infancy, to childhood, and now into the juvenile and adolescence stage of development (Figure 6.22). Similar to the other stages, isomeres are most strongly positively correlated. Additionally, later developing teeth, such as the second and third permanent molars (M2 and M3) and premolars (PM1 and PM2), are more strongly

correlated with each other as compared to earlier forming dentition, such as the first incisor and first permanent molar (I1 and M1, respectively).

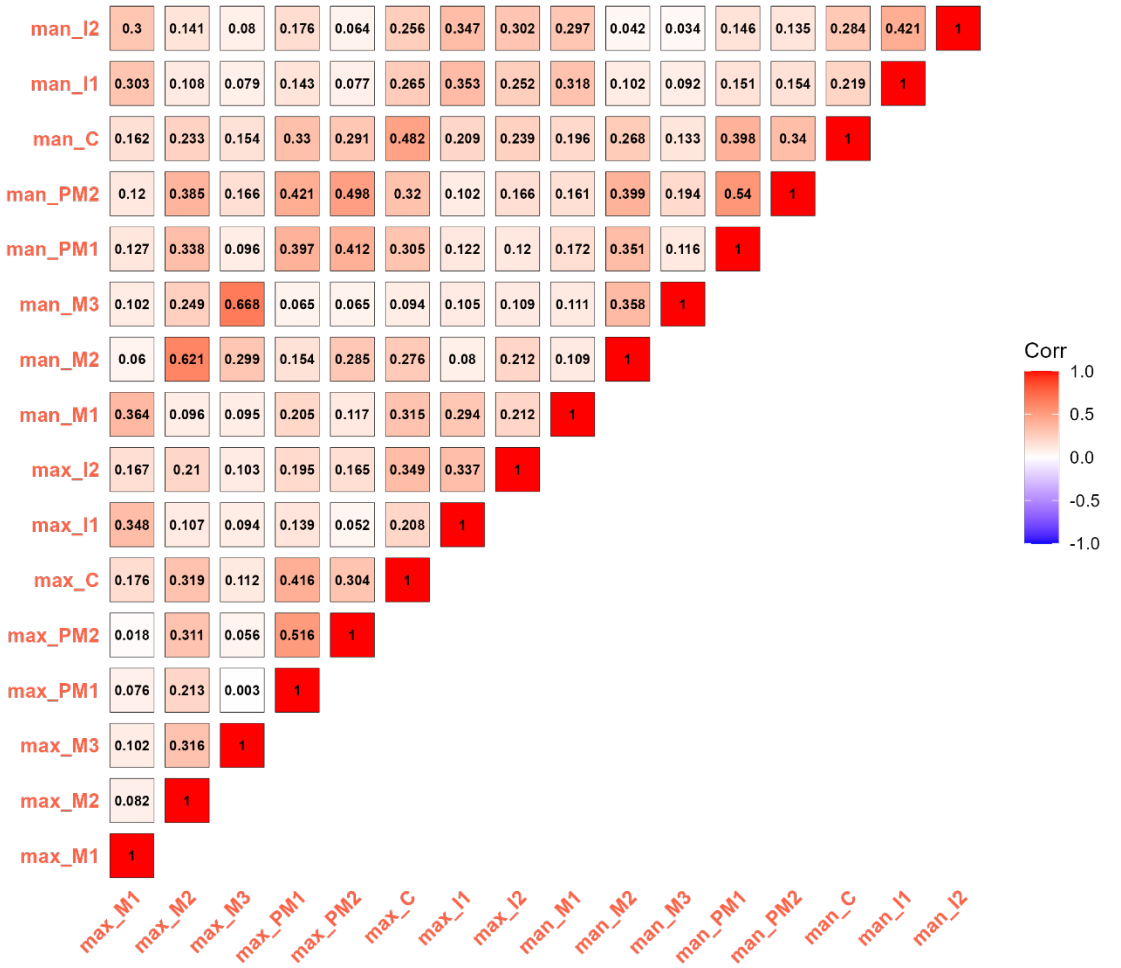

Figure 6. 22. Correlogram showing relationships between traits associated with the dental development module from the juvenile and adolescence model. Red = positive correlation, Blue = negative correlation, White = no correlation.

6.5.4 Skeletal Development Module: Epiphyseal Fusion and Skeletal Ossification

Traits within the skeletal development demonstrate the strongest positive correlations in the juvenile and adolescence periods (Figure 6.23). This is especially apparent between all proximal and distal epiphyses on both the upper and lower limbs.

Importantly, active fusion and development is ongoing during the juvenile and adolescence period coinciding with the stronger positive correlation values. The exception to this active pattern of growth is seen at both the ischio-pubic ramus (ISPR_EF) and ossification of the tarsals (TC_Oss) and carpals (CC_Oss). This is because of ischio-pubic ramus fusion and appearance of carpals and tarsals occurs much earlier during childhood and the very early juvenile period.

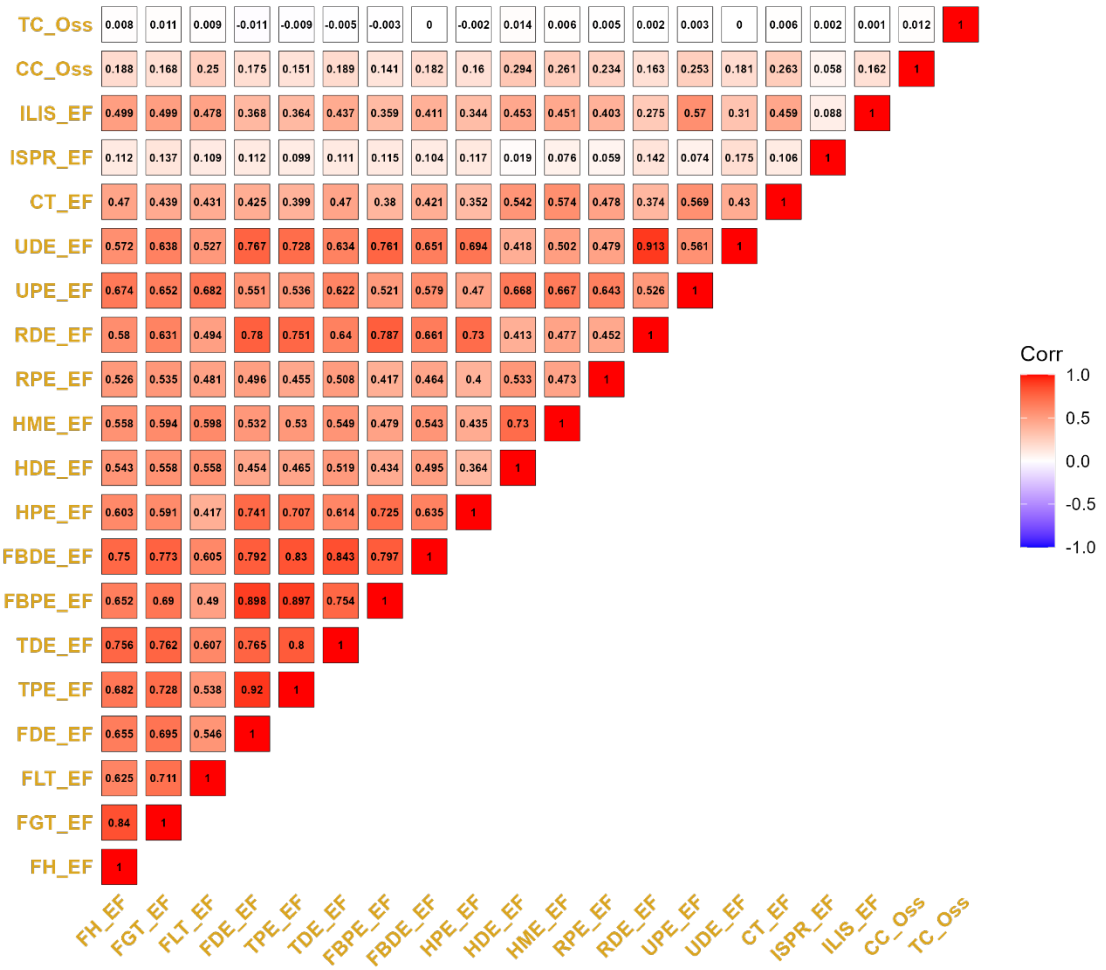

Figure 6. 23. Correlogram showing relationships between traits associated with the skeletal development module from the juvenile and adolescence model. Red = positive correlation, Blue = negative correlation, White = no correlation.

6.6 Biological Sex Models

6.6.1 All Variables

The correlation structure between males and females is similar (Figure 6.3; Figure 6.24 and Figure 6.25, respectively). Relationships are strongest within traits of the same growth module as compared to traits between two different growth modules (Table 6.6). In both males and females, the strongest positive correlation is between diaphyseal growth of the ulna (UDL) and radius (RDL) with $r = 0.989$ in males (Figure 6.26) and $r = 0.988$ in females (Figure 6.27). Similarly, the weakest correlations are also the same between sexes demonstrated by the correlation between proximal epiphysis of the ulna (UPE_EF) and diaphyseal length of the ulna (UDL) (male $r = -0.256$; female $r = -0.271$) (Figure 6.26 and Figure 6.27, respectively). Across both sexes, elements that share similar developmental trajectories, such as early forming dentition (M1, I1, and I2) and growth in length of the diaphyses, are all more strongly correlated as compared to elements that diverge or grow at different periods during development. These results corroborate those from previous sections suggesting growth is patterned within specific growth modules. Females do display marginally weaker relationships across growth modules as compared to males (e.g., LBL x LBL in males is 0.9529, while it is 0.9439 in females) (Table 6.6). However, even with the marginally weaker correlations, there does not appear to be a sex-specific correlation pattern between growth and development traits.

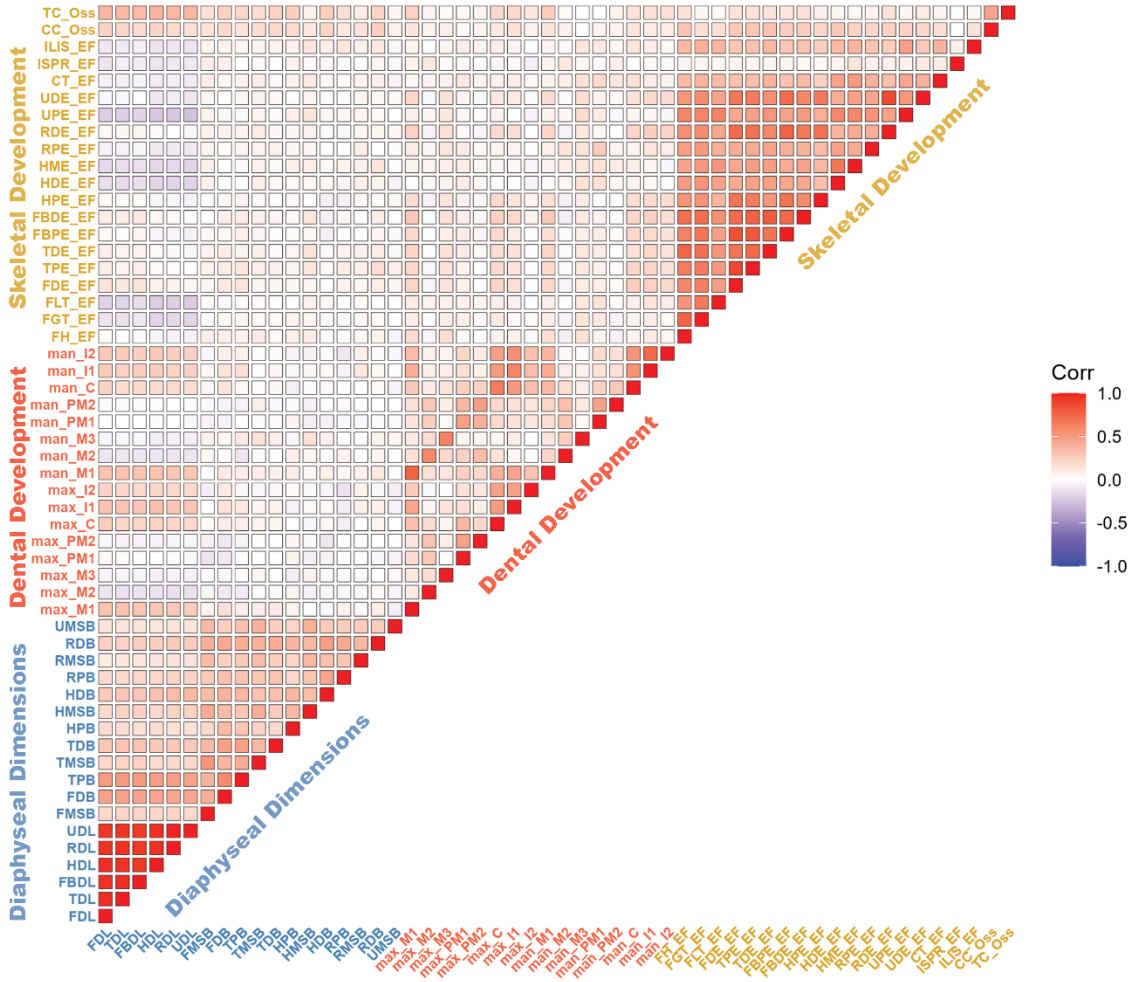

Figure 6.24. Correlogram showing relationship between 54 growth and development indicators from the male model. Labels are colored by growth module. Red = positive correlation, Blue = negative correlation, White = no correlation.

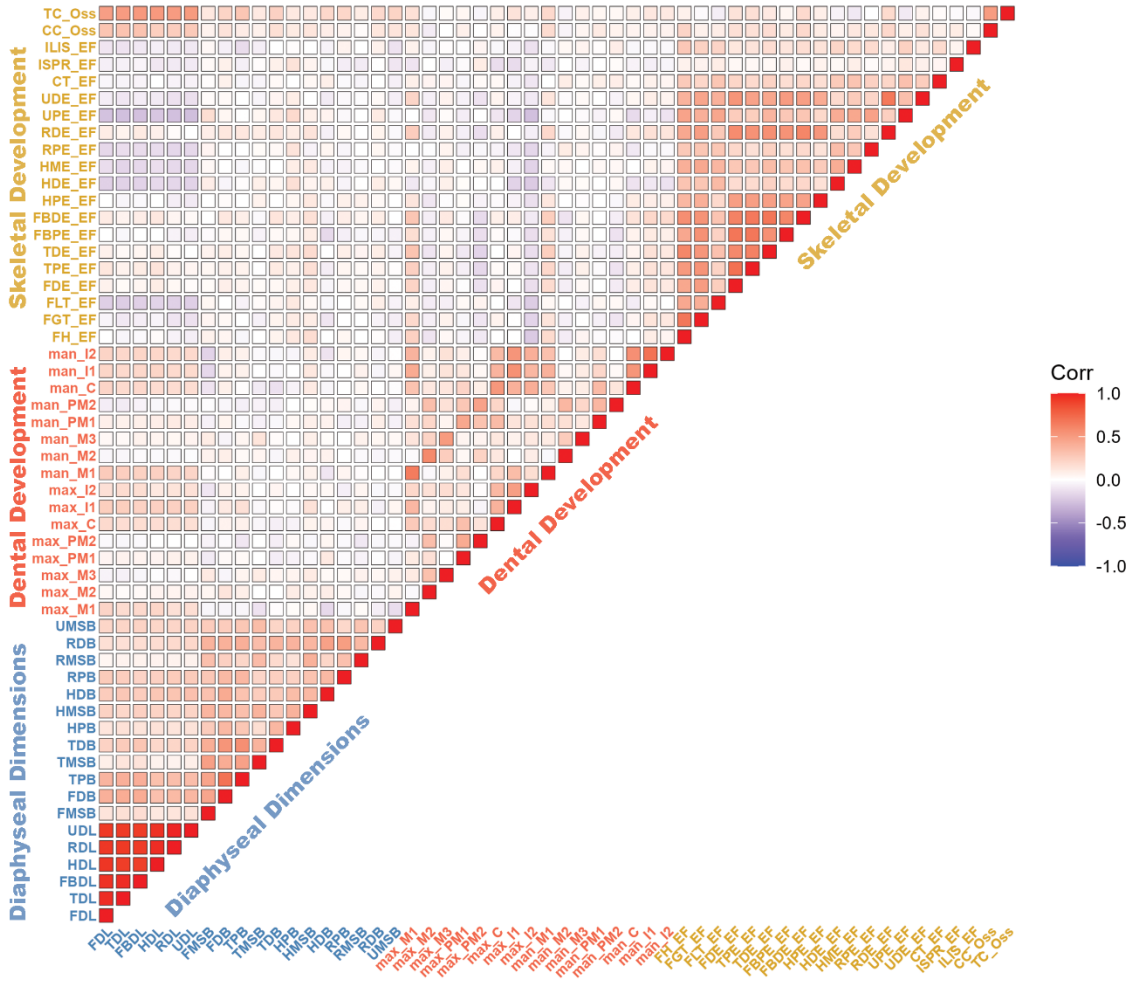

Figure 6.25. Correlogram showing relationship between 54 growth and development indicators from the female model. Labels are colored by growth module. Red = positive correlation, Blue = negative correlation, White = no correlation.

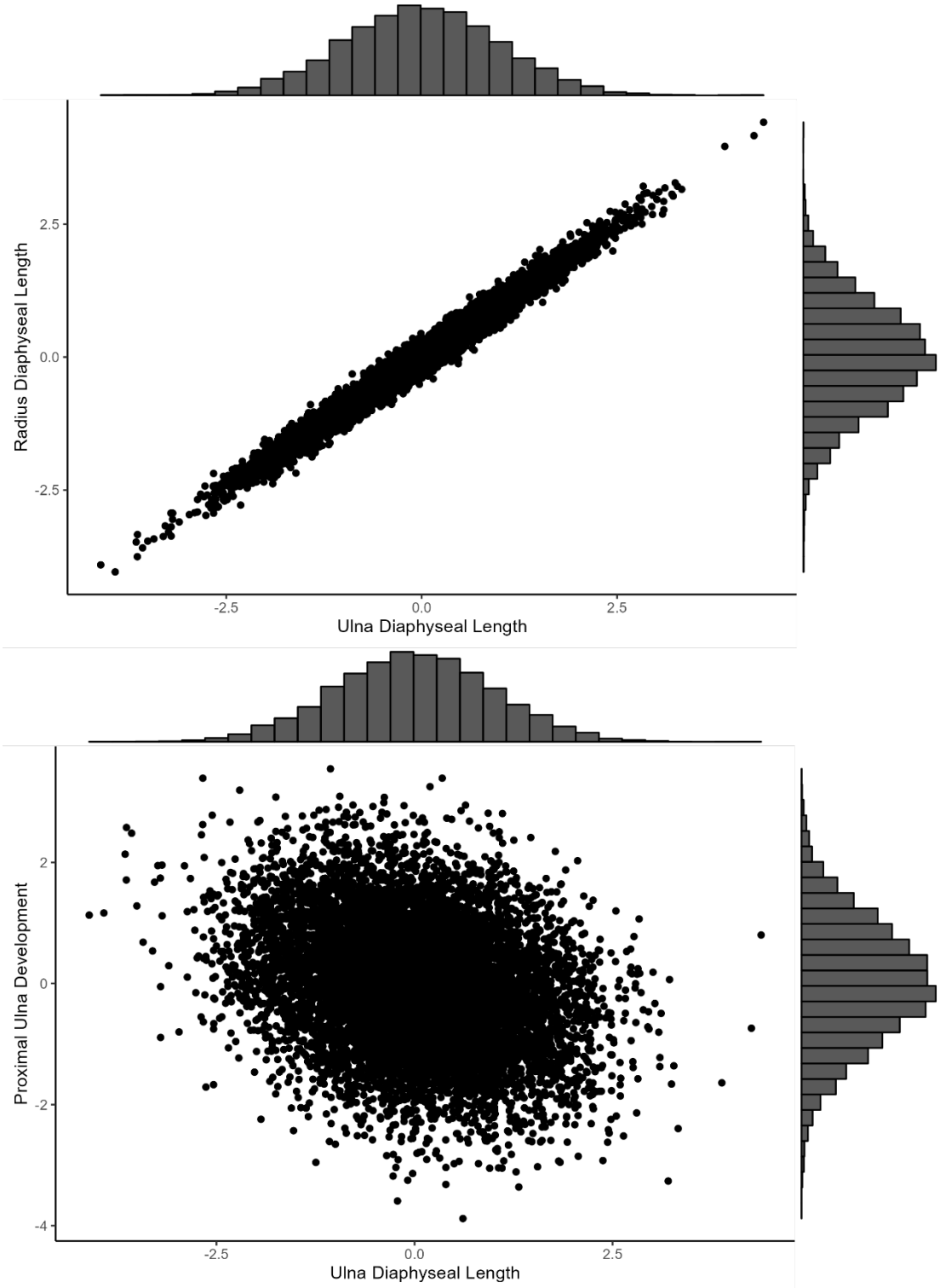

Figure 6. 26. Copula scatterplot displaying the strongest (UDL x RDL, top) and weakest (UDL x UPE_EF, bottom) correlations in the male model. The variables are standardized with each marginal distribution shown as a standard Gaussian distribution along the right and top axis. This is *z* in the equations described in Chapter 5.

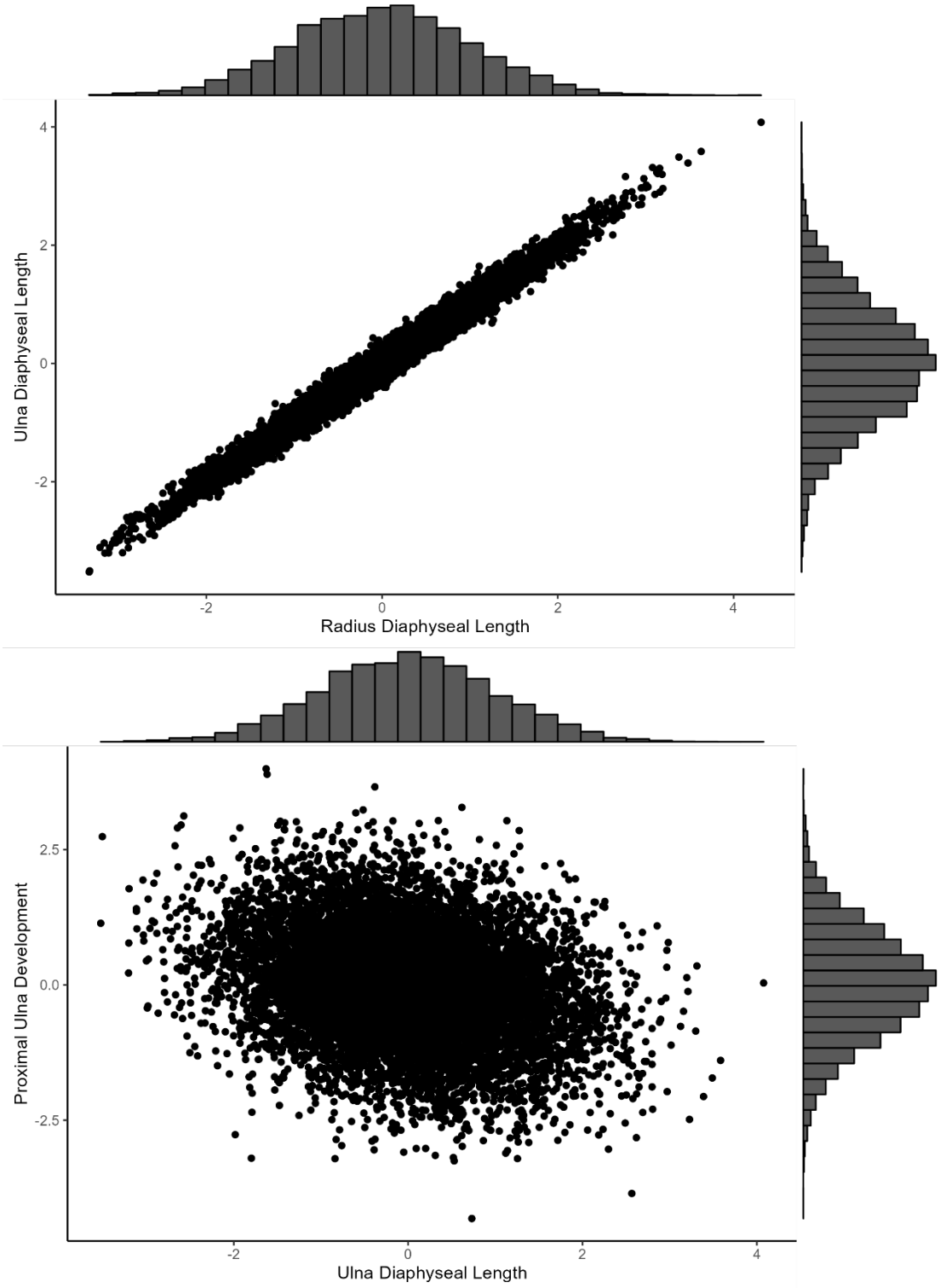

Figure 6.27. Copula scatterplot displaying the strongest (UDL x RDL, top) and weakest (UDL x UPE_EF, bottom) correlations in the female model. The variables are standardized with each marginal distribution shown as a standard Gaussian distribution along the right and top axis. This is *z* in the equations described in Chapter 5.

Table 6. 6. The average posterior correlation within and between growth modules for both the male and female models. Displayed in descending order with the strongest relationship at top. DD = Dental Development; EF = Epiphyseal Fusion; LBB = Long Bone Breadth; LBL = Long Bone Length; OSS = Skeletal Ossification.

Variable Pairs	Mean Posterior Correlations (Male)	Mean Posterior Correlations (Female)
[LBL,LBL]	0.9529	0.9439
[EF,EF]	0.4685	0.3192
[OSS,OSS]	0.4532	0.5014
[LBB,LBB]	0.3420	0.3402
[LBL,OSS]	0.2793	0.3939
[LBB,LBL]	0.2562	0.2144
[DD,DD]	0.2402	0.2049
[LBB,OSS]	0.1701	0.1377
[EF,OSS]	0.1521	0.0810
[DD,LBL]	0.1028	0.1068
[DD,OSS]	0.0974	0.0547
[DD,EF]	0.0818	0.0032
[EF,LBB]	0.0427	0.0267
[DD,LBB]	0.0143	0.0073
[EF,LBL]	-0.0570	-0.0599

6.6.2 Skeletal Growth Module: Diaphyseal Dimensions

Both males and females show stronger, positive correlations between diaphyseal dimensions associated with lengths as compared to variables associated with breadths (Figure 6.28 and Figure 6.29). Females display slightly weaker positive correlations across either growth dimension. In both sexes, midshaft breadths tend to be more weakly correlated with all other variables as compared to proximal and distal breadths. There is no sex-specific correlation pattern to skeletal growth variables.

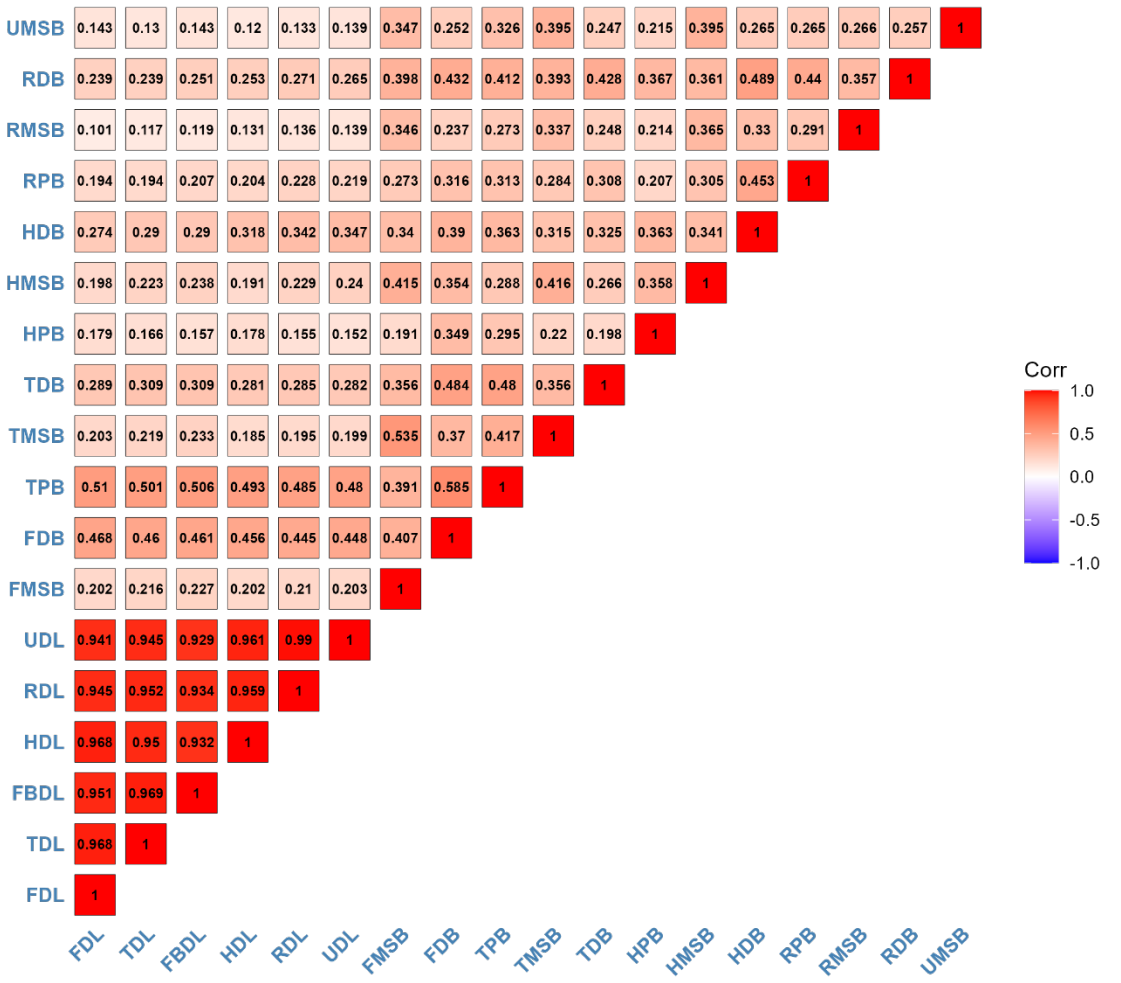

Figure 6. 28. Correlogram showing relationships between traits associated with the skeletal growth module from the male model. Red = positive correlation, Blue = negative correlation, White = no correlation.

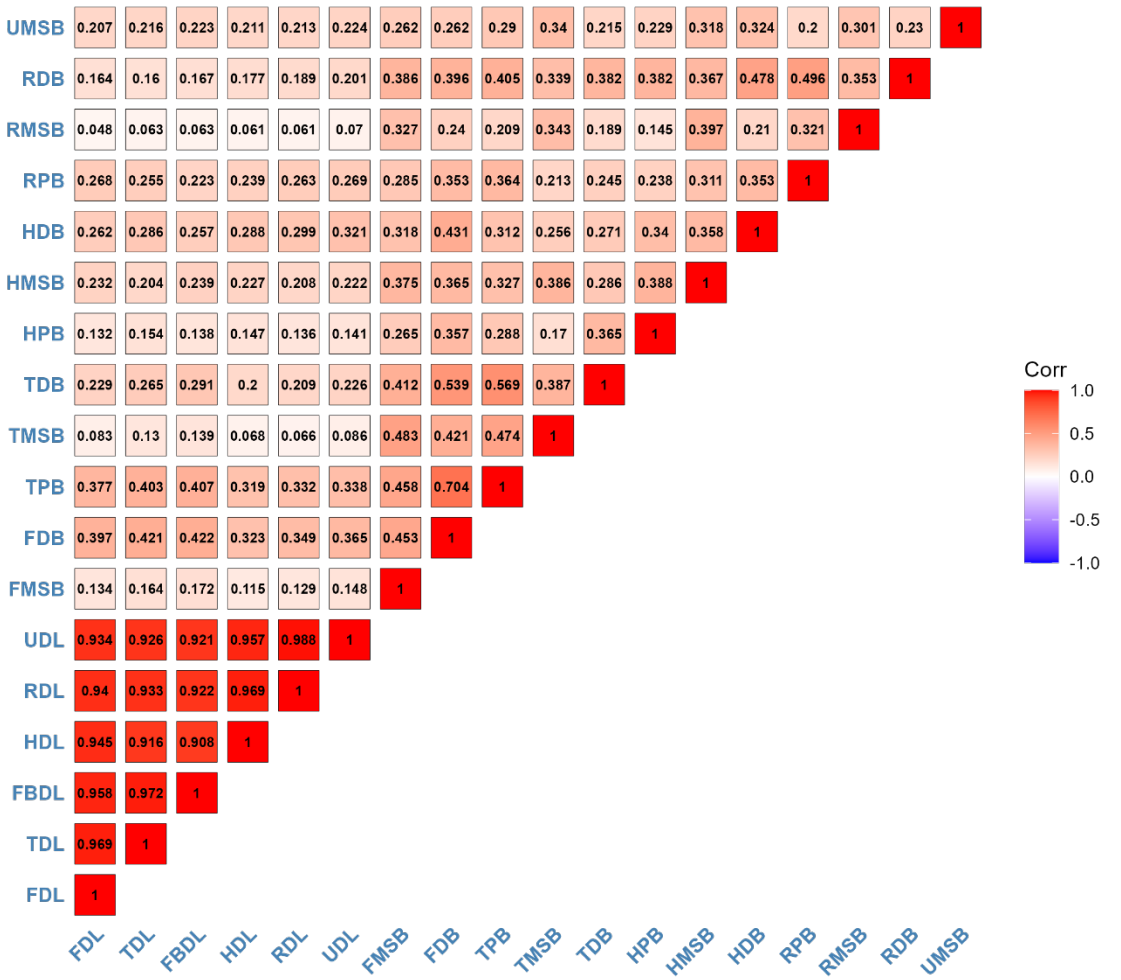

Figure 6. 29. Correlogram showing relationships between traits associated with the skeletal growth module from the female model. Red = positive correlation, Blue = negative correlation, White = no correlation.

6.6.3 Dental Development Module

Males and females show similar correlation patterns in dental development (Figure 6.30, and Figure 6.31, respectively). Isomeres between the upper and lower dentition are the strongest and most positively correlated teeth. The results between both sexes mirror those from previous sections whereby strength of the relationships between individual teeth coincides with developmental period or time frame within which each tooth may develop. In other words, teeth that begin development earlier and cease development at similar period are strongly correlated (e.g., M1 and I1), and teeth that begin development later and complete development later are also more strongly correlated (e.g., M2 and M3). There is no sex-specific correlation pattern suggestive of differences between males or females.

6.6.4 Skeletal Development Module: Epiphyseal Fusion and Skeletal Ossification

There are no sex differences in the pattern of variable correlations associated with skeletal development module (Figure 6.32 and Figure 6.33). Elements related to epiphyseal fusion at the long bones are all moderate to strongly correlated with each other, while those associated with other anatomical locations such as the pelvis (ISPRE_EF), carpals (CC_Oss), and tarsals (TC_Oss and CT_EF) are weakly correlated with all other variables. This is most likely because of the similar developmental timing associated with the appearance and fusion of long bone epiphyses as compared to the appearance and/or fusion of other anatomical locations.

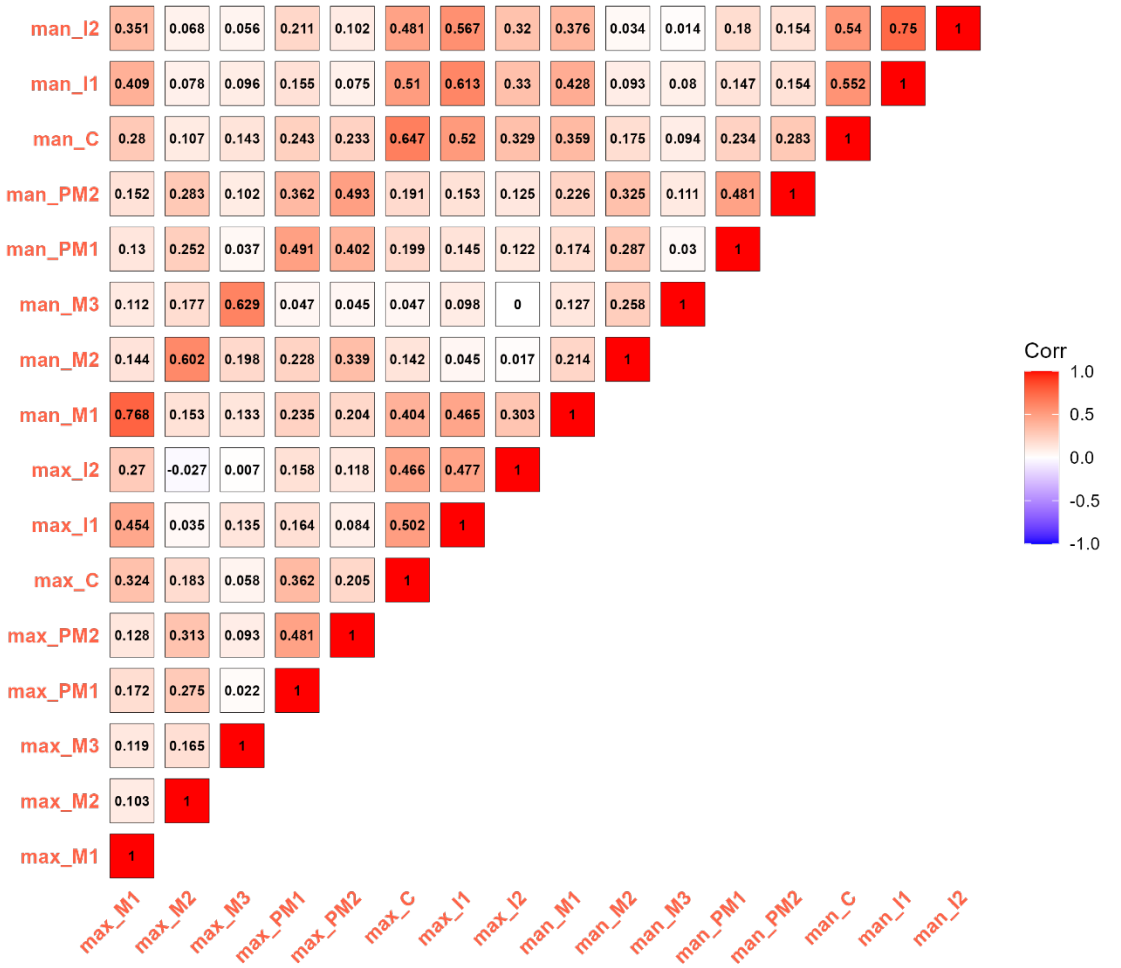

Figure 6. 30. Correlogram showing relationships between traits associated with the dental development module from the male model. Red = positive correlation, Blue = negative correlation, White = no correlation.

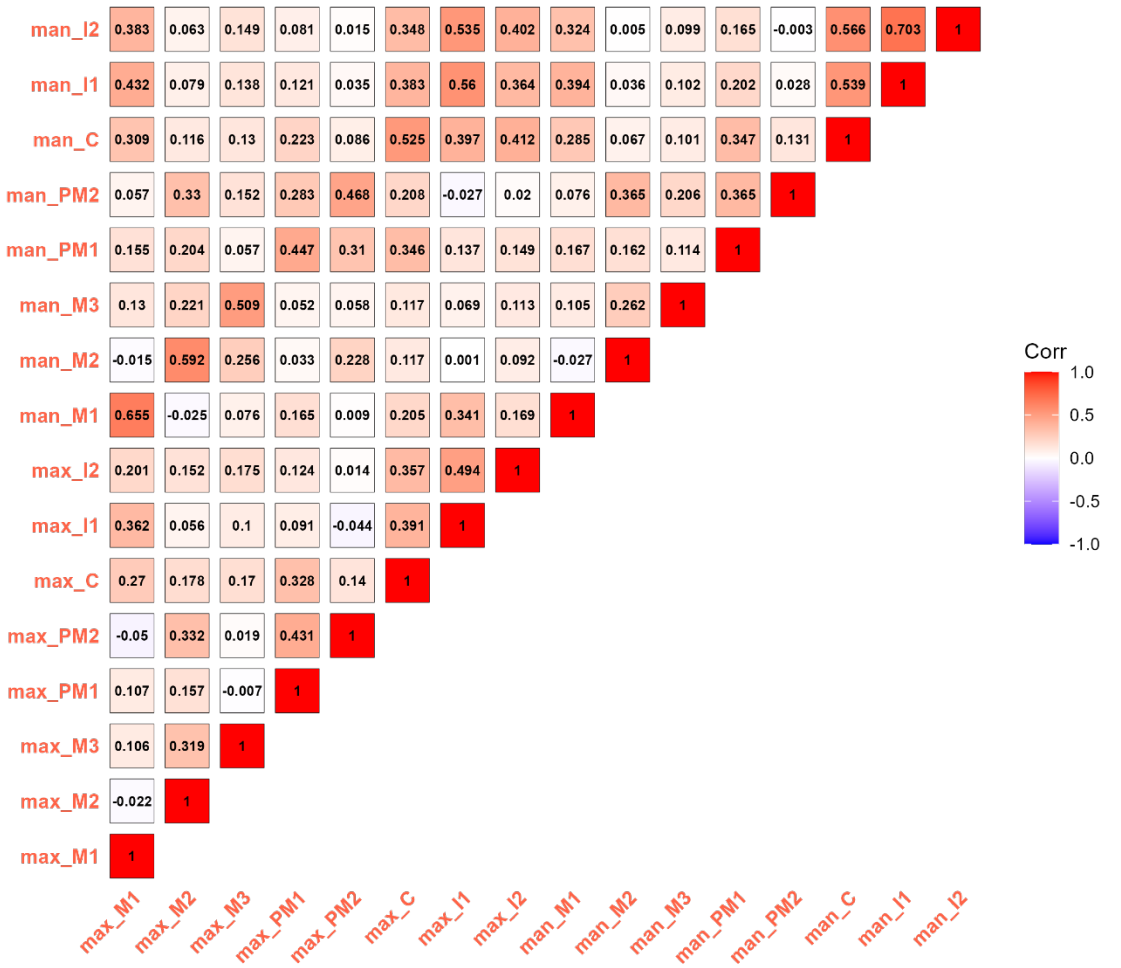

Figure 6. 31. Correlogram showing relationships between traits associated with the dental development module from the female model. Red = positive correlation, Blue = negative correlation, White = no correlation.

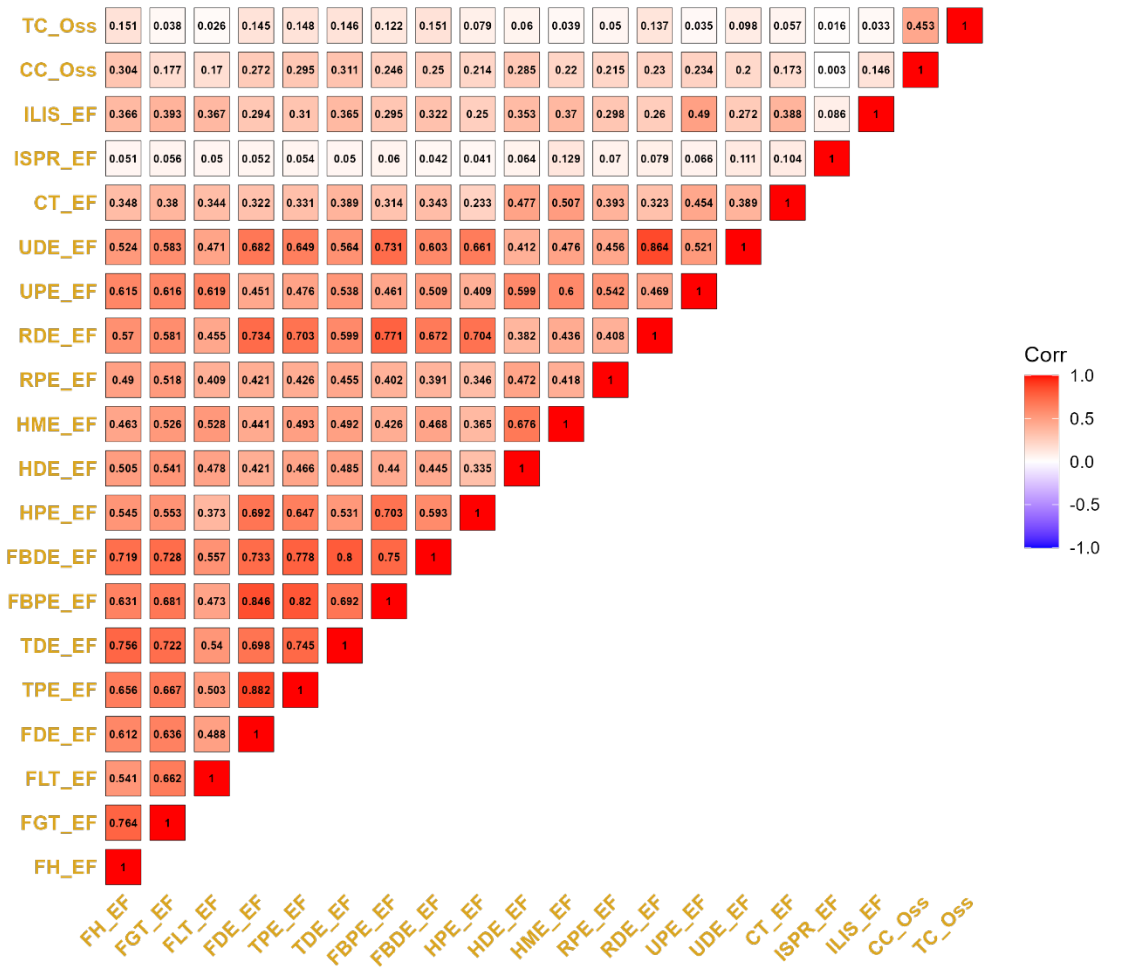

Figure 6. 32. Correlogram showing relationships between traits associated with the skeletal development module from the male model. Red = positive correlation, Blue = negative correlation, White = no correlation.

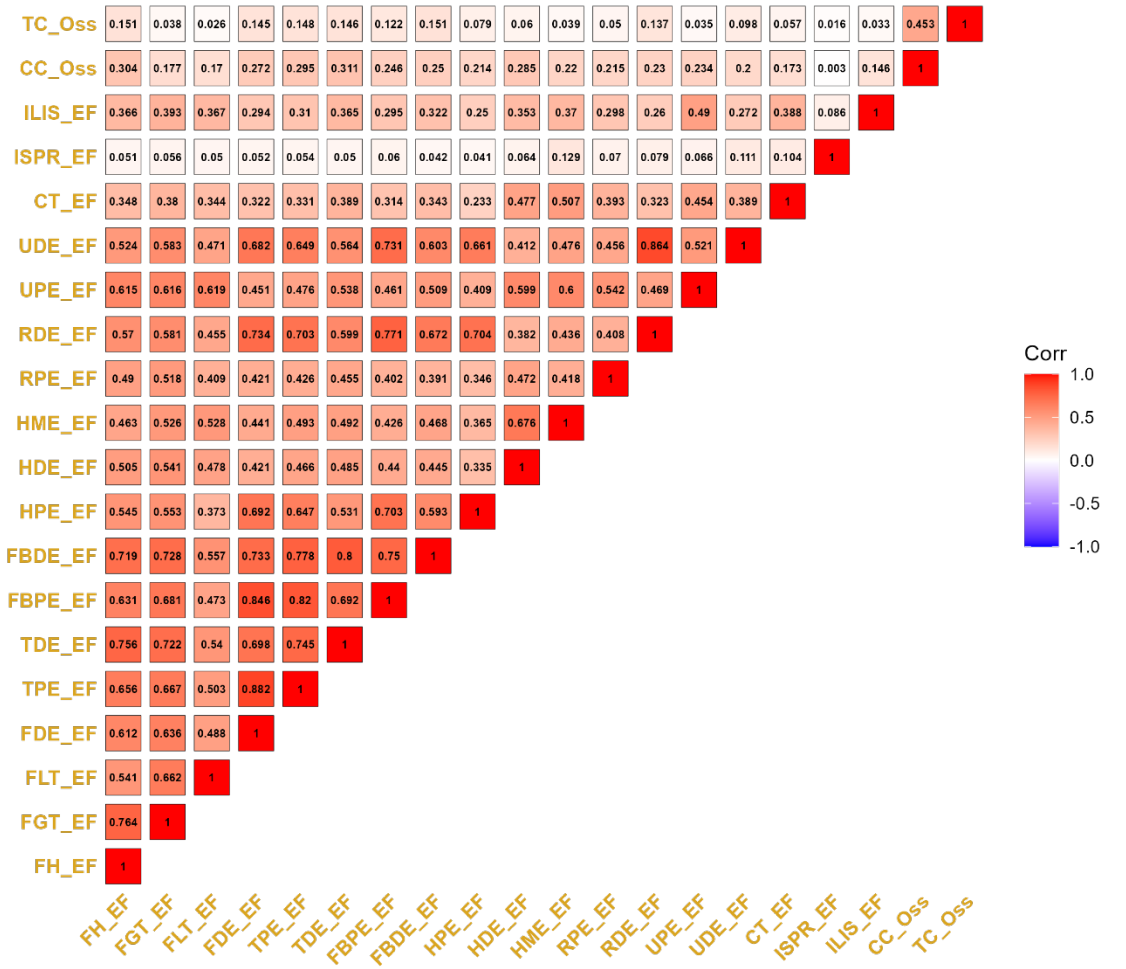

Figure 6. 33. Correlogram showing relationships between traits associated with the skeletal development module from the female model. Red = positive correlation, Blue = negative correlation, White = no correlation.

Chapter 7 – Discussion

This study introduces a novel statistical method to biological anthropology and the multivariate study of the human (or non-human primate) phenotype. Until recently, researchers neither had the data nor the statistical or computational methods to provide efficient, valid, and biologically interpretable results describing the interplay between the multivariate and multifactorial growth and development phenotype. This work and the computational approach offered through the Mixed Discrete-Continuous Gaussian copula results in the most comprehensive investigation into the multivariate and multifactorial processes that define the interplay between skeletal growth, skeletal development, and dental development. With the inclusion of 54 individual growth and development traits made possible with virtual anthropology and the Subadult Virtual Anthropology Database (SVAD), the 1,431 unique pairwise trait relationships learned from the Mixed Discrete-Continuous Gaussian copula leads to the largest known exposition of the growth and development phenotype of any single human population. By applying the Mixed Discrete-Continuous copula to different subsets of the larger sample, the results highlight how learning *more* relationships improves our ultimate understanding of the multivariate phenotype and the proximate understanding of inter-trait relationships. Importantly, interrelationships between *many* raw trait measurements or scores expose the dependency among dental development and skeletal growth and development traits and the variability across modules when considering developmental periods and biological sex. The patterns of correlation are corroborated by genetic, environmental, and embryological origins of variation across human growth and development. Excitingly, the copula enables future

research to easily move beyond the goals of the current study and are easily applicable to various subfields of biological anthropology.

While the immediate work expands upon previous research investigating interrelationships, integration, and phenotypic variation across human ontogeny, the results also contribute tens of thousands of parameters across all models that can be explored further in innumerable research areas. For example, future research questions may include the exploration of trait interrelationships across time (bioarchaeology), the evolution of hominin growth patterns (paleoanthropology), the improvement of chronological age estimation techniques (forensic anthropology), and perhaps most exciting, the use of the joint multivariate distribution to estimate missing components, which can impact all previously described contexts.

7.1 More is Better: Expanding Previous Research into Trait Interrelationships

Previous analyses investigating interrelationships between human growth and development traits were limited in scope to few restrictive and arbitrary pairwise correlations across select traits (e.g., Demirjian, Buschang, Tanguay, & Patterson, 1985; Demisch & Wartmann, 1956; Lamons & Gray, 1958). Such restrictions are the result of study-specific sampling techniques and the traditional usage of longitudinal growth studies which, while useful in delineating individual patterns of growth across a *small* number of traits (e.g., stature, femoral growth, weight, molar development), do not provide the data necessary to study the *multivariate* phenotype. The sampling protocols in the present study broadens the scope of previous research with the usage of 54

individual growth traits to investigate trait interrelationships. Specifically, virtual anthropology and open access repositories, such as those associated with SVAD, lead to both larger sample sizes and a greater number of growth and development traits from which to study interrelationships. The Mixed-Discrete Continuous Gaussian copula is therefore able to take advantage of the increased data availability to provide an even more robust analysis of inter-trait relationships.

With the inclusion of more growth and development traits comes the necessity to analyze the relationships between disparate data types like continuous data and ordinal data. In the past, when traits of different data types were analyzed the researchers often related observed skeletal and/or dental growth and development information to measures of skeletal and/or dental age (e.g., Demirjian, Buschang, Tanguay, & Patterson, 1985; Demisch & Wartmann, 1956; Lamons & Gray, 1958). However, these approaches conflate the known variability between different aspects of biological age and chronological age as evidence for the lack of interrelationships between different growth modules. Instead of relying on disparate, continuous measurements of skeletal versus dental age, which is the result of different variable combinations where you are unsure what trait is contributing more or less or how they are interacting, the copula allows for interpretable comparisons between different data types without introducing added layers of error such as the inclusion of biological age metrics. In fact, by describing interrelationships between *many* raw trait measurements or scores, the results here show that dental development and skeletal growth and development are neither as independent as previously thought nor are their interrelationships uniform across traits comparisons of the same modules. For example, in the full model (Figure 6.4), the correlation between

development and fusion of the distal epiphysis of the fibula (FBDE_EF) and development of the first mandibular molar (man_M1) is 0.357 – a weak to moderate positive relationship. At the same time, the correlation between FBDE_EF and development of the second mandibular premolar (man_PM2) is -0.004 – no dependence or correlation between the traits. This example shows that broad developmental relationships between growth modules cannot be extrapolated from one pairwise comparison. Instead, the relationship between skeletal development and tooth development is variable depending on tooth class and skeletal location. The copula expounds and clarifies historic research and shows that independence between one pair of traits (e.g., FBDE and man_PM2) does not necessarily suggest independence in another (e.g., FBDE_EF and man_M1). Therefore, discussion of (in)dependence between broad growth modules should be conveyed in reference to the variable pairwise relationships across individual trait pairs.

The use of the Mixed Discrete-Continuous Gaussian copula also exposes the variable nature of trait interrelationships across ontogeny (Garn et al., 1965; Lewis & Garn, 1960). It is true to say the results of the copula corroborate previous work. Specifically, both the copula and historic analyses show weak correlations between development of the second mandibular molar (man_M2) and ossification of the carpals (CC_Oss) during childhood (3-6.99 years old) (Lewis & Garn, 1960). However, Lewis and Garn still only rely on a limited number of pairwise relationships and arbitrary age ranges that limit the analysis of interrelationships in other developmental stages (e.g., infancy or adolescence). In contrast, while also investigating the childhood period (Figure 6.14), the present study is neither limited to a small number of pairwise relationships nor is it limited to a specific age range or developmental stage (Figure 6.9, Figure 6.14,

Figure 6.19). In fact, by fitting the copula across three different subsets that encapsulate distinct periods of ontogeny the results show that correlation between traits at one point during development are not the same at a different point in development. For example, during infancy (0-2.99 years old) the correlation between development of the distal epiphysis of the femur (FDE_EF) and distal breadth of the humerus (HDB) is -0.05. In comparison, during the juvenile and adolescence period the correlation between the same traits is 0.34. The difference between these values from the same two traits but different time periods is related to the individual growth trajectories of each trait. Growth in breadth (HDB) is active during infancy and continues throughout the entire ontogenetic period. Development of the distal femoral epiphysis does not begin until 3-5 years old and fuses late in adolescence. Therefore, the increased positive strength between both traits during the juvenile and adolescence period occurs during a time when both could be actively growing and/or developing. Table 6.1 corroborates this with the Spearman's correlation value between the correlation matrices across each developmental period being weak to moderate, which suggests differences across developmental stage. While this study *can* corroborate previous work (Lewis & Garn, 1960), this study also exposed the problems with previous work. The availability of data across human ontogeny allows for different models to be fit during different developmental stages, which shows a more complete picture of how trait interrelationships vary across the growth and development period.

Additionally, the use of the copula and *raw* trait scores / measurements to describe conditional correlations between traits enhances our knowledge of differences in growth and development (or lack thereof) between biological males and females. There are

known sex-specific patterns to the growth and development of individual long bones and the development of the dentition. This includes slightly earlier ossification and fusion timing in females as compared to males (e.g., Callewaert, Sinnesael, Gielen, Boonen, & Vanderschueren, 2010; Duren, Nahhas, & Sherwood, 2015; Noback, 1954; Stinson, 1985), differential timing of mineralization and eruption in the dentition (e.g., Levesque, Demirijian, & Tanguay, 1981; Smith, 1991), and differential magnitude and timing of the pubertal growth spurt and cessation of diaphyseal growth (e.g., Bogin, 1999; Cardoso, 2007; Duren, Seselj, Froehle, Nahhas, & Sherwood, 2013; Stinson, 1985). However, the copula results suggest that, beyond individual traits, multivariate relationships between traits are similar between the sexes. This is most likely because the copula correlation is conditional on chronological age or controls for the influence of age on each trait. Therefore, the copula is measuring *true* relationships between traits. In other words, by controlling for the known variability associated with chronological age, the results here demonstrate that multivariate growth and development between males and females is similar.

The Mixed Discrete-Continuous Gaussian copula demonstrates that the *true* relationships between broad growth modules like skeletal growth, dental development, and skeletal development, cannot be summarized via a few pairwise correlations taken at one point during ontogeny. Instead, analyses should be conducted based on as much trait information as possible and at various points throughout ontogeny. The results of such an approach demonstrate that while traits are indeed tightly integrated within each module (Figure 6.2), the degree of independence or dependence between other modules varies

across ontogeny (Figure 6.7, 6.12, 6.17) and may change according to the traits chosen in the analysis.

7.2 The Integrated Human Growth and Development Phenotype, Redux

Chapter two provided a broad introduction to the study of phenotypic integration and the more specific developmental integration. No previous research had sought to explicitly characterize the human growth and development phenotype as an integrated structure. Further, while there are a myriad of studies describing other processes of variability, such as canalization and plasticity (e.g., Cameron & Demerath, 2002; Debat & David, 2001; Hermanussen, 1997; Hermanussen, Largo, & Molinari, 2001; Temple, 2014; Wells, 2007), these studies do not contextualize how such processes interact within an integrated, multivariate, growing human. The Mixed Discrete-Continuous Gaussian copula provides the first known attempt to describe the pattern of phenotypic variation between growth traits considering the strength (or lack thereof) of their relationships within or across other modules.

The most visible feature of variability demonstrated in the present study is the modularity across each type of growth indicator (Figure 6.2). There are distinct modules of skeletal growth, dental development, and skeletal development and ossification where correlations between individual traits of each module are stronger as compared to correlations between traits of different modules. Embryologically, dental development and skeletal growth and development originate from two different areas of the embryo. The lateral plate mesoderm is responsible for skeletal growth and development, while

neural crest cell lineages are responsible for dental development. Importantly, signaling pathways and growth factors related to bone morphogenetic proteins (BMPs) play a role in both skeletal growth and development and dental development (Wang et al., 2014). The role of certain BMPs reinforces the notion that although growth structures are ultimately representative of tightly knit functional and developmental modules, there are known molecular relationships that could impact each at varying magnitudes. Specifically, BMP4 is known to play an important role in both endochondral bone formation (Tsumaki & Yoshikawa, 2005; Young & Badyaev, 2007) and the formation and development of tooth germs (Li et al., 2019). Therefore, the moderate correlations demonstrated between early forming teeth and diaphyseal dimensions or the additional moderate relationships between later forming teeth and few epiphyseal fusion sites could either be related to these similar BMP pathways, similar developmental timing, or some combination of the two processes. These results demonstrate several important components of modular biological architecture including the distillation into specific components of the human body (skeletal diaphyses, skeletal epiphyses, and the dentition), variable levels of integration with other modules (patterned by similar signaling pathways related to BMPs), and a chronological component suggesting a difference between early and/or later forming elements (Raff, 1996).

An additional component of modular structures is that each module may itself be further decomposed into smaller hierarchical units such that a module may contain modules of its own. This is especially present in the skeletal growth module between longitudinal growth and appositional growth, (e.g., Figure 6.6), the dental development module between individual teeth or isomeres (e.g., Figure 6.7), and the skeletal

development module between primary and secondary ossification centers and later skeletal fusion (e.g., Figure 6.8). The skeletal growth module can be further subdivided into modules associated with longitudinal growth (diaphyseal length) and appositional growth (diaphyseal breadth). Growth of the skeletal diaphysis is representative of a delicate balance of oppositional growth processes to construct bones that are rigid or strong enough to withstand mechanical loading, while remaining functionally efficient to complete their specialized roles (e.g., bipedal walking, shoulder rotation, etc.) (Gkiatas et al., 2015; Jepsen et al., 2009; Kurki et al., 2022; Robling, Duijvelaar, Geevers, Ohashi, & Turner, 2001; Schlecht & Jepsen, 2013). A myriad of research demonstrates the plastic nature of longitudinal growth in children (e.g., Agarwal, 2016; Kuzawa, 2005; Said-Mohamed et al., 2018; Temple, 2019; Wells, 2017), yet far fewer studies delve into questions of plasticity as related to appositional growth (Kurki et al., 2022). Further complicating relationships is that the BMP pathways described above tend to relate to longitudinal growth and not appositional growth, with mechanical forces playing in outsized role in growth in breadth (Gkiatas et al., 2015). Diaphyseal breadths tend to complete growth later than diaphyseal lengths with growth often extending up through an individual's mid-twenties. This means the external environment has longer to interact with the breadth growth process as compared to the length growth process. Additionally, there is a fair degree of sexual dimorphism in skeletal breadth size resulting from complex sex- and ontogenetic timing-specific interactions between sex hormones, growth hormones, and mechanical loading (Callewaert et al., 2010). Unsurprisingly, interrelationships associated with breadth growth are complex and multifactorial.

Here I turn towards the relationship between phenotypic plasticity and developmental integration to clarify the relationship between appositional and longitudinal growth. There is consensus (e.g., Agarwal, 2016; Kuzawa, 2005; Said-Mohamed et al., 2018; Temple, 2019; Wells, 2017) that longitudinal growth is plastic and influenced by external environmental stimuli. The strong correlations between all traits associated with diaphyseal lengths suggest that similar levels of plasticity are patterned across each of the traits (Pigliucci, 2003). If this was not the case and one length was more plastic than the other it would likely show a reduced strength in correlation (Matesanz et al., 2021; Schlichting, 1989). On the other hand, breadth measurements are not strongly correlated with length variables, but are moderately correlated with each other. Therefore, it is likely that levels of phenotypic plasticity, patterned by the differential timing of growth, are different between the two growth processes. Putting it all together, the hierarchical modularity present in the skeletal growth module is likely because of combination of differential growth trajectories, sexual dimorphism in breadth size and growth, variable levels of plasticity patterned differently between longitudinal traits as compared to appositional traits, and the lower size variation (breadths are intrinsically smaller than lengths) mediated by the necessity to create strong and rigid, yet functionally efficient skeletal diaphyses.

The dental development module can be described by even smaller hierarchical units separated into isomere modules. Across all levels of analysis, dental isomeres, or the same tooth between each arcade (e.g., max_M1 and man_M1), are most strongly correlated. Additional relationships between teeth of the same class (e.g., M1 and M2) and between teeth of the same arcade (e.g., man_M1 and man_I1) are weaker in

comparison. Contemporary research into conditional dependence of the dentition does suggest varying levels of integration that are also tied to similar developmental sequences (i.e., early forming teeth are strongly correlated with other early-forming teeth) (Sgheiza, 2022). However, this work only focuses on the mandibular dentition, uses a different ordinal scoring system, and it is unclear whether the learned correlations are or are not conditional upon chronological age. Regardless, not all teeth of the mandible displayed similar correlations to each other. At the core, this study and that of Sgheiza (2022) suggest that dental development is less integrated than initially thought (Braga & Heuze, 2007). In fact, it is likely that each individual tooth or pairs of the same tooth are representative of different developmental modules with individual tooth germs developing largely independent from each other (Wagner, 2015; Wagner, Mezey, & Calabretta, 2001). Evidence of this is the presence of ectopic teeth that form away from the dental arch. The implication that the human dentition is overall less tightly integrated between all 32 permanent teeth is important. Traditional research suggests that teeth (often metonymically used to described the dentition as a whole) are more genetically canalized and therefore less susceptible to environmental perturbation as compared to skeletal growth (e.g., Cardoso, 2007; Conceicao & Cardoso, 2011). However, given the reduced levels of integration beyond isomeres, it is likely that levels of canalization and/or plasticity are not uniform across the dentition. Instead, individual teeth have their own capacity for plasticity, and this may not be stable throughout ontogeny or across the dental arcade.

Additional evidence of separate tooth modules comes from the study of an additional form of integration known as morphological integration, or the relationship

between the shape and form of structures. These studies suggest that antagonist teeth are more integrated and that the mandible displays stronger levels of correlation between teeth as compared to the maxilla (Gómez-Robles & Polly, 2012). An additional factor to consider is the known strong relationship between dental development and emergence with that of life history variables, such as age at weaning with first molar development (Smith, 1992). Onset of weaning suggests the introduction of differential foodstuffs whereby proper occlusion of the jaw is necessary to complete functionally efficient mastication. As such, M1s develop and erupt first, followed by each antagonistic pair, with the order playing a key role in the position of later erupting teeth and serving as a guide to complete the functional layout of the jaw. Importantly, this process is occurring when an individual is weaned, signaling the need for proper occlusion for efficient mastication and healthy nutrient intake (Gómez-Robles & Polly, 2012). Even still, research is ongoing to disentangle the perceived independence of certain tooth elements and how such independent structures may combine into a functional whole (Boughner & Hallgrímsson, 2008).

The relationship within and between traits of a multivariate human growth and development phenotype are complex, ontogenetically variable, and patterned according to any number of signaling pathways, embryological connections, genetic background, and environmental factors. While discrete growth and development modules exist between skeletal growth, skeletal development, and dental development, these modules themselves can be further divided into additional units composed of integrated substructures that themselves have different levels of dependence/independence and differentially influenced by pathways, connections, genetics, and the environment.

To put each of these relationships into perspective, I replicate the epigenetic landscape first described by Waddington (Waddington, 1942b, 1942a). Figure 7.1 demonstrates that each growth module follows their own paths, but there are linkages throughout that dictate the pace and sequence of growth and development. Each module can be further subdivided into additional modules related to individual growth processes within each module. The "end" point on the figure is that of the *whole* person or the integrated biological unit that inevitably ceases growth when adulthood begins. The point is to show that while we may think of growth and development as independent, the processes are multivariate, interrelated, and dynamic.

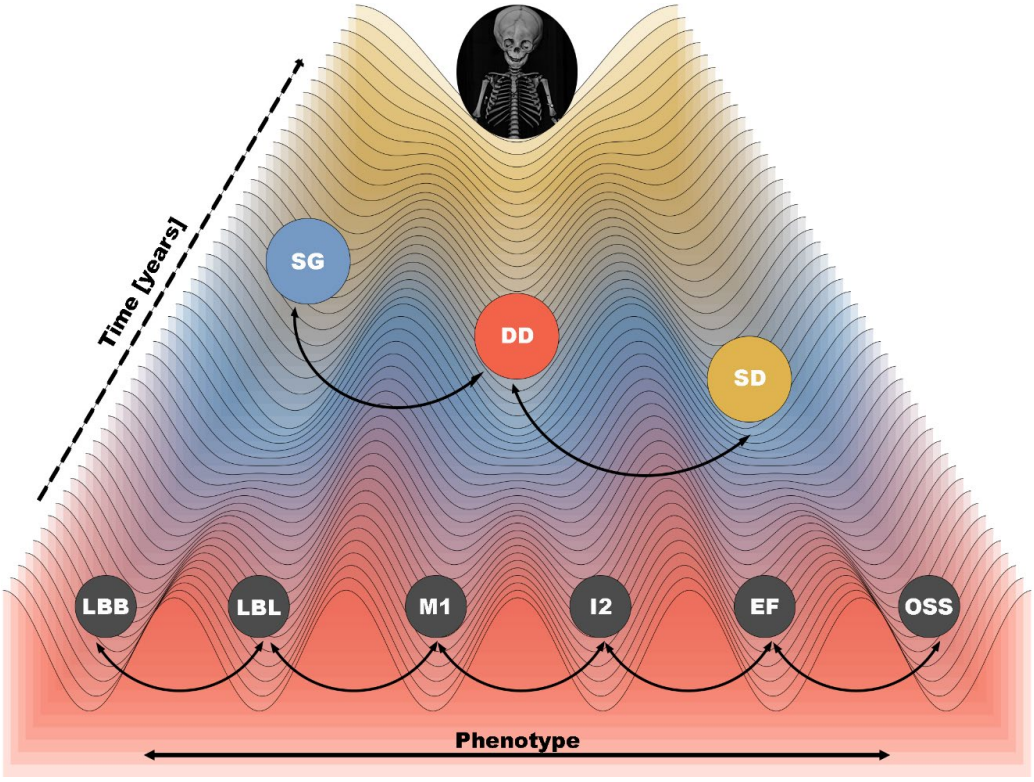

Figure 7.1. The Human Growth and Development Phenotypic Landscape. Individual traits give way to three distinct, yet related modules, that all combine into an integrated, developing human phenotype. LBB = Long Bone Breadth, LBL = Long Bone Length, M1 = 1st Molar, I2 = 2nd Incisor, EF = Epiphyseal Fusion, OSS = Ossification, SG = Skeletal Growth, DD = Dental Development, SD = Skeletal Development.

7.3 The Application of Copula Modeling to Biological Anthropology

The use of multivariate statistical methods has a tenuous history in biological anthropology. Much of the tension stems from the difficulty in interpretation of multivariate results and the theoretical relationship between the proposed statistical model and the underlying biology it is meant to explain (Corruccini, 1975; Kowalski, 1972). The tenor of such arguments falls squarely within George Box's aphorism that "all models are wrong, but some are useful." Or, as a question, do multivariate statistical methods provide greater interpretability of complex biological phenomena as compared to univariate or simpler techniques? In biological anthropology, contemporary theory suggests that with increased data quality and with careful consideration of both biological complexity and its translation to statistical assumptions, multivariate methods provide the best means to identify complex patterns in the human phenotype (Klingenberg, 2014; Vark & Howells, 1984). The Mixed Discrete-Continuous Gaussian copula evidences the utility of multivariate approaches in describing patterns underlying human growth and development.

Although the utility of the multivariate techniques offered in the current study lie at the core of the initial unease demonstrated by early researchers they differ by 1) providing interpretable results in the form of a correlation, and 2) the correlations can be translatable to downstream analyses. Calculating the joint multivariate probability distribution using a copula is one method we can use to ease the historic concerns regarding complex multivariate models (Goda, 2010). In the words of Amiridi and colleagues (2019), "estimating the joint distribution of data sampled from an unknown

distribution is the holy grail for modeling the structure of the dataset…". Once the joint distribution is known, marginal, conditional, and joint subsets of the data can be manipulated in tasks such as classification, regression, prediction, imputation, etc. Thus, the results from the copula modeled in the current study may be extended to applications outside of the initial task of describing the underlying dependency structure of a contemporary, United States sample of children. In the remainder of this section, I provide several examples pertaining to the application of copula modeling across biological anthropology.

7.3.1 Bioarchaeology and Paleoanthropology

The study of human growth and development is not limited in scope to modern human populations. In fact, the same phenotypic traits used in the current study are common in studies of growth in past modern human populations (e.g., Cardoso & Garcia, 2009; Geber, 2014; Hummert & Van Gerven, 1983; Newman, Gowland, & Caffell, 2019; Temple, Bazaliiskii, Goriunova, & Weber, 2014) and in the description and evolution of human growth across the human lineage (e.g., Cameron, Bogin, Bolter, & Berger, 2017; Leigh & Park, 1998; Rosas et al., 2017; Smith, 1992, 1994). Regardless, the Mixed Discrete-Continuous Gaussian copula may be used in either setting to highlight the temporal variation in trait interrelationships or to disentangle plastic relationships (or lack thereof) between the dentition and the human skeleton. A key distinction between the present study and an extension towards these additional areas is the ability to quantify the

multivariate joint distribution and associated dependency structure *without* the known chronological age of an individual.

In bioarchaeological and paleoanthropological settings chronological age is unknown. Even still, the phenotype can be modeled as the joint distribution of traits that may be conditional on other metrics of human growth and maturation, such as emergence of certain elements of the dentition and fusion of certain elements of the skeleton (Roksandic & Armstrong, 2011). Importantly, the utility of copula modeling is not restricted to analyses of only the traits described in the current study. The human phenotype is inherently multivariate and researchers in both bioarcheology and paleoanthropology ask questions that require multivariate solutions. In bioarchaeology, this may include a description of the interrelationships between certain skeletal markers of non-specific stress (e.g., Agarwal, 2016; Geber, 2014; Klaus, 2014; Schug & Goldman, 2014; Yaussy, DeWitte, & Redfern, 2016). In paleoanthropology, this may include the ability to distill the often-multivariate trait lists used to delineate certain hominin taxa into a robust analysis of the relationship between the expression of such traits across individual taxa (e.g., Robson & Wood, 2008). Regardless, a copula provides another piece of the arsenal to explore any component of the multivariate human phenotype.

Studies of past human and hominin populations are riddled with data quality issues and an abundance of missing data. The Mixed Discrete-Continuous Gaussian copula provides a robust method to estimate missing values to enhance downstream research. An important quality of learning the joint distribution of growth traits like that done here is the ability to not only separate out individual traits and ask specific questions

about each marginal distribution, but to also ask questions about the conditional distributions of traits such as what is the measurement of a femur given the measurement of other bones? (Crane & Hoek, 2008; Käärik, Selart, Käärik, & Liivi, 2011). Probabilistically, we can write this as $P(y_1 \mid y_2, \ldots, y_M)$, which asks what the value of the unknown trait is given the information known about the other traits. Put more simply, femoral length is missing, what is that measurement given the length of the humerus and development of the first molar? This question is especially straightforward to answer in the current study because of the Gaussian copula's relationship to the multivariate normal distribution. Further, because both marginals are also assumed standard normal, no transformation is necessary to account for different marginal constructions (external to the Probit link function for the ordinal data). As such, the task of prediction can be completed in R using *condMVNorm* (Varadhan, 2020).

An example of this in application is completed using SVAD and the mean posterior correlations learned from the copula. I simulated missing data in femoral diaphyseal lengths (FDL). I then predict the missing values given fibula diaphyseal length (FBDL), humerus proximal breadth (HPB), development of the first maxillary molar (max_M1), development of the mandibular canine (man_C), tarsal ossification (TC_Oss), and development of the distal radius (RDE_EF). Probabilistically, this can be written out as $P(FDL \mid FBDL, HPB, \max M1, \text{man C}, \text{TC Oss}, \text{RDE EF})$. Figure 7.2 visualizes the relationship between observed femoral growth and predicted femoral growth based on the simulation of missing data. The near perfect fit is indicated by the straight line on the plot and a Pearson's *r* between the observed and predicted values of

0.98. Figure 7.3 provides further evidence of such agreement demonstrating that the growth profile between observed and predicted values is similar. To demonstrate the ability to predict traits that are scored on an ordinal scale, I complete the same task, except predicting development of the first molar ($P(\max M1 \mid FBDL, HPB, FDL, \text{man C}, \text{TC Oss}, \text{RDE EF})$). Figure 7.4 and Figure 7.5 demonstrate the agreement between observed and predicted values. As an additional check, a weighted kappa analysis and a rank correlation such as Spearman's ρ can be used to test agreement between different ordinal scores (Corron et al., 2021). The present results demonstrate a (quadratically) weighted κ value of 0.93 and a Spearman's ρ of 0.94 – both indicating strong agreement between observed and predicted scores. Combined, the Gaussian copula successfully recovers the values of both femoral growth and dental development conditional on other marginals in the model.

The results described above have profound implications for biological anthropology. This is possible because in addition to learning interrelationships, a copula models the joint distribution of all traits in the analyses. Put a different way, one learns the full phenotypic space of all *known* outcomes. Therefore, any downstream tasks related to expectations, conditional probabilities, and marginal probabilities are straightforward computations. While the work in the current study focuses on contemporary human growth, copulas can be extended to any number of settings in bioarchaeology and paleoanthropology. This includes missing data (Wissler, Blevins, & Buikstra, 2022), exploring (in)dependence between traits (Conaway, Schroeder, & von Cramon-Taubadel, 2018), and using conditional analyses to look at the variability of the

data given certain conditions such as an individual's growth given any number of non-specific stress indicators (Schug & Goldman, 2014).

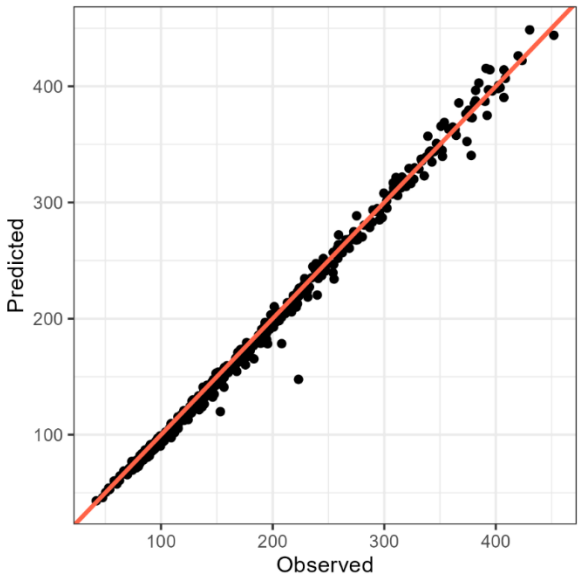

Figure 7.2. A plot of the observed vs predicted value of femur diaphyseal length. The straight line is indicative of perfect agreement.

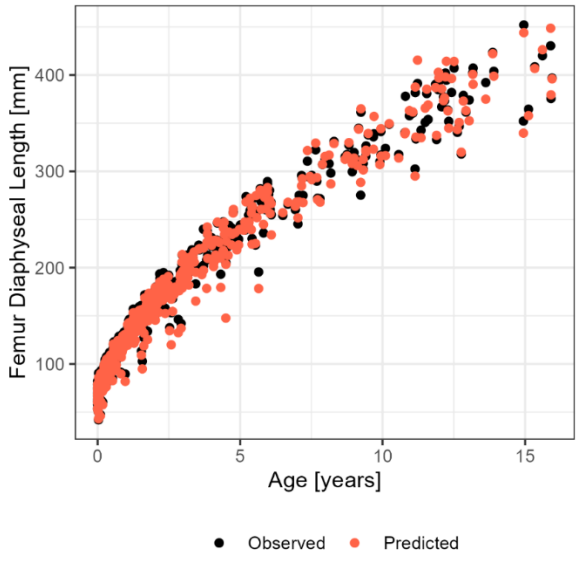

Figure 7.3. A skeletal growth profile of femur diaphyseal length given chronological age. Black is the observed measurement, and the reddish orange is what was predicted conditional on other elements.

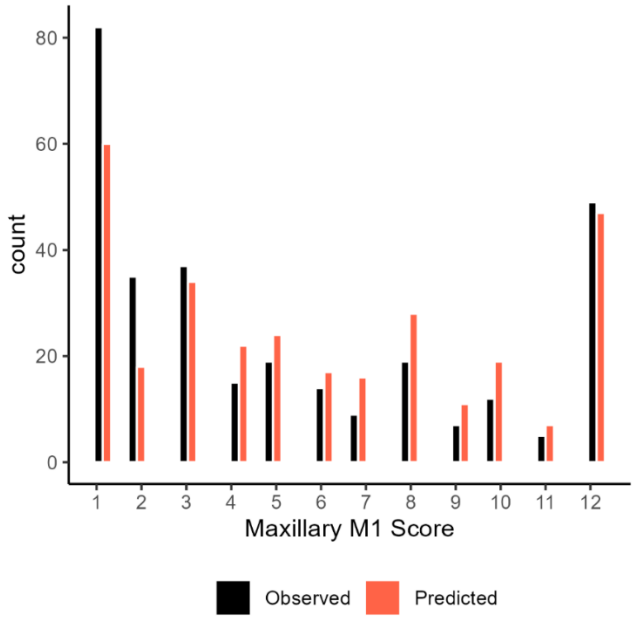

Figure 7.4. Bar plot demonstrating the observed scores vs the predicted scores when learning M1 development conditional on additional growth traits. Black is observed and reddish orange is predicted from the copula.

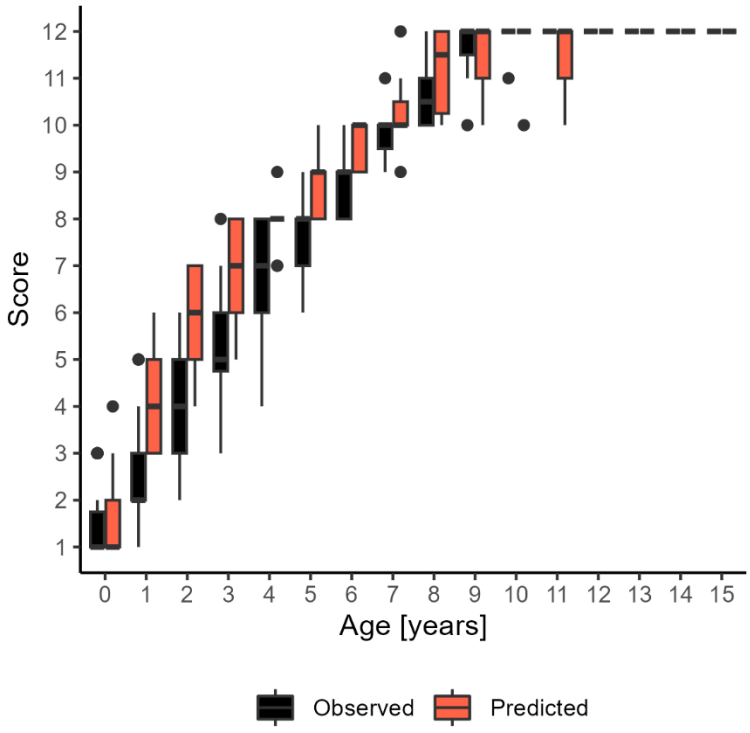

Figure 7.5. Boxplot demonstrating the relationship between age and M1 score. Black are the observed scores, and reddish orange are those predicted using the copula.

7.3.2 Chronological Age Estimation and Forensic Anthropology

Forensic anthropologists and researchers of chronological age estimation utilize human growth and development traits to estimate the age of subadult individuals (Konigsberg, Herrmann, Wescott, & Kimmerle, 2008; Stull et al., 2021; Ubelaker & Khosrowshahi, 2019). Contemporary work suggests that multivariate age estimation techniques are more valid as compared to univariate techniques because of their ability to capture more information about the differential relationship between phenotypes and age (Boldsen et al., 2002; De Tobel et al., 2020; Konigsberg, 2015; Lovejoy, Meindl, Mensforth, & Barton, 1985; Stull, L'Abbe, et al., 2014). With the advent of multivariate techniques comes the necessity to account for the conditional dependence (or lack thereof) between the traits utilized. Failure to account for such relationships leads to an invalid model with unrealistically small error (Stull et al., 2021). The copula proposed here is a direct demonstration of the conditional dependence between traits that is translated to the age estimation of subadults.

In practice, the conditional dependence structure learned with the copula could be directly translatable to current age estimation models that deal with similar data complexities such as missingness, mixed data types, and heteroskedasticity (Stull et al., 2022). Stull and colleagues provide a novel method known as the Mixed Cumulative Probit (MCP) to estimate the age of subadults. Mathematically, the MCP and the Mixed Discrete-Continuous Gaussian copula are identical except for differences in their choice of parametric mean function related to the ordinal data. However, the MCP is computationally inefficient, which leads to the decision to constrain the correlation

structure to allow for similarly grouped variables (e.g., all skeletal growth variables) to share the same correlation coefficient. In comparison, the copula is computationally more efficient (although improvements are necessary) and such efficiency occurs while applying no constraints on the correlation structure. The results of the current study demonstrate that relationships between two different modules cannot be distilled to a single value as the correlation between one tooth and long bone may not be the same as that of another tooth and long bone. Thus, much of the dependency information captured in the present study is missed in the existing MCP parametric fits.

As a validation of the copula method to learn dependencies and a test to see if the model can be improved by *only* adjusting the dependence structure, I modify MCP model structure found at https://github.com/ElaineYChu/aaba_2022 where FDL, RDL, max_M1, man_I2, HME_EF, and TC_Oss are utilized to predict the age of individuals from SVAD – the same data used in the current study. To be precise, here I use the parametric values of the mean and standard deviation from the initial MCP models fits and input the correlation parameter learned from the present copula model. Figure 7.6 visualizes the predicted age ranges between both the initial MCP model with the truncated dependency structure and the predicted ranges when substituting the copula parameters from the model in the current study. Figure 7.7 plots the bias (raw residuals, left) and accuracy (absolute value of the residuals, right) between both models. Figure 7.8 shows the range of the prediction interval between the two models. In general, the results are similar – in fact, model performance statistics are identical as common metrics including accuracy, root mean square error, and standard error of the estimate are

identical at 0.83, 2.40, and 2.08, respectively. Further, Stull and colleagues introduce a metric known as the test mean negative log posterior as an additional model selection technique and both the original MCP model and the model with the updated dependency structure have identical values of approximately 8.7. However, Figure 7.8 demonstrates slightly better precision (i.e., smaller prediction intervals) beginning in childhood when using the correlations from the copula as compared to the initial MCP correlations. Further, while there may not have been drastic differences in the model performance between the copula determined dependency structure and the original dependency structure calculated by the MCP, it is likely not a great subset of variables to demonstrate the potential of a full dependency structure. In context, these results suggest three points: 1) the dependency structure learned in the current work, while different than the MCP, is valid given the similar results between models, 2) perhaps unsurprisingly, while conditional dependence is important, differences in other model parameters such as mean and noise specification, play an outsized role in predictive ability, and 3) the MCP and Gaussian copula in the present study are mathematically identical leading to similar results. Previous research has shown that age estimation models can be constructed using copulas (Faragalli et al., 2023), opening up possible future directions to use a copula *a priori* instead of the post-hoc approach demonstrated here.

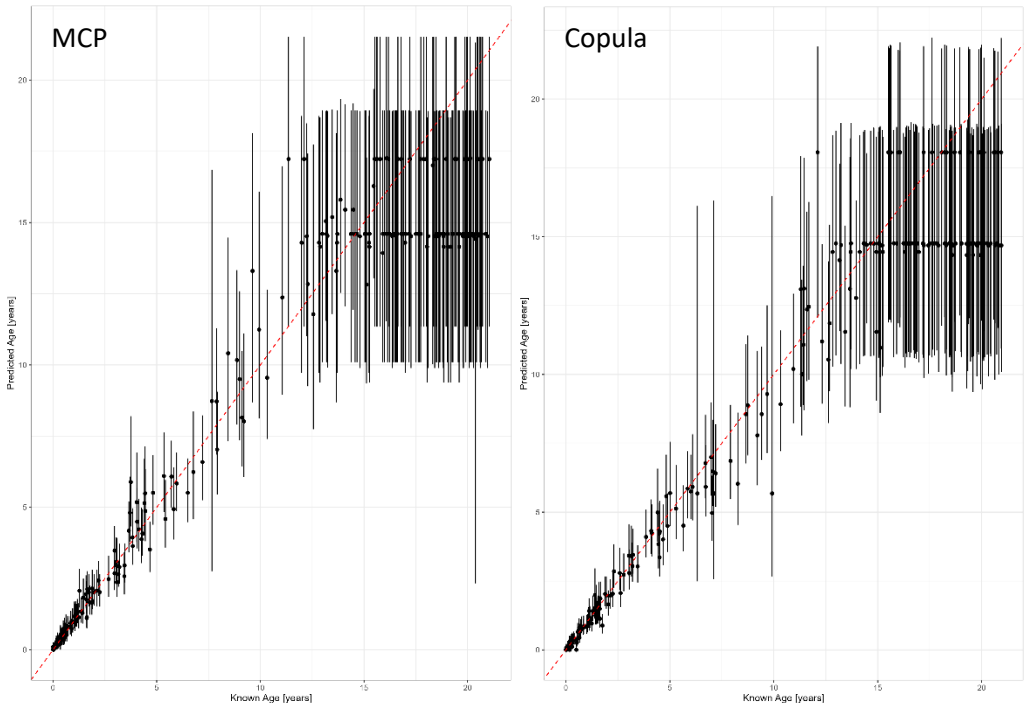

Figure 7.6. Plots displaying the average point estimate and credible intervals around the prediction. The original MCP model is on the left, the same model but with the copula correlations is on the right. The dotted red line indicates perfect agreement.

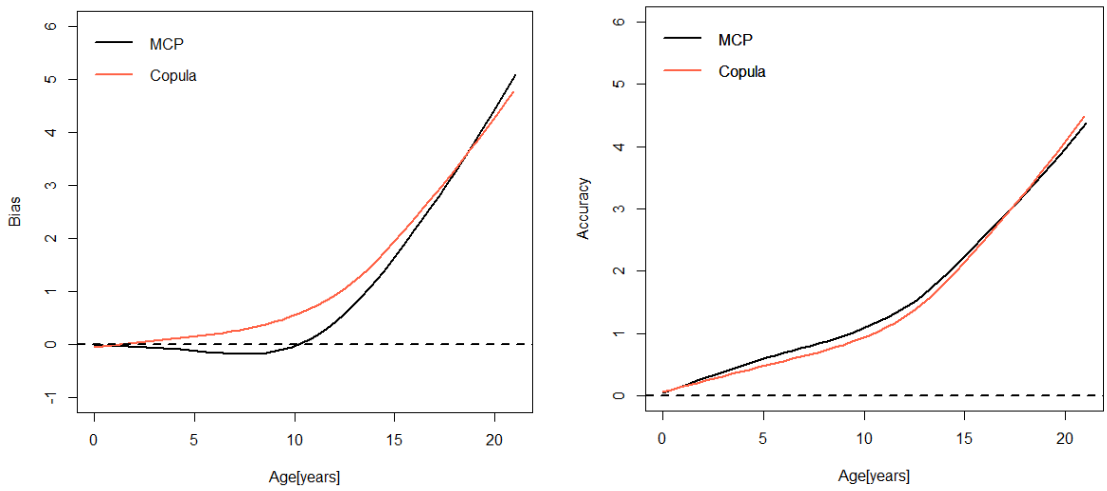

Figure7.7. Bias (left) and accuracy (right) of the MCP results based on the MCP correlations (black) and copula correlations (red).

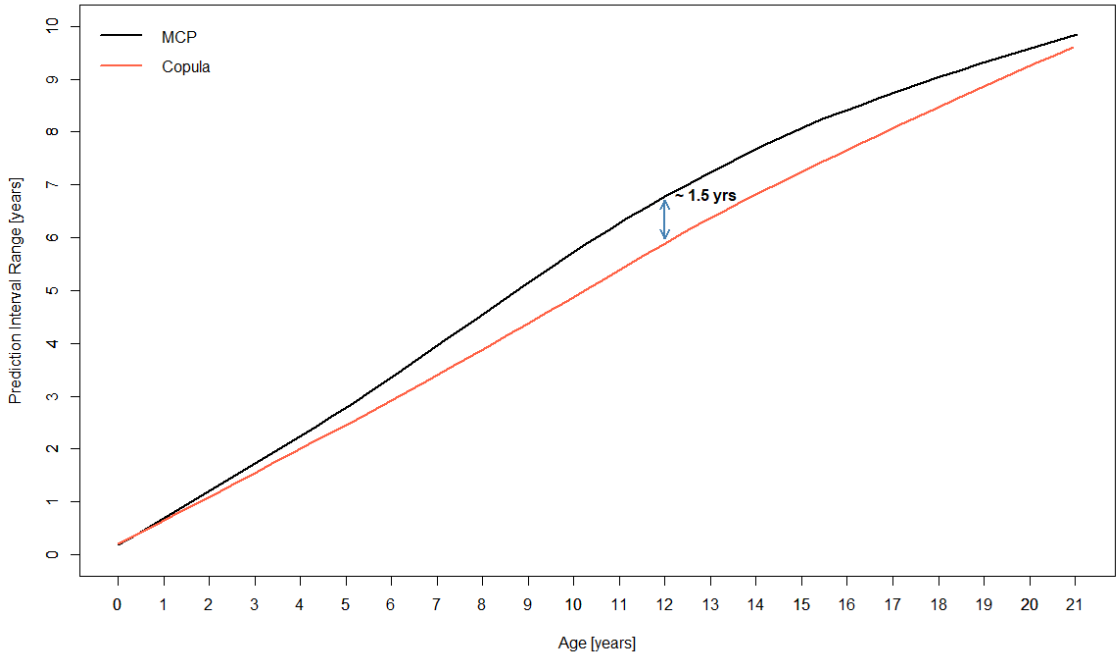

Figure 7.8. Plot demonstrating the size of the prediction intervals (upper95 - lower95) between an MCP model fit with the initial MCP correlations versus the copula correlations.

7.4 Limitations to the Current Study

While the work presented here provides a promising approach to address any number of questions in biological anthropology, there are several limitations to be highlighted that may also point to future work. The limitations can be described as data-specific limitations pertaining to the choice of data in the study, methodological limitations pertaining to the specifics of the copula chosen in the current study, statistical and computational limitations related to the broad application of copulas in Stan and high-dimensional data problems, and model-specific limitations pertaining to current construction of the copula.

7.4.1 Data Limitations

The analysis of a multivariate and multifactorial human growth and development phenotype requires data that captures as many traits as possible across as many individuals as possible. The SVAD (Stull & Corron, 2022) provides the requisite source to obtain this information. The current study uses the United States subset of the databank because it is the most complete portion of the data or contains more data per trait type. However, the results presented here may not equate to those from other samples within SVAD. The results apply to the current United States sample and may not be representative of growth relationships globally. Even though the United States provides the most complete sample, there are uneven sample size across developmental stages – particularly in late childhood into adolescence (Figure 4.1). As a result, it could be likely that the analyses of the childhood developmental stage are skewed because of the

magnitude of missing data. Relatedly, the developmental stage analyses are subset based upon chronological age due to historical precedence and convenience (Bogin, 1999). However, movement across different developmental stages cannot be pinpointed to a single age point and perhaps a more valid approach would be to divide groups based on maturational and developmental markers on the human skeleton. However, such work is predicated on less missing data than is present currently. Lastly, the ordinal scoring protocol used for both the dentition and skeletal development may play an outsized role in the patterning of the dependency structure. Previous research demonstrates that traits with more ordinal categories elucidate more information as compared to those with less (Stull et al., 2021). This fact is why binary variables were excluded from the present analyses. Therefore, although the ability to design methods to quantify mixed-data relationships is important, the nature of those relationships could change if one scores the epiphyses on a 3-stage versus a 7-stage scale.

7.4.2 Methodological Limitations

Like other approaches to parametric modeling, the choice of copula and individual marginal distributions are defined *a priori* or assumed prior to model fit. The Gaussian copula and standard Gaussian marginal distributions were chosen because of historical precedence relating growth data to Gaussian distributions (Quetelet, 1869) and because of the intuitive interpretation of correlations – specifically linear correlations in the form of Pearson's *r*. An additional advantage of the Gaussian copula is the ability to translate to broader terms of rank association such as Spearman's ρ and Kendall's τ.

However, what if dependence amongst growth is non-linear? Or, if there are strong dependencies in the tail – i.e., more extreme values of one trait are associated with extreme values of another trait, but there is weaker association between average values. Gaussian copulas are notoriously poor at capturing such types of dependence (Nelsen, 2006). In fact, the "over simplification" of Gaussian copulas is often blamed for the 2008-2009 Financial Crisis because of several assumptions made related to the linearity (or non-linearity) of the dependence structure between certain financial derivatives (Salmon, 2009). The model was chosen here for its statistical simplicity and the historical precedent set across biological anthropology using traditional multivariate Gaussian models (given the standard normal and probit marginals, the current model is akin to a multivariate Gaussian with mixed data types and is identical to the MCP described in Stull and colleagues, 2023) and using correlations (or covariances) to describe biological relationships. Such an approach has never been tried in biological anthropology and a broader goal of the current work is to provide a more robust means to analyze complex data types beyond traditional methods with faulty statistical assumptions. Future work will need to identify and test additional copula and marginal frameworks beyond that introduced in the current study.

7.4.3 Statistical and Computational Limitations

High dimensional data analysis is a computationally demanding task. The largest model within the current study – the full US dataset – took 25 days to fit on a computer parallelized across 14 CPU cores with 32 GB of RAM. This is a dataset with 54 total

growth traits and 1,316 individuals – hardly high dimensional in comparison to datasets with far more features and millions of unique cases. Part of the reason for the inefficiency is related to the tuning parameters in Stan. I have increased the adapt delta parameter, which decreases step size, thus it takes far more steps to explore the entire parameter space. I have also increased the tree depth parameter, which leads to an increased distance to explore across the parameter space. While such tuning has led to a more valid statistical model, the consequence is an inefficient sampler. A possible solution to this problem is to reparametrize the model to "simplify" the problem or make it so the parameter space is less complex. However, the statistical properties of a copula make this a difficult task in Stan. Specifically, copula intrinsically model correlations between variables and it is likely that some relationship exists between the correlation of different relationships such as FDL-RDL and TDL-HDL. In other words, a strong correlation in one pair is associated with a strong correlation in another. Given the design of Stan and Hamiltonian Monte Carlo more generally, relationships of this sort between parameters may cause identifiability issues, divergences, and autocorrelation in the Markov chains (Stan Development Team, 2022). As such, future work will either need to reparametrize the current models in Stan to increase efficiency, design a sampler from scratch where exact tuning parameters can be better controlled, or methods beyond Bayesian and/or Hamiltonian Monte Carlo introduced (Bao et al., 2023).

7.4.4 Model-Specific Limitations

A large limitation to the current study is the fact that I have presented one single model (across six subsets of data) that utilizes only one single specification of prior distributions, marginal distributions, and likelihood function. Much of this relates to the discussion above regarding the computational burden of the model and the timeframe of this dissertation. As a result, model selection or the comparison of several models to determine which fits the observed data best has not yet occurred. There is no way to know if the Mixed Discrete-Continuous Gaussian copula is the best model available to describe the correlation between traits or if a different construction would perform better. Future work will rectify this limitation and is ongoing.

A component of model specification is tied to the choice of prior distribution on all parameters sampled in the model. As currently constructed, the standard Gaussian priors ($normal(0,1)$) on the parameters associated with the continuous mean function ($\boldsymbol{\theta}^j = [a^j\ r^j\ b^j]^T$) are missprecified. That is, they constrain the parameter value far below the true expectation given that the majority of the probability mass is centered close to one. A comparison between the parameters in the current model and those in Stull and colleagues (2023) corroborate this fact. The result is a parametric mean function that is linear in nature as compared to curvilinear relationship related to specification of the mean (Figure 7.9). The ramifications of this misspecification of the prior density may include invalid prediction in downstream task such as age estimation and imprecise posterior correlations given that the marginal cdfs – the object that is being linked with the correlation coefficient – are conditional on mean and standard deviations that are

themselves functions of age. However, it should be noted that a comparison between correlation values between both models and the identical performance in age estimation using the correlation matrix from the current study (Figure 7.6 and 7.7) suggests that the dependence structure learned within the Gaussian copula – the main parameter of interest in the current study – is valid given the current specification of the model. Further, the missing data example in Figures 7.2-7.5 demonstrate agreement between observed and predicted values based on the posterior correlations from the copula. This may also corroborate the validity of the dependence structure in the current model. While the fit in Figure 7.9 may be poor, the overall relationship (i.e., an increase in length with age) may also provide validity to the overall correlation values and would only be inappropriate in more fine-grained applications such as chronological age estimation. It should also be noted that this misspecification of the priors associated with the parametric mean function is related to the continuous response variables. This is because there is a mismatch between the scale of the prior and the scale of observed data. The priors associated with the discrete-valued responses and resulting latent data augmentation are valid in context and corroborated by the better fit in Figure 5.4, top, as compared to Figure 5.3, top.

Moving forward, model selection will need to be undertaken between several candidate models to determine the best fit to observed data. This will need to test several different iterations of likelihood function (type of copula + marginal distributions) and prior distribution specifications. Testing is underway to adjust the priors to coincide with the scale of the data more appropriately (e.g., $normal(0,100)$). Initial results on small subsets of the data suggest an improved fit of the parametric mean function and identical correlation results to those in the current study (Figure 7.9 and Figure 7.10). While the

above $normal(0,100)$ may be too diffuse in context, it provides a starting point to begin adjustments of other priors in search of a more computationally efficient and statistically valid model. Future work and later publications will ultimately provide the final results of these changes to model and prior specification.

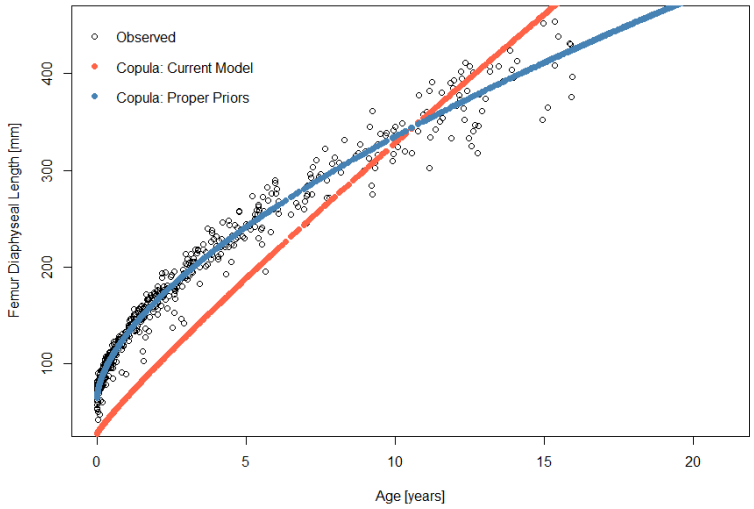

Figure 7.9. Plot demonstrating the lack of fit of the parametric mean function from the current model. The red line is the present parametric values. The blue line is a secondary copula model that tests different prior constructions. This blue line is the appropriate fit and represents future work of the Gaussian copula.

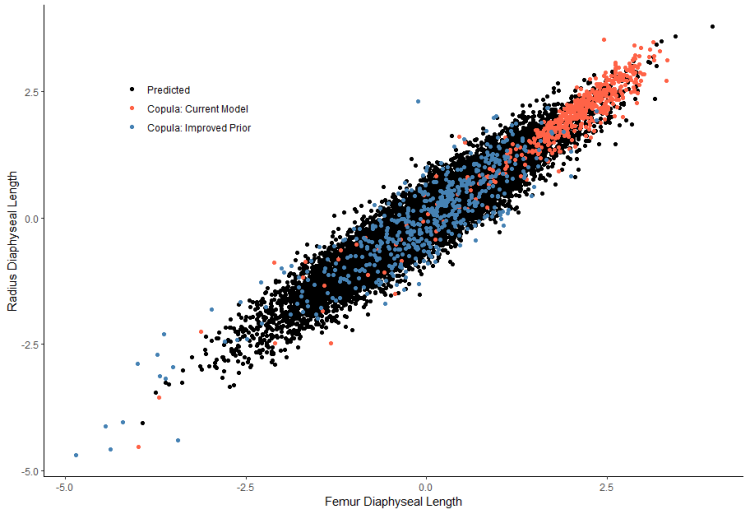

Figure 7.10. An update to Figure 5.3 from Chapter 5. This scatterplot is demonstrative of a posterior predictive check with priors from the current model represented by the red points and priors from a secondary copula fit to improve the present model. Note the better agreement in the blue points versus those in red.

Chapter 8 – Conclusion

The current study combined a novel methodological technique in biological anthropology, the Mixed Discrete-Continuous Gaussian copula, and the largest and most complete dataset of modern children between the ages of birth and 20 years to perform the most comprehensive analysis of the multivariate human growth and development phenotype. The statistical methodology (*i.e.*, copula modeling) and the explicit discussion of the 54 growth and development traits (*i.e.*, skeletal growth, skeletal development, and the dental development) in the context of phenotypic and/or developmental integration has yet to be explored in previous growth and development research. The creation of a joint probability model that learned 1,431 trait-by-trait relationships exposed the changing relationships across life history stages and within growth modules, which emphasizes the need for researchers to stop extrapolating large patterns from one bivariate relationship.

The multivariate human growth and development phenotype is variable across ontogeny with the relationships between and within growth and development modules tied to active growth and development periods and mediated through a suite of molecular, genetic, and environmental factors. These factors are not sex specific as biological males and females display similar patterns of trait interrelationships. Combined, the results of six copula models, thousands of parameters, and 1,431 trait-by-trait relationships shows that skeletal growth, skeletal development, and dental development are neither representative of one single trait nor a single independent process, but instead a series of interconnected pathways moving in conjunction towards adulthood. These pathways are

hierarchically structured within- and between-modules whereas skeletal growth, dental development, and skeletal development can be further broken down into additional modular structures related to direction of growth, tooth class, and primary versus secondary skeletal ossification and fusion. Some of these pathways are more related to each other like regimented soldiers, while others are informal friends meandering about across human ontogeny. Regardless, the relationships formed between each set of traits provides scaffolding for the study of human phenotypic variation and its application across all branches of the human biological sciences.

One of the real strengths of this study is the potential utility of the model in future research designs across the discipline of biological anthropology. The copula provides researchers with a new tool in the arsenal to the study of multivariate human phenotypic variation. A few examples include applications in forensic anthropology to estimate chronological age or biological sex, applications in paleoanthropology to understand either the evolution of the unique human ontogeny or more broadly describe patterns of skeletal traits that define the boundaries of human ancestors, and applications in bioarchaeology to better understand variation between samples and populations across space and time. With the foundation put down through the introduction of the Gaussian copula and the utility of robust data sources such as the SVAD, future research endeavors can continue to explore the infinitely complex multivariate human phenotype.

In the future, this means further application of the copula to all SVAD samples and in extension, to bioarchaeological samples. This also means continuing to refine multivariate statistical techniques to best capture the complex structure realized between

different data types across the human phenotype. Such work may be in the form of differential copula approaches beyond a Gaussian copula or a pivot to more complex machine learning and computer science approaches to the study of multivariate systems. Future work will also need to undergo model selection and present better prior specifications related to the parametric mean function associated with the scalar-valued response variables. In the end, while the Mixed Discrete-Continuous Gaussian copula is not the first technique put forth to study phenotypic relationships, it provides the most comprehensive analysis to date and lays the groundwork for future research into the growing, developing, multivariate, human ontogeny.

References

Adams, D. C., & Collyer, M. L. (2019). Phylogenetic Comparative Methods and the Evolution of Multivariate Phenotypes. *Annual Review of Ecology, Evolution, and Systematics*, *50*(1), 405–425. https://doi.org/10.1146/annurev-ecolsys-110218-024555

Agarwal, S. C. (2016). Bone morphologies and histories: Life course approaches in bioarchaeology. *American Journal of Physical Anthropology*, *159*, 130–149. https://doi.org/10.1002/ajpa.22905

Albert, J. H., & Chib, S. (1993). Bayesian Analysis of Binary and Polychotomous Response Data. *Journal of the American Statistical Association*, *88*(422), 669–679. https://doi.org/10.1080/01621459.1993.10476321

AlQahtani, S. J., Hector, M. P., & Liversidge, H. M. (2010). Brief communication: The London Atlas of Human Tooth Development and Eruption. *American Journal Of Physical Anthropology*, *142*, 481–490. https://doi.org/10.1002/ajpa.21258

Amiridi, M., Kargas, N., & Sidiropoulos, N. D. (2019). Statistical learning using hierarchical modeling of probability tensors. *2019 IEEE Data Science Workshop (DSW)*, 290–294. IEEE.

Armbruster, W. S., Pelabon, C., Bolstad, G. H., & Hansen, T. F. (2014). Integrated phenotypes: Understanding trait covariation in plants and animals. *Philosophical Transactions of the Royal Society B*, *369*. https://doi.org/10.1098/rstb.2013.0245

Baker, P. T. (1997). The Raymond Pearl Memorial Lecture, 1996: The eternal triangle—Genes, Phenotypes, and Environment. *American Journal of Human Biology*, *9*, 93–101.

Bao, F., Nie, S., Xue, K., Li, C., Pu, S., Wang, Y., … Zhu, J. (2023). *One Transformer Fits All Distributions in Multi-Modal Diffusion at Scale*.

Berry, S. D., & Edgar, H. J. H. (2017). Development of a large-scale, whole body CT image database. *Proceedings of the AMIA Annual Symposium, Washington, DC, USA*, 6–8.

Betancourt, M. (2017). *A Conceptual Introduction to Hamiltonian Monte Carlo*. arXiv. https://doi.org/10.48550/ARXIV.1701.02434

Bogin, B. (1999). *Patterns of Human Growth* (2nd ed.). Cambridge: Cambridge University Press.

Bogin, B., & Smith, B. H. (1996). Evolution of the human life cycle. *American Journal of Human Biology*, *8*(6), 703–716. https://doi.org/10.1002/(SICI)1520-6300(1996)8:6<703::AID-AJHB2>3.0.CO;2-U

Boldsen, J. L., Milner, G. R., Konigsberg, L. W., & Wood, J. W. (2002). Transition analysis: A new method for estimating age from skeletons. In R. D. Hoppa & J. W. Vaupel (Eds.), *Paleodemography: Age distributions from skeletal samples* (pp. 73–106). Cambridge: Cambridge University Press.

Bollen, K.-A. (1989). *Stuructural equations with latent variables*. Hoboken, NJ: John Wiley & Sons.

Boughner, J. C., & Hallgrímsson, B. (2008). Biological spacetime and the temporal integration of functional modules: A case study of dento–gnathic developmental timing. *Developmental Dynamics: An Official Publication of the American Association of Anatomists*, *237*(1), 1–17.

Braga, J., & Heuze, Y. (2007). Quantifying variation in human dental development sequences: An EVO-DEVO perspective. In S. E. Bailey & J.-J. Hublin (Eds.), *Dental Perspectives on Human Evolution* (pp. 247–261). Dordrecht, The Netherlands: Springer.

Brimacombe, C. S. (2017). The enigmatic relationship between epiphyseal fusion and bone development in primates. *Evolutionary Anthropology*, *26*, 325–335. https://doi.org/10.1002/evan.21559

Callewaert, F., Sinnesael, M., Gielen, E., Boonen, S., & Vanderschueren, D. (2010). Skeletal sexual dimorphism: Relative contribution of sex steroids, GH–IGF1, and mechanical loading. *Journal of Endocrinology*, *207*(2), 127–134. https://doi.org/10.1677/JOE-10-0209

Cameron, N. (2015). Can maturity indicators be used to estimate chronological age in children? *Annals of Human Biology*, *42*(4), 300–305. https://doi.org/10.3109/03014460.2015.1032349

Cameron, N., & Bogin, B. (2012). *Human Growth and Development* (2nd ed.). London: Academic Press.

Cameron, N., Bogin, B., Bolter, D., & Berger, L. R. (2017). The postcranial skeletal maturation of Australopithecus sediba. *American Journal of Physical Anthropology*, *163*(3), 633–640. https://doi.org/10.1002/ajpa.23234

Cameron, N., & Demerath, E. W. (2002). Critical periods in human growth and their relationship to diseases of aging. *Yearbook of Physical Anthropology*, *45*, 159–184.

Cardoso, H. F. V. (2007). Environmental effects on skeletal versus dental development: Using a documented subadult skeletal sample to test a basic assumption in human osteological research. *American Journal of Physical Anthropology*, *132*(2), 223–233. https://doi.org/10.1002/ajpa.20482

Cardoso, H. F. V., & Garcia, S. (2009). The Not-so-Dark Ages: Ecology for human growth in medieval and early Twentieth Century Portugal as inferred from skeletal growth profiles. *American Journal of Physical Anthropology*, *138*(2), 136–147. https://doi.org/10.1002/ajpa.20910

Carpenter, B., Gelman, A., Hoffman, M. D., Lee, D., Goodrich, B., Betancourt, M., … Riddell, A. (2017). Stan: A Probabilistic Programming Language. *Journal of Statistical Software*, *76*(1), 1–32. https://doi.org/10.18637/jss.v076.i01

Cavallo, F., Mohn, A., Chiarelli, F., & Giannini, C. (2021). Evaluation of Bone Age in Children: A Mini-Review. *Frontiers in Pediatrics*, *9*, 580314. https://doi.org/10.3389/fped.2021.580314

Chen, G., Shin, Y.-W., Taylor, P. A., Glen, D. R., Reynolds, R. C., Israel, R. B., & Cox, R. W. (2016). Untangling the relatedness among correlations, part I: Nonparametric approaches to inter-subject correlation analysis at the group level. *NeuroImage*, *142*, 248–259. https://doi.org/10.1016/j.neuroimage.2016.05.023

Cherubini, U., Luciano, E., & Vecchiato, W. (2004). *Copula methods in finance*. John Wiley & Sons.

Cheverud, J. M. (1982). Phenotypic, genetic, and environmental integration in the cranium. *Evolution*, *36*, 499–516.

Cheverud, J. M. (1996). Developmental integration and the evolution of pleiotropy. *American Zoologist*, *36*, 44–50.

Chib, S., & Greenberg, E. (1998). Analysis of multivariate probit models. *Biometrika*, *85*(2), 347–361. https://doi.org/10.1093/biomet/85.2.347

Cole, T. (2007). Babies, bottles, breasts: Is the WHO growth standard relevant? *Significance*, *4*(1), 6–10. https://doi.org/10.1111/j.1740-9713.2007.00211.x

Colman, K. L., Dobbe, J. G. G., Stull, K. E., & Ruijter, J. M. (2017). The geometrical precision of virtual bone models derived from clinical computed tomography data for forensic anthropology. *International Journal of Legal Medicine*, *131*(4), 1155–1163.

Colman, Kerri L., de Boer, H. H., Dobbe, J. G. G., Liberton, N. P. T. J., Stull, K. E., van Eijnatten, M., … van der Merwe, A. E. (2019). Virtual forensic anthropology: The accuracy of osteometric analysis of 3D bone models derived from clinical computed tomography (CT) scans. *Forensic Science International*, *304*, 109963. https://doi.org/10.1016/j.forsciint.2019.109963

Conaway, M. A., Schroeder, L., & von Cramon-Taubadel, N. (2018). Morphological integration of anatomical, developmental, and functional postcranial modules in the crab-eating macaque (Macaca fasicularis). *American Journal of Physical Anthropology*, *166*, 661–670. https://doi.org/10.1002/ajpa.23456

Conceicao, E. L. N., & Cardoso, H. F. V. (2011). Environmental effects on skeletal versus dental development II: Further testing of a basic assumption in human osteological research. *American Journal of Physical Anthropology*, *144*, 463–470. https://doi.org/10.1002/ajpa.21433

Corron, L. K., Condemi, S., & Chaumoitre, K. (2017). Evaluating the consistency, repeatability, and reproducibility of osteometric data on dry bone surfaces, scanned dry bone surfaces, and scanned bone surfaces from living individuals. *Bulletins et Memoires de La Societe d'Anthropologie de Paris*, *29*(1), 33. https://doi.org/10.1007/s13219-016-0172-7

Corron, L. K., Stock, M. K., Cole, S. J., Hulse, C. N., Garvin, H. M., Klales, A. R., & Stull, K. E. (2021). Standardizing ordinal subadult age indictaors: Testing for observer agreement and consistency across modalities. *Forensic Science International*, *320*. https://doi.org/10.1016/j.forsciint.2021.110687

Corron, L., Marchal, F., Condemi, S., & Adalian, P. (2018). A critical review of sub-adult age estimation in biological anthropology: Do methods comply with published recommendations? *Forensic Science International*, *288*, 328.e1-328.e9. https://doi.org/10.1016/j.forsciint.2018.05.012

Corruccini, R. S. (1975). Multivariate analysis in biological anthropology: Some considerations. *Journal of Human Evolution*, *4*(1), 1–19. https://doi.org/10.1016/0047-2484(75)90086-X

Crane, G. J., & Hoek, J. van der. (2008). CONDITIONAL EXPECTATION FORMULAE FOR COPULAS. *Australian & New Zealand Journal of Statistics*, *50*(1), 53–67. https://doi.org/10.1111/j.1467-842X.2007.00499.x

Danaher, P. J., & Smith, M. S. (2011). Modeling multivariate distributions using copulas: Applications in marketing. *Marketing Science*, *30*(1), 4–21.

Darwin, C. (1859). On the origin of species. *Published On*, *24*, 1.

de Onis, M., Garza, C., Victora, C. G., Bhan, M. K., & Norum, K. R. (2004). The WHO multicentre growth reference study (MGRS): Rationale, planning, and implementation. *Food and Nutrition Bulletin*, *25*(1).

De Tobel, J., Fieuws, S., Hillewig, E., Phlypo, I., van Wijk, M., de Hass, M. B., … Thevissen, P. W. (2020). Multi-factorial age estimation: A Bayesian approach combining dental and skeletla magnetic resonance imaging. *Forensic Science International*, *306*, 110054. https://doi.org/10.1016/j.forsciint.2019.110054

Dearborn, W. F., & Shuttleworth, F. K. (1938). Data on the Growth of Public School Children.(From the Materials of the Harvard Growth Study). *Monographs of the Society for Research in Child Development*, *3*(1), 1–136.

Debat, V., & David, P. (2001). Mapping phenotypes: Canalization, plasticity, and developmental stability. *Trends in Ecology & Evolution*, *16*, 555–561.

Demirjian, A., Buschang, P. H., Tanguay, R., & Patterson, D. K. (1985). Interrelationships among measures of somatic, skeletal, dental, and sexual maturity. *American Journal of Orthodontics*, *88*(5), 433–438. https://doi.org/10.1016/0002-9416(85)90070-3

Demirjian, A., Goldstein, H., & Tanner, J. M. (1973). A new system of dental age assesment. *Human Biology*, *45*, 211–227.

Demisch, A., & Wartmann, P. (1956). Calcification of the Mandibular Third Molar and Its Relation to Skeletal and Chronological Age in Children. *Child Development*, *27*(4), 459–473. JSTOR. https://doi.org/10.2307/1125899

Dias, A., & Embrechts, P. (2004). Dynamic copula models for multivariate high-frequency data in finance. *Manuscript, ETH Zurich*, *81*, 1–42.

Duren, D. L., Nahhas, R. W., & Sherwood, R. J. (2015). Do secular trends in skeletal maturity occur equally in both sexes? *Clinical Orthopaedics and Related Research*, *473*, 2559–2567.

Duren, D. L., Seselj, M., Froehle, A. W., Nahhas, R. W., & Sherwood, R. J. (2013). Skeletal growth and the changing genetic landscape during childhood and adulthood. *American Journal of Physical Anthropology*, *150*(1), 48–57. https://doi.org/10.1002/ajpa.22183

Ellison, P. T., & Jasienska, G. (2007). Constraint, pathology, and adaptation: How can we tell them apart? *American Journal of Human Biology*, *19*, 622–630. https://doi.org/10.1002/ajhb.20662

Emura, T., Nakatochi, M., Murotani, K., & Rondeau, V. (2017). A joint frailty-copula model between tumour progression and death for meta-analysis. *Statistical Methods in Medical Research*, *26*(6), 2649–2666.

Erdely, A., & Rubio-Sanchez, M. (2022). *Copula-based statistical dependence visualizations*. arXiv. https://doi.org/10.48550/ARXIV.2204.00265

Eveleth, P. B., & Tanner, J. M. (1990). *Worldwide variation in human growth* (2nd ed.). Cambridge: Cambridge University Press.

Fan, Y., & Patton, A. J. (2014). Copulas in econometrics. *Annu. Rev. Econ.*, *6*(1), 179–200.

Faragalli, A., Skrami, E., Bucci, A., Gesuita, R., Cameriere, R., Carle, F., & Ferrante, L. (2023). Combining Bayesian Calibration and Copula Models for Age Estimation. *International Journal of Environmental Research and Public Health*, *20*(2). https://doi.org/10.3390/ijerph20021201

Fazekas, I. G., & Kosa, F. (1978). *Forensic Fetal Osteology*. Budapest: Akademiai Kiado.

Fieuws, S., Willems, G., Larsen-Tangmose, S., Lynnerup, N., Boldsen, J., & Thevissen, P. (2016). Obtaining appropriate interval estimates for age when multiple indicators are used: Evaluation of an ad-hoc procedure. *International Journal of Legal Medicine*, *130*, 489–499. https://doi.org/10.1007/s00414-015-1200-8

Frees, E. W., & Valdez, E. A. (1998). Understanding relationships using copulas. *North American Actuarial Journal*, *2*(1), 1–25.

Friedman, N., & Koller, D. (2003). Being Bayesian about network structure: A Bayesian approach to structure discovery in Bayesian networks. *Machine Learning*, *50*, 95–125.

Frisancho, A. R. (2009). Developmental adaptation: Where we go from here. *American Journal of Human Biology*, *21*, 694–703. https://doi.org/10.1002/ajhb.20891

Gabry, J., & Cesnovar, R. (2022). *cmdstanr: R Interface to "CmdStan."* Retrieved from https://mc-stan.org/cmdstanr

Garn, S. M., Lewis, A. B., & Kerewsky, R. S. (1965). GENETIC, NUTRITIONAL, AND MATURATIONAL CORRELATES OF DENTAL DEVELOPMENT. *Journal of Dental Research*, *44*, SUPPL:228-242. https://doi.org/10.1177/00220345650440011901

Geber, J. (2014). Skeletal manifestations of stress in child victims of the Great Irish Famine (1845-1852): Prevalence of enamel hypoplasia, Harris lines, and growth retardation. *American Journal of Physical Anthropology*, *155*, 149–161. https://doi.org/10.1002/ajpa.22567

Gelman, A., Carlin, J. B., Stern, H. S., Dunson, D. B., Vehtari, A., & Rubin, D. B. (2014). *Bayesian Data Analysis* (3rd ed.). Boca Raton: Chapman & Hall/CRC.

Gelman, A., Carlin, J. B., Stern, H. S., & Rubin, D. B. (1995). *Bayesian Data Analysis*. London: Chapman & Hall.

Genest, C., & Nešlehová, J. (2007). A Primer on Copulas for Count Data. *ASTIN Bulletin: The Journal of the IAA*, *37*(2), 475–515. https://doi.org/10.1017/S0515036100014963

Genest, C., & Rivest, L.-P. (1993). Statistical Inference Procedures for Bivariate Archimedean Copulas. *Journal of the American Statistical Association*, *88*(423), 1034–1043. JSTOR. https://doi.org/10.2307/2290796

Gkiatas, I., Lykissas, M., Kostas-Agnantis, I., Korompilias, A., Batistatou, A., & Beris, A. (2015). Factors affecting bone growth. *American Journal of Orthopedics (Belle Mead, N.J.)*, *44*(2), 61–67.

Gluckman, P. D., Hanson, M. A., & Beedle, A. S. (2007). Early life events and their consequences for later disease: A life history and evolutionary perspective. *American Journal of Human Biology*, *19*, 1–19. https://doi.org/10.1002/ajhb.20590

Goda, K. (2010). Statistical modeling of joint probability distribution using copula: Application to peak and permanent displacement seismic demands. *Structural Safety*, *32*(2), 112–123. https://doi.org/10.1016/j.strusafe.2009.09.003

Gómez-Robles, A., & Polly, P. D. (2012). Morphological integration in the hominin dentition: Evolutionary, developmental, and functional factors. *Evolution*, *66*(4), 1024–1043.

Goodrich, B. (2017). *Truncated Multivariate Normal Variate in Stan*.

Gould, S. J., & Lewontin, R. C. (1979). The spandrels of San Marco and the Panglossian paradigm: A critique of the adaptionist programme. *Proceedings of the Royal Society of London B: Biological Sciences*, *205*, 581–598.

Greulich, W., & Pyle, S. I. (1959). *Radiographic Atlas of Skeletal Development of the Hand and Wrist* (2nd ed.). Stanford: Stanford University press.

Hallgrimsson, B., Jamniczky, H., Young, N. M., Rolian, C., Parsons, T. E., Boughner, J. C., & Marcucio, R. S. (2009). Deciphering the palimpsest: Studying the relationship between morphological integration and phenotypic covariation. *Evolutionary Biology*, *36*, 355–376. https://doi.org/10.1007/s11692-009-9076-5

Hallgrimsson, B., Willmore, K., & Hall, B. K. (2002). Canalization, developmental stability, and morphological integration in primate limbs. *Yearbook of Physical Anthropology*, *45*, 131–158. https://doi.org/10.1002/ajpa.10182

Herath, H. S., & Herath, T. C. (2011). Copula-based actuarial model for pricing cyber-insurance policies. *Insurance Markets and Companies*, *2*(1).

Hermanussen, M. (1997). Plasticity of adolescent growth in boys. *American Journal of Human Biology*, *9*, 469–480.

Hermanussen, M., Largo, R. H., & Molinari, L. (2001). Canalisation in human growth: A widely accepted concept reconsidered. *European Journal of Pediatrics*, *160*, 163–167.

Hicks, K., & Leonard, W. R. (2014). Developmental systems and inequality: Linking evolutionary and political-economic theory in biological anthropology. *Current Anthropology*, *55*(5), 523–550. https://doi.org/10.1086/678055

Hobbs, N. T., & Hooten, M. B. (2015). *Bayesian Models: A statistical guide for ecologists*. Princeton, NJ: Princeton University Press.

Hoffman, M. D., & Gelman, A. (2014). The No-U-Turn Sampler: Adaptively Setting Path Lengths in Hamiltonian Monte Carlo. *J. Mach. Learn. Res.*, *15*(1), 1593–1623.

Holly Smith, B., Crummett, T. L., & Brandt, K. L. (1994). Ages of eruption of primate teeth: A compendium for aging individuals and comparing life histories. *Yearbook of Physical Anthropology*, *37*, 177–231.

Howells, W. W. (1951). Factors of human physique. *American Journal of Physical Anthropology*, *9*, 159–192.

Hughes, J. (2022). A unified Gaussian copula methodology for spatial regression analysis. *Scientific Reports*, *12*(1), 15915. https://doi.org/10.1038/s41598-022-20171-1

Hummert, J. R., & Van Gerven, D. P. (1983). Skeletal growth in a medieval population from Sudanese Nubia. *American Journal of Physical Anthropology*, *60*, 471–478.

Huttegger, S. M., & Mitteroecker, P. (2011). Invariance and Meaningfulness in Phenotype spaces. *Evolutionary Biology*, *38*(3), 335–351. https://doi.org/10.1007/s11692-011-9123-x

Huxley, J. (1932). *Problems of Relative Growth*. London: Methuen & Company.

Jantz, R. L., & Ousley, S. (2005). *FORDISC 3.0: Computerized Forensic Discriminant Functions*. The University of Tennessee, Knoxville.

Jepsen, K. J., Hu, B., Tommasini, S. M., Courtland, H.-W., Price, C., Cordova, M., & Nadeau, J. H. (2009). Phenotypic integration of skeletal traits during growth buffers genetic variants affecting the slenderness of femora in inbred mouse strains. *Mammalian Genome*, *20*(1), 21–33. https://doi.org/10.1007/s00335-008-9158-1

Joe, H. (1997). *Multivariate Models and Dependence Concepts*. Chapman & Hall.

Joe, H. (2014). *Dependence Modeling with Copulas*. Chapman & Hall.

Johnston, F. E. (1969). Approaches to the study of developmental variability in human skeletal populations. *American Journal of Physical Anthropology*, *31*, 335–342.

Jones, H. E., & Bayley, N. (1941). The Berkeley Growth Study. *Child Development*, *12*(2), 167–173. JSTOR. https://doi.org/10.2307/1125347

Junker, B. H. (2008). Networks in Biology. In B. H. Junker & F. Schreiber (Eds.), *Analysis of Biological Systems* (pp. 3–14). Hoboken, NJ: John Wiley & Sons.

Käärik, M., Selart, A., Käärik, E., & Liivi, J. (2011). The use of copulas to model conditional expectation for multivariate data. *ISI Proc. 58th World Statistical Congress*, 5533–5538.

Kamnikar, K. R., Herrmann, N. P., & Plemons, A. M. (2018). New Approaches to Juvenile Age Estimation in Forensics: Application of Transition Analysis via the Shackelford et al. Method to a Diverse Modern Subadult Sample. *Human Biology*, *90*(1), 1–20.

Kaplan, D., & Depaoli, S. (2012). Bayesian structural equation modeling. In R. H. Hoyle (Ed.), *Handbook of Structural Equation Modeling* (pp. 650–673). New York: The Guilford Press.

Klaus, H. D. (2014). Frontiers in the bioarchaeology of stress and disease: Cross-disciplinary perspectives from pathophysiology, human biology, and epidemiology. *American Journal of Physical Anthropology*, *155*(2), 294–308. https://doi.org/10.1002/ajpa.22574

Klingenberg, C. P. (2008). Morphological integration and developmental modularity. *Annual Review of Ecology, Evolution, and Systematics*, *39*, 115–132. https://doi.org/10.1146/annurev.ecolsys.37.091305.110054

Klingenberg, Christian Peter. (2014). Studying morphological integration and modularity at multiple levels: Concepts and analysis. *Philosophical Transactions of the Royal Society of London. Series B, Biological Sciences*, *369*(1649), 20130249. https://doi.org/10.1098/rstb.2013.0249

Konigsberg, L. W. (2015). Multivariate cumulative probit for age estimation using ordinal categorical data. *Annals of Human Biology*, *42*, 366–376. https://doi.org/10.3109/03014460.2015.1045430

Konigsberg, L. W., Herrmann, N. P., Wescott, D. J., & Kimmerle, E. H. (2008). Estimation and evidence in forensic anthropology: Age-at-Death. *Journal of Forensic Sciences*, *53*, 541–557. https://doi.org/10.1111/j.1556-4029.2008.00710.x

Konigsberg, Lyle W., & Frankenberg, S. R. (1992). Estimation of age structure in anthropological demography. *American Journal Of Physical Anthropology*, *89*, 235–256.

Konigsberg, Lyle W., Frankenberg, S. R., & Liversidge, H. M. (2016). Optimal trait scoring for age estimation. *American Journal of Physical Anthropology*, *159*(4), 557–576. https://doi.org/10.1002/ajpa.22914

Konigsberg, Lyle W., & Hens, S. M. (1998). Use of ordinal categorical variables in skeletal assessment of sex from the cranium. *American Journal of Physical Anthropology*, *107*(1), 97–112. https://doi.org/10.1002/(SICI)1096-8644(199809)107:1<97::AID-AJPA8>3.0.CO;2-A

Kowalski, C. J. (1972). A commentary on the use of multivariate statistical methods in anthropometric research. *American Journal of Physical Anthropology*, *36*(1), 119–131.

Kurki, H. K., Holland, S., MacKinnon, M., Cowgill, L., Osipov, B., & Harrington, L. (2022). Appositional long bone growth: Implications for measuring cross-sectional geometry. *American Journal of Biological Anthropology*, *179*(2), 291–306. https://doi.org/10.1002/ajpa.24602

Kuzawa, C. W. (2005). Fetal origins of developmental plasticity: Are fetal cues reliable predictors of future nutritional environments? *American Journal of Human Biology*, *17*, 5–21. https://doi.org/10.1002/ajhb.20091

Kuzawa, C. W., & Bragg, J. M. (2012). Plasticity in human life history strategy: Implications for contemporary human variation and the evolution of Genus Homo. *Current Anthropology*, *53*, s369–s382. https://doi.org/10.1086/667410

Lamons, F. F., & Gray, S. W. (1958). A study of the relationship between tooth eruption age, skeletal development age, and chronological age in sixty-one Atlanta children. *American Journal of Orthodontics*, *44*(9), 687–691. https://doi.org/10.1016/0002-9416(58)90146-5

Lampl, M. (2012). Perspectives on modelling human growth: Mathematical models and growth biology. *Annals of Human Biology*, *39*(5), 342–351. https://doi.org/10.3109/03014460.2012.704072

Lampl, M., & Jeanty, P. (2003). Timing is everything: A reconsideration of fetal growth velocity patterns identifies the importance of individual and sex differences. *American Journal of Human Biology*, *15*, 667–680. https://doi.org/10.1002/ajhb.10204

Lande, R. (2019). Developmental integration and evolution of labile plasticity in a complex quantitative character in a multiperiodic environment. *Proceedings of the National Academy of Sciences*, *116*(23), 11361–11369. https://doi.org/10.1073/pnas.1900528116

Lasker, G. W. (1969). Human biological adaptability. *Science*, *166*, 1480–1486.

LAUTERSTEIN, A. M. (1961). A cross-sectional study in dental development and skeletal age. *Journal of the American Dental Association (1939)*, *62*, 161–167. https://doi.org/10.14219/jada.archive.1961.0032

Leigh, S. R. (2001). Evolution of human growth. *Evolutionary Anthropology*, *10*, 223–236.

Leigh, S. R., & Park, P. B. (1998). Evolution of human growth prolongation. *American Journal of Physical Anthropology*, *107*, 331–350.

Lenover, M. B., & Seselj, M. (2019). Variation in the fusion sequence of primary and secondary ossification centers in the human skeleton. *American Journal of Physical Anthropology*, *170*, 373–392. https://doi.org/10.1002/ajpa.23921

Levesque, G. Y., Demirijian, A., & Tanguay, R. (1981). Sexual dimorphism in the development, emergence, and agenesis of the mandibular third molar. *Journal of Dental Research*, *60*(10), 1735–1741. https://doi.org/10.1177/00220345810600100201

Lewandowski, D., Kurowicka, D., & Joe, H. (2009). Generating random correlation matrices based on vines and extended onion method. *Journal of Multivariate Analysis*, *100*(9), 1989–2001. https://doi.org/10.1016/j.jmva.2009.04.008

Lewis, A. B., & Garn, S. M. (1960). The relationship between tooth formation and other maturational factors. *The Angle Orthodontist*, *30*, 70–77.

Lewontin, R. (1978). Adaptation. *Scientific American*, *239*(3), 157–169.

Li, Q., Zhang, S., Sui, Y., Fu, X., Li, Y., & Wei, S. (2019). Sequential stimulation with different concentrations of BMP4 promotes the differentiation of human embryonic stem cells into dental epithelium with potential for tooth formation. *Stem Cell Research & Therapy*, *10*(1), 276. https://doi.org/10.1186/s13287-019-1378-7

Little, B. B., Malina, R. M., Buschang, P. H., DeMoss, J. H., & Little, L. R. (1986). Genetic and environmental effects on growth of children from a subsistence agricultural community in southern Mexico. *American Journal of Physical Anthropology*, *71*, 81–87.

Lovejoy, C. O., Meindl, R. S., Mensforth, R. P., & Barton, T. J. (1985). Multifactorial determination of skeletal age at death: A method and blind tests of its accuracy. *American Journal of Physical Anthropology*, *68*(1), 1–14. https://doi.org/10.1002/ajpa.1330680102

Low, W. (1970). The cross-sectional, longitudinal and mixed longitudinal methods in the study of human growth. *Zeitschrift Für Morphologie Und Anthropologie*, (H. 3), 249–258.

Ma, X., Luan, S., Ding, C., Liu, H., & Wang, Y. (2019). Spatial interpolation of missing annual average daily traffic data using copula-based model. *IEEE Intelligent Transportation Systems Magazine*, *11*(3), 158–170.

Ma, X., Luan, S., Du, B., & Yu, B. (2017). Spatial copula model for imputing traffic flow data from remote microwave sensors. *Sensors*, *17*(10), 2160.

Malina, R. M., Zavaleta, A., & Little, B. B. (1987). Secular changes in the stature and weight of Mexican American school children in Brownsville, Texas. *Human Biology*, *59*, 509–522.

Maresh, M. M. (1955). Linear growth of long bones of extremities from infancy through adolescence. *American Journal of Disabled Children*, *89*, 725–742.

Maresh, M. M. (1972). A forty-five year investigation for secular changes in physical maturation. *American Journal of Physical Anthropology*, *36*, 103–110.

Marquez-Grant, N. (2015). An overview of age estimation in forensic anthropology: Perspectives and practical considerations. *Annals of Human Biology*, *42*, 306–320. https://doi.org/10.3109/03014460.2015.1048288

Martorell, R. (2020). History and Design of the INCAP Longitudinal Study (1969-1977) and Its Impact in Early Childhood. *Food and Nutrition Bulletin*, *41*(1_suppl), S8–S22. https://doi.org/10.1177/0379572120906062

Matesanz, S., Blanco-Sánchez, M., Ramos-Muñoz, M., de la Cruz, M., Benavides, R., & Escudero, A. (2021). Phenotypic integration does not constrain phenotypic plasticity: Differential plasticity of traits is associated to their integration across environments. *New Phytologist*, *231*(6), 2359–2370. https://doi.org/10.1111/nph.17536

Milner, G. R., Ousley, S. D., Boldsen, J. L., Getz, S. M., Weise, S., & Tarp, P. (2020). *Transition Analysis 3 (TA3): Trait Manual*.

Mitteroecker, P., & Bookstein, F. (2007). The conceptual and statistical relationship between modularity and morphological integration. *Systems Biology*, *56*, 818–836.

Mitteroecker, P., & Bookstein, F. (2009). The ontogenetic trajectory of the phenotypic covariance matrix, with examples from craniofacial shape in rats and humans. *Evolution*, *63*, 727–737. https://doi.org/10.1111/j.1558-5646.2008.00587.x

Mitteroecker, P., Gunz, P., Neubauer, S., & Muller, G. (2012). How to explore morphological integration in human evolution and development. *Evolutionary Biology*, *39*, 536–553. https://doi.org/10.1007/s11692-012-9178-3

Moffat, T., & Galloway, T. (2007). Adverse environments: Investigating local variation in child growth. *American Journal of Human Biology*, *19*, 676–683. https://doi.org/10.1002/ajhb.20664

Moore-Jansen, P. J., Ousley, S. D., & Jantz, R. L. (1994). *Data Collection Procedures for Forensic Skeletal Material* (Report of Investigations No. 48). Knoxville, TN: Department of Anthropology, University of Tennessee, Knoxville.

Moorrees, C. F. A., Fanning, E. A., & Hunt, E. E. Jr. (1963). Age variation of formation stages for ten permanent teeth. *Journal of Dental Research*, *42*, 1490–1502.

Navega, D., Costa, E., & Cunha, E. (2022). Adult Skeletal Age-at-Death Estimation through Deep Random Neural Networks: A New Method and Its Computational Analysis. *Biology*, *11*(4). https://doi.org/10.3390/biology11040532

Nelsen, R B. (2006). *An Introduction to Copulas* (2nd ed.). Springer.

Nelsen, Roger B. (2005). 14—Copulas and quasi-copulas: An introduction to their properties and applications. In E. P. Klement & R. Mesiar (Eds.), *Logical, Algebraic, Analytic and Probabilistic Aspects of Triangular Norms* (pp. 391–413). Amsterdam: Elsevier Science B.V. https://doi.org/10.1016/B978-044451814-9/50014-8

Newman, S. L., Gowland, R. L., & Caffell, A. C. (2019). North and south: A comprehensive analysis of non-adult growth and health in the industrial revolution (AD 18th-19th C), England. *American Journal of Physical Anthropology*, *169*, 104–121. https://doi.org/10.1002/ajpa.23817

Noback, C. R. (1954). The appearance of ossification centers and the fusion of bones. *American Journal of Physical Anthropology*, *12*, 63–70.

Olson, E. C., & Miller, R. L. (1958). *Morphological Integration*. Chicago: The University of Chicago Press.

Othus, M., & Li, Y. (2010). A Gaussian Copula Model for Multivariate Survival Data. *Statistics in Biosciences*, *2*(2), 154–179. https://doi.org/10.1007/s12561-010-9026-x

Park, E. S., Oh, R., Ahn, J. Y., & Oh, M.-S. (2021). Bayesian analysis of multivariate crash counts using copulas. *Accident Analysis and Prevention*, *149*, 105431. https://doi.org/10.1016/j.aap.2019.105431

Patton, Andrew J. (2009). Copula–based models for financial time series. In *Handbook of financial time series* (pp. 767–785). Springer.

Patton, Andrew John. (2002). *Applications of copula theory in financial econometrics*. University of California, San Diego.

Pearl, J. (2000). *Causality: Models, reasoning, and inference*. New York: Cambridge University Press.

Pigliucci, M. (2001). *Phenotypic Plasticity: Beyond Nature and Nurture: Syntheses in Ecology and Evolution*. Baltimore: Johns Hopkins University Press.

Pigliucci, Massimo. (2003). Phenotypic integration: Studying the ecology and evolution of complex phenotypes. *Ecology Letters*, *6*(3), 265–272. https://doi.org/10.1046/j.1461-0248.2003.00428.x

Pinhasi, R., Teschler-Nicola, M., & Shaw, P. (2005). Cross-population analysis of the growth of long bones and the Os Coxae of three Early Medieval Austrain populations. *American Journal of Human Biology*, *17*, 470–488. https://doi.org/10.1002/ajhb.20406

Pitt, M., Chan, D., & Kohn, R. (2006). Efficient Bayesian Inference for Gaussian Copula Regression Models. *Biometrika*, *93*, 537–554. https://doi.org/10.1093/biomet/93.3.537

Poulsen, A. R., & Sonnesen, L. (2023). Association between dental and skeletal maturation in Scandinavian children born between 2005 and 2010. *Acta Odontologica Scandinavica*, 1–9. https://doi.org/10.1080/00016357.2023.2176920

Quetelet, L. A. J. (1869). *On Man and the Development of His Faculties, or Essay in Social Physics* (Vol. 2).

R Core Team. (2022). *R: a language and environment for statistical computing*. Vienna, Austria: R Foundationf for Statistical Computing. Retrieved from https://www.R-project.org/

Raff, R. A. (1996). *The Shape of Life: Genes, Development and the Evolution of Animal Form*. Chicago: University of Chicago Press.

Relethford, J. H., Lees, F. C., & Byard, P. J. (1978). The use of principal components in the analysis of cross-sectinoal growth data. *Human Biology*, *50*, 461–475.

Robling, A. G., Duijvelaar, K. M., Geevers, J. V., Ohashi, N., & Turner, C. H. (2001). Modulation of appositional and longitudinal bone growth in the rat ulna by applied static and dynamic force. *Bone*, *29*(2), 105–113. https://doi.org/10.1016/S8756-3282(01)00488-4

Robson, S. L., & Wood, B. (2008). Hominin life history: Reconstruction and evolution. *Journal of Anatomy*, *212*(4), 394–425. https://doi.org/10.1111/j.1469-7580.2008.00867.x

Roche, A. F. (1992). *Growth, maturation, and body composition: The Fels Longitudinal Study 1929-1991*. Cambridge University Press.

Roksandic, M., & Armstrong, S. D. (2011). Using the life history model to set the stage(s) of growth and senescence in bioarchaeology and paleodemography. *American Journal of Physical Anthropology*, *145*(3), 337–347. https://doi.org/10.1002/ajpa.21508

Rosas, A., Ríos, L., Estalrrich, A., Liversidge, H., García-Tabernero, A., Huguet, R., … Dean, C. (2017). The growth pattern of Neandertals, reconstructed from a juvenile skeleton from El Sidrón (Spain). *Science*, *357*(6357), 1282–1287. https://doi.org/10.1126/science.aan6463

Rudwick, M. J. S. (2008). *Georges Cuvier, Fossil Bones, and Geological Catastrophes: New Translations and Interpretations of the Primary Texts*. University of Chicago Press. Retrieved from https://books.google.com/books?id=-LrMY1qd0Z8C

Said-Mohamed, R., Pettifor, J. M., & Norris, S. A. (2018). Life History theory hypotheses on child growth: Potential implications for short and long-term child growth, development and health. *American Journal of Physical Anthropology*, *165*(1), 4–19. https://doi.org/10.1002/ajpa.23340

Salmon, F. (2009). Recipe for Disaster: The Formula That Killed Wall Street. *Wired*.

Sardi, M. L., & Rozzi, F. R. (2007). Developmental connections between cranial components and the emergence of the first permanent molar in humans. *Journal of Anatomy*, *210*(4), 406–417. https://doi.org/10.1111/j.1469-7580.2007.00701.x

Scammon, R. E. (1927). The first seriatim study of human growth. *American Journal of Physical Anthropology*, *10*, 329–336.

Schell, L. M., Gallo, M. V., & Ravenscroft, J. (2009). Environmental influences on human growth and development: Historical review and case study of contemporary influences. *Annals of Human Biology*, *36*(5), 459–477. https://doi.org/10.1080/03014460903067159

Schlecht, S. H., & Jepsen, K. J. (2013). Functional integration of skeletal traits: An intraskeletal assessment of bone size, mineralization, and volume covariance. *Bone (New York, N.Y.)*, *56*(1), 127–138.

Schlichting, C. D. (1989). Phenotypic integration and environmental change: What are the consequences of differential phenotypic plastciity of traits? *BioScience*, *39*.

Schour, I., & Massler, M. (1940). The development of the human dentition. *Journal of the American Dental Association*, *28*, 1953–1160.

Schug, G. R., & Goldman, H. M. (2014). Birth is but our death begun: A bioarchaeological assessment of skeletal emaciation in immature human skeletons in the context of environmental, social, and subsistence transition. *American Journal of Physical Anthropology*, *155*(2), 243–259. https://doi.org/10.1002/ajpa.22536

Schultz, A. H. (1923). Fetal growth in man. *American Journal of Physical Anthropology*, *6*, 389–399.

Šešelj, M. (2013). Relationship between dental development and skeletal growth in modern humans and its implications for intepreting ontogeny in fossil hominins. *American Journal of Physical Anthropology*, *150*(1), 38–47.

Sgheiza, V. (2022). Conditional independence assumption and appropriate number of stages in dental developmental age estimation. *Forensic Science International*, *330*, 111135. https://doi.org/10.1016/j.forsciint.2021.111135

Shackelford, L. L., Harris, A. E. S., & Konigsberg, L. W. (2012). Estimating the distribution of probable age-at-death from dental remains of immature human fossils. *American Journal of Physical Anthropology*, *147*(2), 227–253. https://doi.org/10.1002/ajpa.21639

Silventoinen, K., Kaprio, J., & Yokoyama, Y. (2011). Genetics of pre-pubertal growth: A longitudinal study of Japanese twins. *ANNALS OF HUMAN BIOLOGY*, *38*(5), 608–614.

Simmons, K., & Greulich, W. W. (1944). The Brush Foundation Study of child growth and development: II. Physical growth and development. *Monographs of the Society for Research in Child Development*, *9*(1), i–87.

Skylar, A. (1959). Fonctions de r´epartition `a n dimensions et leurs marges. *Publications de l'Institut de Statistique de L'Universit´e de Paris*, *8*, 229–231.

Slice, D. (2005). *Modern Morphometrics in Physical Anthropology* (1st ed. 2005.). New York, NY: Springer US.

Smith, B. H. (1991). Standards of Human Tooth formation and dental age assessment. In M. A. Kelley & C. S. Larsen (Eds.), *Advances in Dental Anthropology*. New York: Wiley-Liss.

Smith, B. H. (1992). Life history and the evolution of human maturation. *Evolutinoary Anthropology*, *1*, 134–142.

Smith, B. H. (1994). Sequence of emergence of the permanent teeth in Macaca, Pan, Homo, and Australopithecus: Its evolutioary significance. *American Journal of Human Biology*, *6*, 61–76.

Smith, M S. (2013). 336Bayesian approaches to copula modelling. In P. Damien, P. Dellaportas, N. G. Polson, & D. A. Stephens (Eds.), *Bayesian Theory and Applications* (p. 0). Oxford University Press. https://doi.org/10.1093/acprof:oso/9780199695607.003.0017

Smith, Michael S, & Khaled, M. A. (2012). Estimation of Copula Models with Discrete Margins via Bayesian Data Augmentation. *Journal of the American Statistical Association*, *107*(497), 290–303. https://doi.org/10.1080/01621459.2011.644501

Smith, S. L., & Buschang, P. H. (2004). Variation in longitudinal long bone growth in children three to ten years of age. *American Journal of Human Biology*, *16*, 648–657.

Smith, T. M., Tafforeau, P., Reid, D. J., Grün, R., Eggins, S., Boutakiout, M., & Hublin, J.-J. (2007). Earliest Evidence of Modern Human Life History in North African Early Homo sapiens. *Proceedings of the National Academy of Sciences of the United States of America*, *104*(15), 6128–6133.

Song, P. X.-K. (2000). Multivariate Dispersion Models Generated from Gaussian Copula. *Scandanavian Journal of Statistics*, *27*, 305–320.

Spradley, M. K. (2014). Toward estimating geographic origin of migrant remains along the United States-Mexico Border. *Annals of Anthropological Practice*, *38*, 101–110.

Stan Development Team. (2022). *Stan Modeling Language Users Guide and Reference Manual*. Retrieved from https://mc-stan.org

Stearns, S. C. (1992). *The evolution of life histories*. New York: Oxford University Press.

Stearns, S. C., & Koella, J. C. (1986). The evolution of phenotypic plasticity in life-history traits: Predictions of reaction norms for age and size at maturity. *Evolution*, *40*, 893–915.

Stinson, S. (1985). Sex differences in environmental sensitivity during growth and development. *Yearbook of Physical Anthropology*, *28*, 123–147.

Stock, M. K., Garvin, H. M., Corron, L. K., Hulse, C. N., Cirillo, L. E., Klales, A. R., … Stull, K. E. (2020). The importance of processing procedures and threshold values in CT scan segmentation of skeletal elements: An example using the immature os coxa. *Forensic Science International*, *309*, 110232. https://doi.org/10.1016/j.forsciint.2020.110232

Stull, K. E., & Armelli, K. A. (2021). Combining variables to improve subadult age estimation. *Forensic Anthropology*. https://doi.org/10.5744/fa.2019.0039

Stull, K. E., Chu, E. Y., Corron, L. K., & Price, M. H. (2022). Subadult Age Estimation Using the Mixed Cumulative Probit and a Contemporary United States Population. *Forensic Science*, *2*, 741–779. https://doi.org/10.3390/forensicsci2040055

Stull, K. E., & Corron, L. K. (2021). SVAD_US (1.0.0) [Data Set]. *Zenodo*. https://doi.org/10.5281/zenodo.5193208

Stull, K. E., Corron, L. K., & Price, M. H. (2021). Subadult age estimation variables: Exploring their varying roles across ontogeny. In B. F. B. Algee-Hewitt & J. Kim (Eds.), *Remodeling Forensic Skeletal Age: Modern Applications and New Research Directions* (pp. 50–74). London: Academic Press.

Stull, K.E., Chu, E. Y., Corron, L. K., & Price, M. H. (2023). Mixed cumulative probit: A multivariate generalization of transition analysis that accommodates variation in the shape, spread and structure of data. *Royal Society Open Science*, *10*, 220963. https://doi.org/10.1098/rsos.220963

Stull, Kyra E, & Corron, L. K. (2021a). Subadult Virtual Anthropology Database (SVAD) Data Collection Protocol: Amira. *Zenodo*. https://doi.org/10.5281/zenodo.5348411

Stull, Kyra E, & Corron, L. K. (2021b). Subadult Virtual Anthropology Database (SVAD) Data Collection Protocol: Epiphyseal Fusion, Diaphyseal Dimensions, Dental Development Stages, Vertebral Neural Canal Dimensions. *Zenodo*. https://doi.org/10.5281/zenodo.7293977

Stull, Kyra E, & Corron, L. K. (2022). The Subadult Virtual Anthropology Database (SVAD): An Accessible Repository of Contemporary Subadult Reference Data. *Forensic Science*, *2*, 20–36. https://doi.org/10.3390/forensicsci2010003 doi

Stull, Kyra E., L'Abbe, E. N., & Ousley, S. (2014). Using multivariate adaptive regression splines to estimate subadult age from diaphyseal dimensions. *American Journal of Physical Anthropology*, *154*, 376–386. https://doi.org/10.1002/ajpa.22522

Stull, Kyra E., Tise, M. L., Ali, Z., & Fowler, D. R. (2014). Accuracy and reliability of measurements obtained from computed tomography 3D volume rendered images. *Forensic Science International*, *238*, 133–140. https://doi.org/10.1016/j.forsciint.2014.03.005

Stulp, G., & Barrett, L. (2016). Evolutionary perspectives on human height variation. *Biological Reviews*, *91*, 206–234.

Tanner, J. M. (1981). *A history of the study of human growth*. Cambridge university press.

Tanner, J. M., Whitehouse, R. H., Marshall, W. A., Healy, M. J. R., & Goldstein, H. (1975). *Assessment of Skeletal Maturity and Prediction of Adult Height (TW2 Method)*. London: Academic Press.

Temple, D. H. (2019). Bioarchaeological evidence for adaptive plasticity and constraint: Exploring life-history trade-offs in the human past. *Evolutionary Anthropology*, *28*, 34–46. https://doi.org/10.1002/evan.21754

Temple, D. H., Bazaliiskii, V. I., Goriunova, O. I., & Weber, A. W. (2014). Skeletal growth in Early and Late Neolithic foragers from the Cis-Baikal region of Eastern Siberia. *American Journal of Physical Anthropology*, *153*, 377–386. https://doi.org/10.1002/ajpa.22436

Temple, Daniel H. (2014). Plasticity and constraint in response to early-life stressors among late/final Jomon period foragers from Japan: Evidence for life history trade-offs from incremental microstructures of enamel. *American Journal of Physical Anthropology*, *155*(4), 537–545.

Thompson, D. W. (1917). *On Growth and Form* (1st ed.). Cambridge: Cambridge University Press.

Tsumaki, N., & Yoshikawa, H. (2005). The role of bone morphogenetic proteins in endochondral bone formation. *Cytokine & Growth Factor Reviews*, *16*(3), 279–285. https://doi.org/10.1016/j.cytogfr.2005.04.001

Ubelaker, D. H. (1987). Estimating age at death from immature human skeletons: An overview. *1987*, *32*, 1254–1263.

Ubelaker, D. H., & Khosrowshahi, H. (2019). Estimation of age in forensic anthropology: Historical perspective and recent methodlogical advances. *Forensic Sciences Research*, *4*, 1–9.

University of Iowa Child Welfare Research Station. (1924). *Administration and scope of the Iowa Child Welfare research station* (Vol. 78). The University.

Varadhan, R. (2020). *condMVNorm: Conditional Multivariate Normal Distribution*. Retrieved from https://CRAN.R-project.org/package=condMVNorm

Vark, G. N., & Howells, W. W. (1984). *Multivariate Statistical Methods in Physical Anthropology: A Review of Recent Advances and Current Developments*. Springer.

Venables, W. N., & Ripley, B. D. (2002). *Modern Applied Statistics with S* (Fourth). New York: Springer. Retrieved from https://www.stats.ox.ac.uk/pub/MASS4/

Voje, K. L., Hansen, T. F., Egset, C. K., Bolstad, G. H., & Pélabon, C. (2014). ALLOMETRIC CONSTRAINTS AND THE EVOLUTION OF ALLOMETRY. *Evolution*, *68*(3), 866–885. https://doi.org/10.1111/evo.12312

Waddington, C. H. (1942a). Canalization of development and the inheritance of acquired characteristics. *Nature*, *150*, 563–565.

Waddington, C. H. (1942b). The epigenotype. *Endeavor*, *1*, 18–20.

Wagner, G. P. (2015). Homologues, Natural Kinds and the Evolution of Modularity1. *American Zoologist*, *36*(1), 36–43. https://doi.org/10.1093/icb/36.1.36

Wagner, G. P., Booth, G., & Bagheri-Chaichian, H. (1997). A populations genetic theory of canalization. *Evolution*, *51*, 329–347.

Wagner, Günter P., Mezey, J. G., & Calabretta, R. (2001). *Natural Selection and the Origin of Modules*.

Walker, P. L. (2008). Sexing skulls using discriminant function analysis of visually assessed traits. *American Journal of Physical Anthropology*, *136*(1), 39–50. https://doi.org/10.1002/ajpa.20776

Wang, R. N., Green, J., Wang, Z., Deng, Y., Qiao, M., Peabody, M., … Shi, L. L. (2014). Bone Morphogenetic Protein (BMP) signaling in development and human diseases. *Genes & Diseases*, *1*(1), 87–105. https://doi.org/10.1016/j.gendis.2014.07.005

Weber, G. W. (2015). Virtual Anthropology. *American Journal of Physical Anthropology*, *156*(S59), 22–42. https://doi.org/10.1002/ajpa.22658

Wells, J. C. K. (2007). Environmental quality, developmental plasticity, and the thrifty phenotype. *Evolutionary Bioinformatics*, *3*, 109–120.

Wells, J. C. K. (2017). Worldwide variability in growth and its association with health: Incorporating body composition, developmental plasticity, and intergenerational effects. *American Journal of Human Biology*, *29*, e22954. https://doi.org/10.1002/ajhb.22954

Wissler, A., Blevins, K. E., & Buikstra, J. E. (2022). Missing data in bioarchaeology I: A review of the literature. *American Journal of Biological Anthropology*, *179*(3), 339–348. https://doi.org/10.1002/ajpa.24609

Wright, S. (1932). General, group, and special size factors. *Genetics*, *17*, 603–619.

Wund, M. A. (2012). Assessing the impact of phenotypic plasticity on evolution. *Integrative and Comparative Biology*, *52*, 5–15. https://doi.org/10.1093/icb/ics050

Yaussy, S. L., DeWitte, S. N., & Redfern, R. C. (2016). Frailty and famine: Patterns of mortality and physiological stress among victims of famine in medieval London: FRAILTY AND FAMINE: MORTALITY AND STRESS IN MEDIEVAL LONDON. *American Journal of Physical Anthropology*, *160*(2), 272–283. https://doi.org/10.1002/ajpa.22954

Young, R. L., & Badyaev, A. V. (2007). Evolution of ontogeny: Linking epigenetic remodeling and adaptation in skeletal structures. *Integrative and Comparative Biology*, *47*, 234–244. https://doi.org/10.1093/icb/icm025

Zangirolami-Raimundo, J., de Oliveira Echeimberg, J., & Leone, C. (2018). Research methodology topics: Cross-sectional studies. *Journal of Human Growth and Development*, *28*(3), 356–360.

Zhao, X., & Zhou, X. (2012). Estimation of medical costs by copula models with dynamic change of health status. *Insurance: Mathematics and Economics*, *51*(2), 480–491.

Appendix – Stan Code for the Mixed Discrete-Continuous Gaussian Copula

**** All code and data can be found at https://github.com/ChristopherAWolfe/Mixed-Discrete-Gaussian-copula.***

```
functions{

 // All associated code is adapted from:
 // https://spinkney.github.io/helpful_stan_functions/group__gaussian__copula.html

 // There are 2 functions that define a Gaussian Copula in Stan. First, `multi_
 // normal_cholesky_copula_lpdf` and second, `centered_gaussian_copula_choelsky_`
 // These work in tandom to first aggregate all the marginal calculations and
 // jacobian adjustment and then increment the log-probability.

 real multi_normal_cholesky_copula_lpdf(matrix U, matrix L) {
  int N = rows(U);
  int J = cols(U);
  matrix[J, J] Gammainv = chol2inv(L);
  return -N * sum(log(diagonal(L))) - 0.5 * sum(add_diag(Gammainv, -1.0) .* crossprod(U));
 }

 real centered_gaussian_copula_cholesky_(array[,] matrix marginals, matrix L) {
  // Extract dimensions of final outcome matrix
  int N = rows(marginals[1][1]);
  int J = rows(L);
  matrix[N, J] U;

  // Iterate through marginal arrays, concatenating the outcome matrices by column
  // and aggregating the log-likelihoods (from continuous marginals) and jacobian
  // adjustments (from discrete marginals)
  real adj = 0;
  int pos = 1;
  for (m in 1 : size(marginals)) {
   int curr_cols = cols(marginals[m][1]);

   U[ : , pos : (pos + curr_cols - 1)] = marginals[m][1];
```

```
    adj += sum(marginals[m][2]);
    pos += curr_cols;
  }

  // Return the sum of the log-probability for copula outcomes and jacobian adjustments
  return multi_normal_cholesky_copula_lpdf(U | L) + adj;
}

// There are 2 function types that define each univariate marginal distribution depending
// on data type: polychotomous ordinal or continuous.The ordinal is adapted into
// two separate functions depending on data structure: (N x K matrix vs. N vector)
// The ordinal data follows the data augmentation approach highlighted in Albert
// & Chib, 1993. The continuous marginal is std_normal.

array[] matrix ordered_probit_marginal(array[,] int y, matrix mu_glm, matrix u_raw, array[] vector cutpoints) {
  int N = rows(mu_glm); // number of observations
  int K = cols(mu_glm); // number of polytomous variables
  array[2] matrix[N, K] rtn; // empty 2D array to return

  for(k in 1:K){
    for(n in 1:N){
      int C = num_elements(cutpoints[k,]) + 1; // total number of ord categories
      if(y[n,k] == 99){ // missing data
        rtn[1][n,k] = inv_Phi(u_raw[n,k]); // missing RV
        rtn[2][n,k] = 0;
      } else if(y[n,k] == 1){ // lowest bound
        real bound = Phi((cutpoints[k,1] - mu_glm[n,k])); // data augmentation
        rtn[1][n,k] = inv_Phi((bound*u_raw[n,k])); // latent RV
        rtn[2][n,k] = log(bound); // jacobian
      } else if (y[n,k] == C){ // highest bound
        real bound = Phi((cutpoints[k, C - 1] - mu_glm[n,k])); // data augmentation
        rtn[1][n,k] = inv_Phi(bound + (1-bound)*u_raw[n,k]); // latent RV
        rtn[2][n,k] = log1m(bound); // jacobian
```

```
    } else { // in between
      real ub = Phi((cutpoints[k ,y[n,k]] - mu_glm[n,k])); // data augmentation
      real lb = Phi((cutpoints[k, y[n,k] - 1] - mu_glm[n,k])); // data augmentation
      rtn[1][n,k] = inv_Phi((lb + (ub-lb)*u_raw[n,k])); // latent RV
      rtn[2][n,k] = log(ub-lb); // jacobian
    }
   }
  }
return rtn;
}

array[] matrix ordered_probit_marginal_uni(int[] y, real[] mu_glm, real[] u_raw, vector cutpoints) {
  int N = num_elements(mu_glm); // number of observations
  array[2] matrix[N, 1] rtn; // empty 2D array to return

  for(n in 1:N){
    int C = num_elements(cutpoints) + 1; // total number of ord categories
    if(y[n] == 99){ // missing data
      rtn[1][n,1] = inv_Phi(u_raw[n]); // missing RV
      rtn[2][n,1] = 0;
     } else if(y[n] == 1){ // lowest bound
      real bound = Phi((cutpoints[1] - mu_glm[n])); // data augmentation
      rtn[1][n,1] = inv_Phi((bound*u_raw[n])); // latent RV
      rtn[2][n,1] = log(bound); // jacobian
    } else if (y[n] == C){ // highest bound
      real bound = Phi((cutpoints[C - 1] - mu_glm[n])); // data augmentation
      rtn[1][n,1] = inv_Phi(bound + (1-bound)*u_raw[n]); // latent RV
      rtn[2][n,1] = log1m(bound); // jacobian
    } else { // in between
      real ub = Phi((cutpoints[y[n]] - mu_glm[n])); // data augmentation
      real lb = Phi((cutpoints[y[n] - 1] - mu_glm[n])); // data augmentation
      rtn[1][n,1] = inv_Phi((lb + (ub-lb)*u_raw[n])); // latent RV
      rtn[2][n,1] = log(ub-lb); // jacobian
    }
```

```
  }
  return rtn;
 }

 matrix[] normal_marginal(matrix y, matrix mu_glm, matrix sigma) {
  int N = rows(mu_glm); // number of observations
  int J = cols(mu_glm); // number of continuous variables
  matrix[N, J] rtn[2]; // empty 2D array to return
  // Initialise the jacobian adjustments to zero, as vectorised lpdf will be used
  rtn[2] = rep_matrix(0, N, J);

  for (j in 1 : J) {
   rtn[1][ : , j] = (y[ : , j] - mu_glm[ : , j]) ./ sigma[ :,j]; // center RV
   rtn[2][1, j] = normal_lpdf(y[ : , j] | mu_glm[ : , j], sigma[ :,j]); // "jacobian"
  }
 return rtn;
 }

}
data{

 // size variables //
 int N; // total # of observations (rows)
 int J; // total # of continuous observations
 int K_dentition; // total # of dental variables
 int K_ef; // total # of ef variables
 int K_pelvis; // total # of pelvic variables
 int K_all; // all ordinal variables

 //continuous prep //
 int present; // total # of complete data in continuous responses
 int missing; // total # of missing data in continuous responses
 real y_continuous[present]; // vector of reals of responses across all vars
 int index_pres[present, 2]; // Matrix (row, col) of non-missing value indices
```

```
  int index_miss[missing, 2]; // Matrix (row, col) of missing value indices

  // polychotomous prep //
  int y_dentition[N,K_dentition]; // 2D array of integers n obs by k_dentition
  int y_ef[N,K_ef]; // 2D array of integers n obs by k_ef
  int y_pelvis[N,K_pelvis]; // 2D array of integers n obs by k_pelvis
  int y_carpal[N]; // 2D array of integers n obs by k_carpal
  int y_tarsal[N]; // 2D array of integers n obs by k_tarsal

  // predictor (age) //
  real X[N]; //scaled

}
parameters{

  // continuous parameters //
  real y_missing_cont[missing]; // missing data parameter the size of all missing vars
  vector<lower=0>[J] constant; //constant in continuous mean function
  vector<lower=0>[J] exponent; // exponent in continuous mean function
  vector[J] offset; // offset in continuous mean function
  vector<lower=0>[J] noise1; // param of linear noise function
  vector<lower=0>[J] noise2; // param of linear noise function

  // Polychotomous parameters //
  vector<lower=0>[K_dentition] constant_dentition;
  vector<lower=0>[K_ef] constant_ef;
  vector<lower=0>[K_pelvis] constant_pelvis;
  real<lower=0> constant_carpal;
  real<lower=0> constant_tarsal;
  matrix<lower=0, upper=1>[N,K_dentition] u_dentition; // nuisance dentition
  matrix<lower=0, upper=1>[N,K_ef] u_ef; // nuisance ef
  matrix<lower=0, upper=1>[N,K_pelvis] u_pelvis; // nuisance pelvis
  real<lower=0, upper=1> u_carpal[N]; // nuisance carpal
  real<lower=0, upper=1> u_tarsal[N]; // nuisance tarsal
```

```
  ordered[11] threshold_dentition[16]; // dental thresholds
  ordered[6] threshold_ef[16]; // ef thresholds
  ordered[2] threshold_pelvis[2]; // pelvis thresholds
  ordered[8] threshold_carpal; // carpal thresholds
  ordered[7] threshold_tarsal; // tarsal thresholds

  // Cholesky factor (copula parameter) //
  cholesky_factor_corr[J+K_all] L;

}
transformed parameters{

  // Parameter Declarations //
  matrix[N,J] mu_continuous; // continuous mean
  matrix[N,J] sd_continuous; // continuous sd
  matrix[N,J] y_full_continuous; // full y matrix including missing data parameters
  matrix[N,K_dentition] mu_dentition; // dental mean
  matrix[N,K_ef] mu_ef; // ef mean
  matrix[N,K_pelvis] mu_pelvis; // pelvis mean
  real mu_carpal[N]; // carpal mean
  real mu_tarsal[N]; // tarsal mean

  // Continuous Parameters //
  for(i in 1:N){
    for(j in 1:J){
      mu_continuous[i,j] = constant[j]*X[i]^exponent[j] + offset[j];
      sd_continuous[i,j] = noise1[j]*(1 + X[i]*noise2[j]);
    }
  }
  // Fill y_full continuous with present data
  for(n in 1:present) {
      y_full_continuous[index_pres[n,1]][index_pres[n,2]] = y_continuous[n];
    }
  // Fill the rest of y_full continuous with missing value "parameters"
```

```
 for(n in 1:missing){
    y_full_continuous[index_miss[n,1]][index_miss[n,2]] = y_missing_cont[n];
  }

// Polytomous Parameters //
for(i in 1:N){
  for(k in 1:K_dentition){
    mu_dentition[i,k] = constant_dentition[k]*X[i];
  }
 }
for(i in 1:N){
  for(k in 1:K_ef){
    mu_ef[i,k] = constant_ef[k]*X[i];
  }
 }
for(i in 1:N){
  for(k in 1:K_pelvis){
    mu_pelvis[i,k] = constant_pelvis[k]*X[i];
  }
 }
for(i in 1:N){
    mu_carpal[i] = constant_carpal*X[i];
 }
for(i in 1:N){
    mu_tarsal[i] = constant_tarsal*X[i];
 }

}
model{

 // Priors //
 constant ~ std_normal();
 exponent ~ std_normal();
 offset ~ std_normal();
```

```
noise1 ~ std_normal();
noise2 ~ std_normal();
constant_dentition ~ std_normal();
constant_ef ~ std_normal();
constant_pelvis ~ std_normal();
constant_carpal ~ std_normal();
constant_tarsal ~ std_normal();

// Threshold Priors //
for(i in 1:K_dentition){
  for(t in 1:11){
    threshold_dentition[i,t] ~ normal(t+1,1);
  }
}
for(i in 1:K_ef){
  for(t in 1:6){
    threshold_ef[i,t] ~ normal(t+1,1);
  }
}
for(i in 1:K_pelvis){
  for(t in 1:2){
    threshold_pelvis[i,t] ~ normal(t+1,1);
  }
}

  for(t in 1:8){
    threshold_carpal[t] ~ normal(t+1,1);
  }

  for(t in 1:7){
    threshold_tarsal[t] ~ normal(t+1,1);
  }
```

```
  // Copula Parameter Prior //
  L ~ lkj_corr_cholesky(8);

  // Likelihood //
  target += centered_gaussian_copula_cholesky_(
    {normal_marginal(y_full_continuous, mu_continuous, sd_continuous),
    ordered_probit_marginal(y_dentition, mu_dentition, u_dentition, threshold_dentition),
    ordered_probit_marginal(y_ef, mu_ef, u_ef, threshold_ef),
    ordered_probit_marginal(y_pelvis, mu_pelvis, u_pelvis, threshold_pelvis),
    ordered_probit_marginal_uni(y_carpal, mu_carpal, u_carpal, threshold_carpal),
    ordered_probit_marginal_uni(y_tarsal, mu_tarsal, u_tarsal, threshold_tarsal)}, L);

}
generated quantities{

  // Here I put the correlation matrix back together for ease of interpretation
  corr_matrix[J+K_all] cor_mat = multiply_lower_tri_self_transpose(L);
```